THE UNIVERSITY OF MICHIGAN

INDUSTRY PROGRAM OF THE COLLEGE OF ENGINEERING

STRUCTURE OF FIBROUS PROTEINS: FEATHER KERATIN

Robert Schor

A dissertation submitted in partial fulfillment
of the requirements for the degree of
Doctor of Philosophy in the
University of Michigan
1958

September, 1958

IP-316

Doctoral Committee:

Assistant Professor Samuel Krimm, Chairman
Professor H. Richard Crane
Professor David M. Dennison
Assistant Professor Karl T. Hecht
Assistant Professor Christer E. Nordman

ACKNOWLEDGMENTS

The author would like to express his appreciation for the financial assistance given to him by the Engineering Research Institute, the Quartermaster Corps, and the United States Public Health Service.

The assistance of the following people is gratefully acknowledged:

Professor Samuel Krimm, for suggesting this problem and for his constant guidance and encouragement.

Mr. Lee Cross, for valuable assistance in model building.

Dr. D. L. Brown and Mrs. Virginia Richardson, of Willow Run Laboratories for expediting the use of MIDAC facilities.

Mr. H. Roemer and his associates in the Physics Instrument Shop, for their construction of the set of molecular models and auxiliary equipment which was used in this work.

Dr. Peter Geiduschek of the Department of Chemistry for a discussion which clarified some of the important chemical aspects of the problem.

Mr. Jerry Davenport of the Photography Department for photographing the molecular model.

The author is grateful for the invaluable aid of the College of Engineering Industry Program in the preparation of this manuscript.

TABLE OF CONTENTS

		Page
ACKNOWLEDGMENTS		iii
LIST OF TABLES		vi
LIST OF ILLUSTRATIONS		vii
I	REVIEW OF WORK ON FIBROUS PROTEINS	1
1.1	Introduction	1
1.2	The Astbury Classification Scheme for the Fibrous Proteins	13
1.3	Review of Previous Work on Feather Keratin	19
II	X RAY-DATA	29
2.1	Introductory Remarks	29
2.2	Experimental Techniques	29
2.3	Preliminary X-Ray Studies	30
2.4	Spacings in the Feather Keratin Diffraction Pattern	32
2.5	Alterations in the Diffraction Pattern	40
2.6	Cylindrical Patterson Function	46
III	CHEMICAL AND INFRARED STUDIES	67
3.1	Introductory Remarks	67
3.2	The Amino Acid Compositon of Feather Keratin	67
3.3	Amino Acid Sequence Studies	69
3.4	Solution Studies	69
3.5	Infrared Studies	74
IV	THE β-HELIX HYPOTHESIS	77
4.1	Introductory Remarks	77
4.2	Inadequacy of the Existing Configurations	77
4.3	Assumption of a Regular Sequence of Proline Residues	83
4.4	β-Helix Structure for Feather Keratin	86
4.5	Uniqueness of the Helical Structure	88
4.6	Construction of a Molecular Model	97

TABLE OF CONTENTS CONT'D

		Page
V	EVALUATION OF THE β-HELIX HYPOTHESIS	105
	5.1 Introductory Remarks	105
	5.2 Equatorial Diffraction Pattern	106
	5.3 Meridional Diffraction Pattern	128
	5.4 Radial Fourier Synthesis	135
	5.5 Cylindrical Patterson Function	144
	5.6 Alterations in the Diffraction Pattern	149
	5.7 Agreement with the Infrared Data	155
	5.8 Agreement with the Chemical Data	157
	5.9 Agreement with the Density	163
VI	CONCLUSIONS	167
	6.1 Experimental Results	167
	6.2 Structural Conclusions	168
	6.3 Perspectives	173
APPENDIX A.	THE APPLICATION OF THE THEORY OF FOURIER TRANSFORMS TO THE DIFFRACTION OF A SIMPLE HELIX	175
APPENDIX B.	CONSTRUCTION OF PURE β-HELICES	185
APPENDIX C.	ROUGH CALCULATIONS OF THE COORDINATES OF A β-HELIX	199
BIBLIOGRAPHY		203

LIST OF TABLES

Table		Page
I-I	Amino Acids Accepted as Being Direct Products of Hydrolysis of Proteins	3
II-I	Meridian and Layer-Line Spacings in the Feather Keratin Diffraction Pattern	36
II-II	Equatorial Spacings in the Feather Keratin Diffraction Pattern	37
II-III	Changes in Meridian Spacings in Feather Quill on Stretching 5.5%	41
III-I	Amino Acid Composition of the Calamus of White Turkey Feathers	68
III-II	Summary of Physical Chemical Properties for Feather Keratin Monomer	71
IV-I	Pitch Angle, Residue Length, and Radius of the Helix as a Function of the Number of Chains	88
IV-II	$C_{\beta 1}H_1'$ Contact as a Function of the Angle ψ	96
V-I	Equatorial Reflections of the Proposed Feather Structure	119
V-II	Intensities and Positions of the Equatorial Reflections of Feather keratin	138
B-I	Coordinates of the Atoms in the Amide Group	189
B-II	Coordinates of the Atoms of a Possible Pure β-Helix	194
C-I	Rough Coordinates of the Atoms of a Possible β-Helix	199

LIST OF ILLUSTRATIONS

Figure		Page
1-1	Diagrammatic representation of a fully extended polypeptide chain with the bond lengths and angles derived from crystal structures	5
1-2	Diagrammatic representation of two polypeptide chains cross-linked by a disulfide bond	6
1-3	Hypothetical fiber diagram	11
1-4	Drawings of left-handed and right-handed α-helices	17
1-5	X-ray diffraction pattern of sea gull quill	21
2-1	X-ray diffraction pattern of turkey calamus	33
2-2	Reciprocal lattice representation of the diffraction pattern of turkey calamus	34
2-3	X-ray diffraction pattern of "tilted sample" of turkey calamus	39
2-4	Comparison photographs of the diffraction patterns obtained from stretched and unstretched samples of turkey calamus	42
2-5	Comparison photographs of the x-ray diffraction patterns obtained from samples of turkey calamus at room humidity and from water-soaked samples	45
2-6	Optical density on equatorial layer line for 100 hour exposure photograph of turkey calamus	52
2-7	Optical density on equatorial layer line for 250 hour exposure photograph of turkey calamus	53
2-8	P(r) turkey calamus calculated from the data obtained from the 100 hour exposure photograph	55
2-9	P(r) turkey calamus calculated from the data obtained from the 250 hour exposure photograph	56
2-10	P(r) turkey calamus calculated by treating reflections as discrete	57

LIST OF ILLUSTRATIONS CONT'D

Figure		Page
2-11	P(r) silk fibroin calculated from the data of Pauling, Corey, and Marsh.....	58
2-12	Cylindrical Patterson Function (1).....	60
2-13	Cylindrical Patterson Function (2).....	61
2-14	Cylindrical Patterson Function (3).....	62
2-15	Cylindrical Patterson Function (4).....	63
2-16	Cylindrical Patterson Function (5).....	64
4-1	Hydrogen-bonding scheme.....	91
4-2	Schematic diagram of a Pauling-Corey extended polar polypeptide chain.....	93
4-3	Diagrammatic representation of short van der Waals contact.....	95
4-4	Photograph of molecular model of proposed feather structure.....	104
5-1	Hexagonal packing arrangement of three-unit groups...	108
5-2	Orthorhombic packing arrangement of three-unit groups	110
5-3	Seven cylinder unit.....	111
5-4	Equatorial scattering of the seven cylinder unit.....	114
5-5	Hexagonal packing of seven cylinder units.....	116
5-6	Equatorial transforms of the cylindrical units.....	117
5-7	Cylindrical lattice of three sheets.....	122
5-8	Equatorial scattering from a cylindrical lattice of three sheets for a_o = 34A.....	124
5-9	Diagrammatic representation of idealized model of the proposed cylindrical unit of structure.....	130

LIST OF ILLUSTRATIONS CONT'D

Figure		Page
5-10	Radial fourier$_1$ turkey calamus.....	140
5-11	Radial fourier$_2$ turkey calamus.....	142
5-12	Calculated "Paterson function" for idealized model of a cylindrical unit of structure.....	146
A-1	Ewald's construction for the diffraction maxima using the reciprocal lattice and the sphere of reflection..	176
A-2	Coordinates of a point on a helix.....	178
A-3	The maxima of the squares of Bessel functions.....	180
A-4	Schematic representation of the diamond shaped array of spots expected from a discontinuous helix (P = 4P).	182
B-1	Skeleton of α-carbon atoms.....	185
B-2	Coordinate systems.....	187
B-3	Parameters in the amide group.....	188
B-4	The Euler angles.....	190
B-5	Orientation of the amide group.....	190
B-6	Basal projection of the atoms in the main chains of a possible pure β-helix.....	195

CHAPTER I

REVIEW OF WORK ON FIBROUS PROTEINS

1.1 Introduction

The problem of the determination of the structure of proteins is of considerable importance since the proteins constitute one of the principal organic constituents of living matter. The great size, variety, and complexity of the proteins enable them to carry out thousands of diverse and important biological functions in a human organism. The following are some typical examples: the protein collagen, a constituent of the tendons, bones and skin, contributes to the mechanical stability of the body; myosin plays an essential role in the phenomenon of muscular contraction; keratin in the hair and epidermis, provides protection for the body; hemoglobin, found inside the red blood cells, combines with the oxygen in the lungs and liberates it in the tissues.

It is convenient to divide the study of the structure of a protein into two separate but closely related problems: 1) the determination of the chemical structure of the protein 2) the determination of the three-dimensional configuration of the protein.

We shall first consider some of the more important general facts relating to the determination of the chemical structure of a protein. It is well known that when a protein is broken down, by boiling it in water for a long time or by treating it with acid or alkali, the resulting products obtained are the relatively simple amino acids. The determination of the amino acid composition of a protein represents one of the first stages in the elucidation of its

chemical structure. Table I-I lists the amino acids which have been isolated as being the direct products of the hydrolysis of proteins.

The next question that arises is the nature of the chemical bonding in proteins. The important role played by polypeptide chains in the structure of proteins was demonstrated by Emil Fischer's experiments over fifty years ago[1]. Figure 1-1 shows that a polypeptide chain is a repeating structure whose backbone consists of identical units ($C_\alpha C'CONH$) called peptide groups to which are attached the side-groups $R_1R_2R_3$.. which characterize the different amino acids that constitute the chain. When a hydrogen atom of the amino group (NH_2) of one amino acid, $RCH(NH_2)COOH$, combines with the carboxyl group (COOH) of another amino acid, a water molecule is split off and in the process the peptide bond, which joins the alpha-carbon atom of the second amino acid to the nitrogen atom of the first amino acid, is formed.

From the point of view of determining the three-dimensional configuration of a polypeptide chain, most of the amino acids have no special structural significance. Proline, hydroxyproline, cystine and glycine, however, have particular structural importance. Proline is in fact an imino acid (NH) and lacks a hydrogen atom to form the important hydrogen bond (CO...HN). The side chain of proline can exert a constraint on the main chain atoms. Hydroxyproline is similar to proline in the constraint it imposes on the atoms in the main chain, and differs only by the replacement of a H on the γ-carbon atom by an OH group, giving rise to the possibility of the formation of an additional hydrogen bond. Figure 1-2 shows that the double unit of cystine can form cross-links between two different polypeptide chains, which

TABLE I-I

Amino Acids Accepted as Being Direct Products of Hydrolysis of Proteins

1. Neutral α-Amino Acids $RCH(NH_2)COOH$

(a) Aliphatic Side Chains (R)

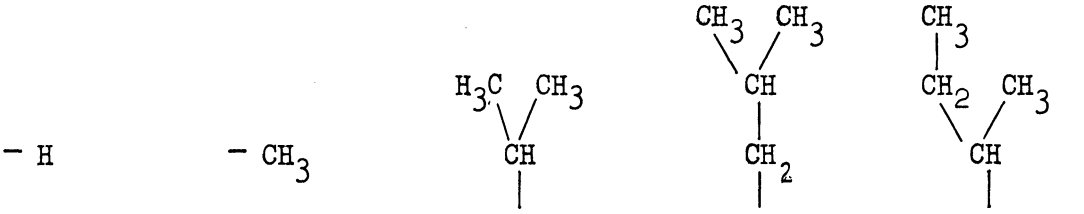

Glycine Alanine Valine Leucine Isoleucine

(b) Side Chains Containing Unsubstituted Aromatic Systems

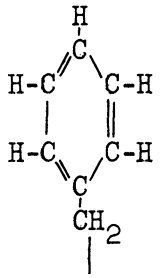

Phenylalanine

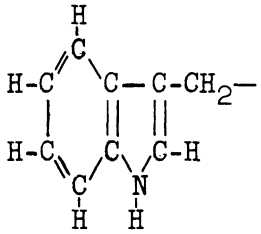

Tryptophan

(c) Side Chains Containing Hydroxy Groups

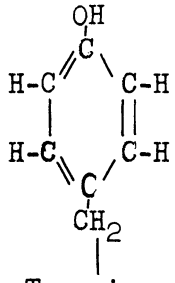

Tyrosine

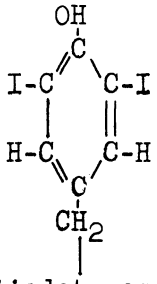

Diiodotyrosine

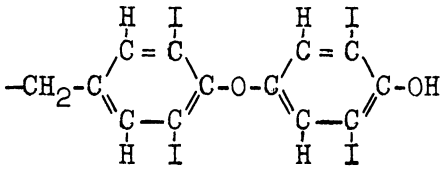

Thyroxine

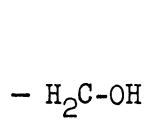

Serine

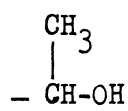

Threonine

TABLE I-I CONT'D

(d) Side Chains Containing Sulfur

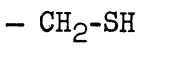

Cysteine

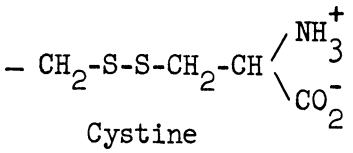

Cystine

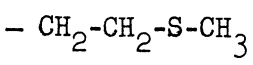

Methionine

(e) Side Chains Cyclized: Imino Acids

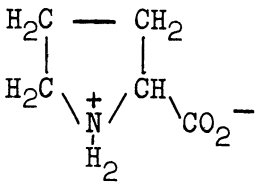

Proline

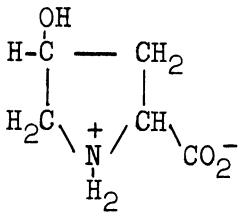

Hydroxyproline

2. Basic α-Amino Acids

Side Chains

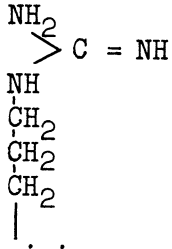

Arginine

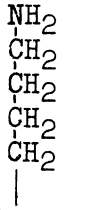

Lysine

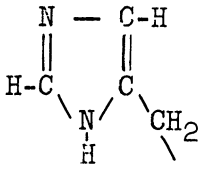

Histidine

3. Acidic α-Amino Acids

Side Chains

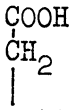

Aspartic Acid

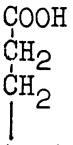

Glutamic Acid

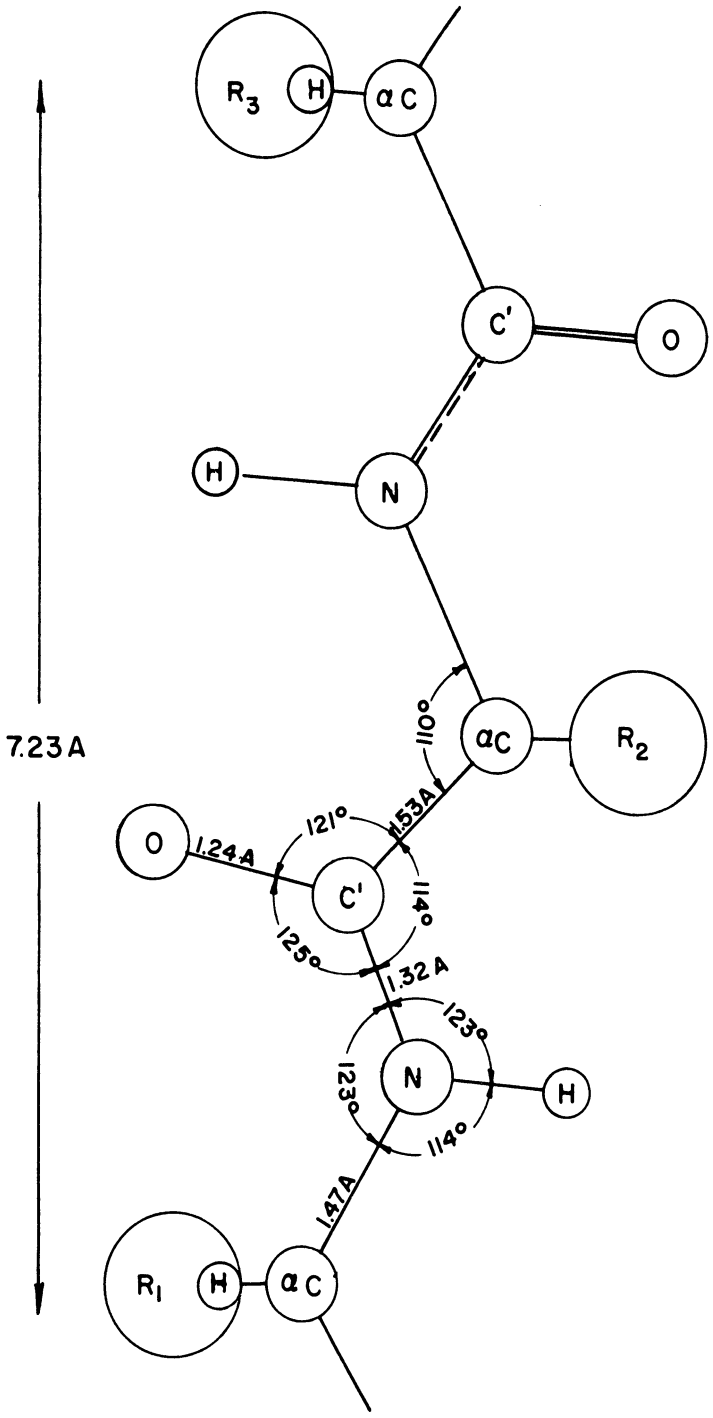

Figure 1-1 Diagrammatic representation of a fully extended polypeptide chain with the bond lengths and angles derived from crystal structures (2). The dotted lines indicate the partial double bond character of the peptide bond. The residues are in the trans configuration (succesive α-carbon atoms on opposite sides of the peptide bond). The cis configuration (succesive α-carbon atoms on the same side of the peptide bond) is unlikely to occur in a protein structure (3). The first carbon atom in the side chain, which is attached to the α-carbon atom, is designated the β-carbon atom.

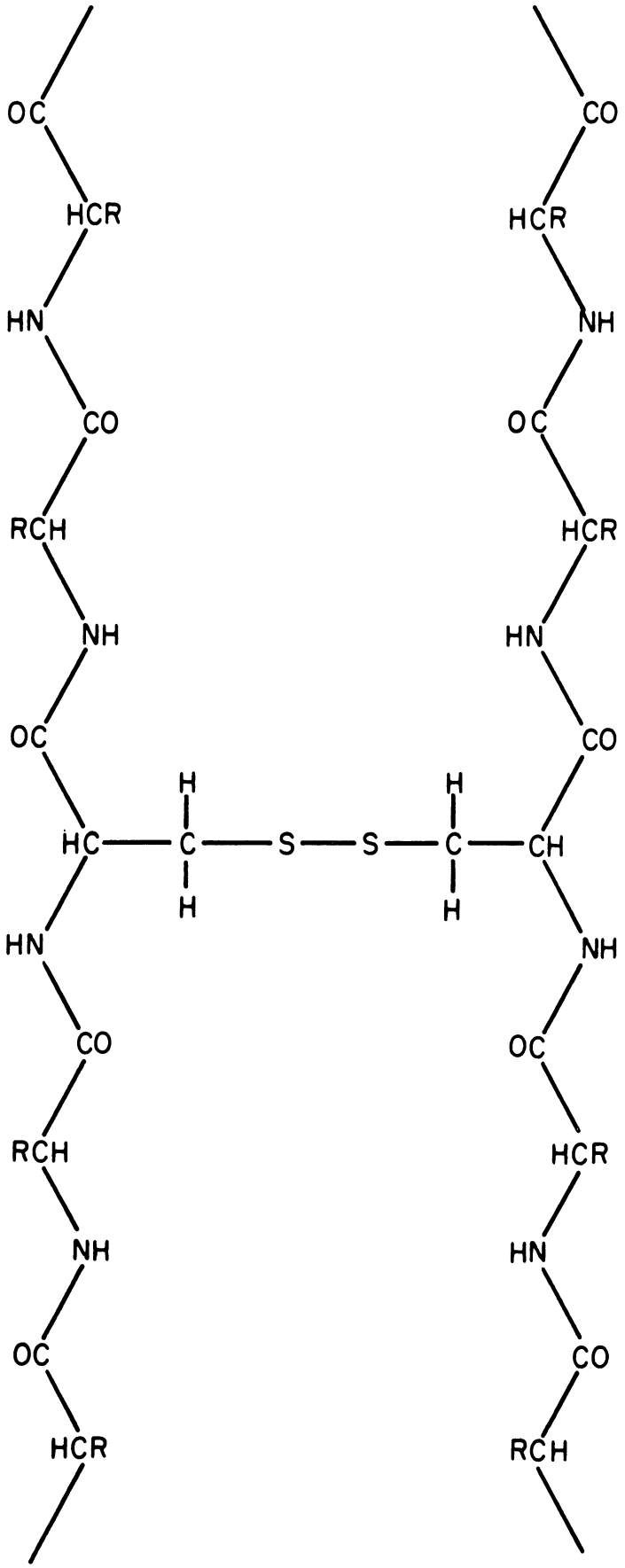

Figure 1-2 - Diagrammatic representation of two polypeptide chains cross-linked by a disulfide bond.

also can constrain the main chain configuration. Glycine is structurally significant because it has only a single hydrogen atom in its side chain. The small side chain of glycine can squeeze into regions of space which could not be occupied by the larger side chains. This property of glycine is of great importance in some recent models for collagen[4].

The difficult and important problems relating to the sequence of the amino acids in the consitituent polypeptide chains of a protein are being studied by chemical methods. Complete success has been obtained in the case of insulin as a result of the work of Sanger and his co-workers[5,6].

Even a complete knowledge of its chemical structure, however, does not completely determine the properties and biological functions of a protein. The three-dimensional configuration of the polypeptide chain must also be taken into account. Inspection of Figure 1-1 shows that the alpha-carbon atom is linked by single bonds to the nitrogen atom and to the carbonyl (C') carbon atom. By rotating one portion of the polypeptide chain relative to the other around these single bonds, the chain can assume, in principle, an infinite number of different spatial configurations. It is in fact found that the proteins fall into two distinct classes with respect to their spatial configurations: 1) the fibrous proteins 2) the globular proteins. The fibrous proteins consist of threadlike bundles of polypeptide chains which possess a linear periodicity along a unique structural axis, i.e., the fiber axis. In the globular proteins, (globe-shaped) no such simplification exists and the axes of the polypeptide chains may describe complex paths

in space. It is of interest to note that the differences in the configurations of the fibrous and the globular proteins seem to be associated with significant biological differences in the functions of these proteins. Enzymes and the hormones are globular proteins. The fibrous proteins, on the other hand, mainly serve to provide a suitable mechanical framework for the protection and functioning of the organism.

It has just been suggested that the configuration of a protein may be of importance in determining its role in a biological system. One method of indicating a more direct relationship between the spatial configuration of a protein and its biological properties is by a consideration of the phenomena involved in the "denaturation" of proteins[7]. The characteristic solubility of a globular protein (fibrous proteins are in general insoluble) may be lost by subjecting the protein to small increases in temperature or to mild acidity. The shape of such a "denatured" protein often approximates more closely to the shape of a fibrous protein than it does to the shape of the native protein. It is found that the denaturation of a biologically active globular protein such as an enzyme or a hormone usually results in the loss of its characteristic biological activity. In those cases where the denaturation is reversible, the protein regains both its characteristic solubility and its biological activity. From these facts it is generally inferred that the process of denaturation may involve the conversion of a globular protein into a fibrous protein with the accompanying loss of some important biological properties of the protein. The conclusion that the polypeptide chains are folded or coiled in a highly specific manner in a globular protein and that the configuration is held together by specific but weak bonds between the polypeptide chains

seems to be a reasonable one. It is thought that such a specific spatial configuration "imparts to the protein" its biological properties.

If the conclusion that the three-dimensional structure of a protein is relevant to the understanding of its function in a biological system is accepted, then the importance of a detailed knowledge of the configurations of proteins becomes evident. This point of view may be summarized as follows: the primary reason for studying the structure of proteins is the reasonable hope that knowledge derived from such studies will be essential to the full understanding of the basic biological processes of growth, metabolism, reproduction, etc.

It should be emphasized that although much progress has been made in the elucidation of the configurations of both the globular and the fibrous proteins, we do not yet have a complete picture of the three-dimensional structure of more than one or two particular proteins. With respect to the biologically important globular proteins, progress has been slow, probably primarily as a result of the difficulties associated with the lack of a unique direction defining the axes of the polypeptide chains. In fact, all of the structural principles which may be assumed to form the underlying basis of the structure of the globular proteins are not understood. The greatest progress has been made, in recent years, in the field of the fibrous proteins where the simplifications which arise from the assumption of a linear periodicity along the polypeptide chain itself have permitted the elucidation of some very general structural principles. In particular, as will be discussed later in greater detail, the hypothesis that the polypeptide chains assume helical configurations has proved to be enormously fruitful. Thus, in addition to the intrinsic

importance of the fibrous proteins, the study of the fibrous proteins is of importance in that such studies may supply additional structural principles and information which will be relevant to a successful attack on the problem of the determination of the structure of the globular proteins.

The x-ray diffraction method has proved to be the most powerful tool in studying the spatial configuration of a protein. The essential reason is that periodicities in structure of the order of atomic dimensions can easily be detected by x-ray methods. The x-ray information relative to the problem in the case of a fibrous protein is contained in the fiber diagram of the material under investigation. For purposes of clarifying the subsequent discussion, some of the general properties characteristic of the diffraction patterns obtained from fibrous systems will be discussed briefly. Figure 1-3 shows a schematic diagram of the scattering from a hypothetical material taken with the x-ray beam perpendicular to the fiber axis, which is assumed to be vertical. In general, a reflection at the point (R,ζ)* can be conceived of as arising from a set of Bragg planes whose normals make an angle ψ with the fiber axis such that $\tan \psi = \frac{R}{\zeta}$. It follows that the meridional reflections ($R = 0$) arise from the scattering of planes perpendicular to the fiber axis and that the equatorial reflections ($\zeta = 0$) arise from the scattering of planes parallel to the fiber axis. Physically, these two types of reflections represent periodicities along the polypeptide chains, and between chains in the lateral direction, respectively. The spots C, D, and E_1 are seen to lie on the layer line $\ell = 1$ ($\zeta = \ell/c$ where c is the fiber axis identity period). In general, the spots lying on the ℓth layer line can be conceived of as arising from the ℓth order diffraction of rows of

* See Appendix A for a definition of ζ. R is the two-dimensional radial coordinate in reciprocal space.

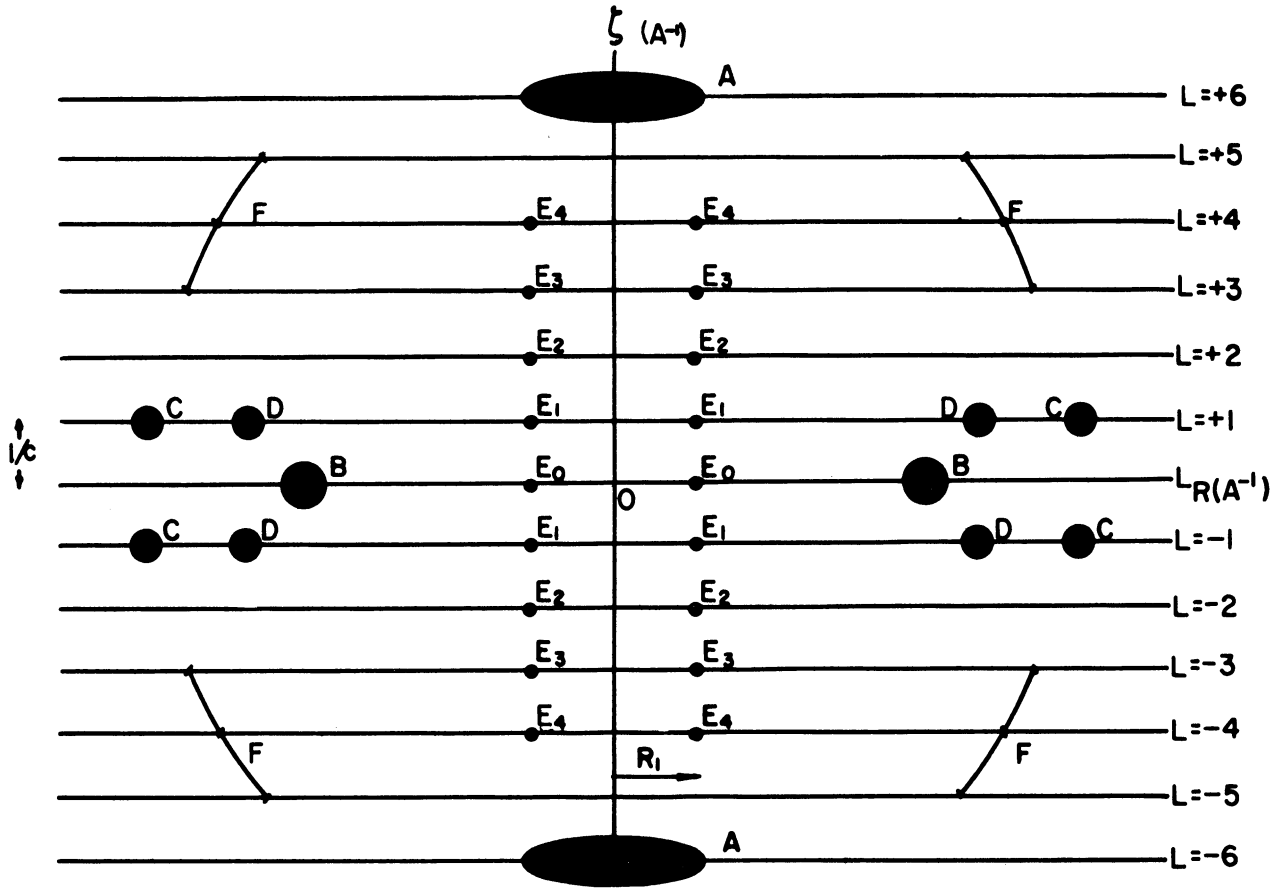

Figure 1-3 - Hypothetical fiber diagram.

points whose repeat distance is c. The only symmetry present in a fiber diagram is of a simple nature. It can be seen from Figure 1-3 that the meridian and the equator of the pattern form mirror planes. This is a result of the fact that the intensity transform of a fiber is cylindrically symmetric about the ζ axis in reciprocal space and also possesses a center of symmetry through the origin of reciprocal space. The cylindrical symmetry of the intensity transform results from the fact that all orientations of the polypeptide chain crystallites around the fiber axis are equally probable. Another general feature of the scattering from fibrous systems is the breadth and/or arcing of some of the reflections, indicating various forms of disorder in the system[8]. For example, reflection F is considerably spread along the arc of a circle, indicating a lack of parallelism of the fibers with respect to the fiber axis. Reflection A exhibits spreading transverse to the layer line indicating limitations in the dimension of the fibril along the repeat direction. The lateral spreading of a reflection, such as is observed for reflection B, indicates a combination of limitations in the lateral dimensions in the fibril and the lack of a perfect packing arrangement. The spots $E_0E_1E_2E_3E_4$ lie at a constant distance R_1 from the ζ axis. Such a sequence of reflections is called a row line. The determination of the Bragg spacings of the reflections and the fiber axis identity period can be accomplished by elementary geometrical considerations which will not be discussed here[9].

From the preceding discussion, it is clear that although a fiber diagram contains significant information relative to the positions and

intensities of the diffracted x-rays, this information is far from sufficient to permit a straightforward approach to the determination of the structure. A study of the historical development of the subject shows that the powerful symmetry considerations and three-dimensional data of classical crystallography are not available, and other approaches are necessary.

1.2 The Astbury Classification Scheme for the Fibrous Proteins

Astbury[10] has classified the native fibrous proteins, on the basis of the regularity in tneir wide-angle diffraction patterns, into the keratin-myosin-epidermin-fibrinogen group and the collagen group. The k-m-e-f group was found to consist of the subgroups α - keratin and β - keratin[11]. Alpha-keratin (e.g., human hair) can be stretched continuously and reversibly approximately 100% along the fiber axis to give the β configuration. The three-fold division of the fibrous proteins into α, β, and collagen (γ), although independent of any structural hypothesis concerning polypeptide chain configurations, gave hope to the early investigators that important generalizations in terms of a few basic configurations would be discovered.

The outstanding features of the α-keratin diffraction pattern are strong meridian reflections at 5.1A and 1.5A and a strong equatorial reflection at 9.8A[2,12]. The β pattern has strong meridian reflections at 3.33A and 1.1A[13] and strong equatorial reflections at 9.8A and 4.65A. In addition, the β pattern exhibits a strong reflection on the 6.66A layer line[14]. These reflections in the α-keratin and β-keratin diffraction patterns are diffuse and are essentially the only reflections in the patterns.

The diffraction pattern of collagen is quite distinct from the α and β patterns[2]. Air-dried collagen shows a strong meridian reflection at 2.86A and strong equatorial reflections at 11.6A and 4.6A. Attempts to stretch collagen, the maximum elongation being approximately 15%, give rise to a proportional increase in the wide-angle spacings but no fundamentally new pattern is obtained.

The β pattern was the first to be successfully interpreted in terms of a detailed configuration of the polypeptide chain. Silk fibroin, which gives the best diffraction pattern of the β type, may be considered the prototype of the β configuration. On the basis of a detailed study of silk fibroin, Brill[15] concluded that the data could be accounted for by a monoclinic unit cell containing eight amino acid residues, 2 amino acid residues from each of the 4 polypeptide chains passing through the unit cell. The dimension of the unit cell in the direction of the fiber axis was 7A. Meyer and Mark[16] noted that this dimension corresponded to two residues in a nearly extended polypeptide chain. There have been several other investigations of silk fibroin, culminating in the work of Marsh, Corey, and Pauling[17]. These authors have concluded that:

"The structure consists of extended polypeptide chains bonded together by lateral NH....O hydrogen bonds to form antiparallel-chain pleated sheets[18]. The sequence -G-X-G-X-G-X- in which G represents glycyl and X alanyl or seryl residues predominates throughout the structure, so that adjacent sheets pack together at 3.5 and 5.7A."

The relationship of the β-keratin diffraction pattern to that of silk fibroin helped in establishing a model for the other β-proteins.

The 3.33A meridian reflection has been interpreted as the axial projection of one slightly collapsed amino acid residue along the polypeptide chain[19]. The maximum extension for a single residue (see Figure 1-1) is approximately 3.63A[20]. The strong and diffuse 4.65A equatorial reflection has been identified with the distance between adjacent polypeptide chains within a given hydrogen-bonded sheet, while the 9.8A equatorial reflection is a side-chain spacing (at right angles to the plane of the sheet) and represents the distance between adjacent sheets of the three-dimensional network[19].

The ability to go reversibly from the α to the β pattern by stretching and relaxing the sample indicates that the basic process is a molecular folding phenomenon. Since the β configuration corresponds to a nearly fully extended polypeptide chain, the unstretched configuration must consist of chains in a contracted state. The early efforts[21-24] to obtain a satisfactory model for the α form were based on an attempt to account for the existence of the 5.1A meridional reflection. The strong 1.5A meridional reflection was discovered only later by Perutz[12]. In an attempt to determine the configuration of the α - proteins, as well as to contribute to the general understanding of protein structure, Pauling and Corey[25] set out to examine in more detail the basic principles underlying the configuration of polypeptide chains. By employing the known distances and bond angles in the polypeptide chain and assuming the structural principles of the equivalence of the residues, the planarity of the amide group ($C_\alpha NHC'OC_\alpha$) and the formation of a maximum number of hydrogen bonds, they[25,26] were able to construct two new helical

configurations of the polypeptide chain, the α-helix and the γ-helix.* In the 3.6 residue per turn α-helix, shown in Figure 1-4, each amide group is hydrogen-bonded to the third amide group beyond it in either direction along the helix. The axial projection of each residue is 1.5A (in agreement with the 1.5A reflection discovered by Perutz), giving a pitch of 5.4A. Allowing approximately 2A for the projecting side-chains, the diameter of an α-helix would be of the order of 10A. The length of the hydrogen-bonds is about 2.85A and the angle between the NH and NO vectors is approximately 15°[27].

The α-helix is a configuration of maximum stability[28], and appears to be in agreement with much of the experimental data on synthetic polypeptides. Cochran, Crick, and Vand[29] have shown that the diffraction pattern of the synthetic polypeptide poly-γ-methyl-L-glutamate is in good agreement with that expected for an α-helix. Small quantitative discrepancies exist in the case of the α form of poly-L-alanine between the experimentally observed intensities and those predicted on the basis of an α-helix, but it is expected that distortions of the methyl groups will ultimately account for them[30]. When the α proteins are considered, the situation is not as certain. In particular, the α-helix predicts a near-meridional reflection at 5.4A instead of the observed meridional reflection at 5.1A. Crick[31] has shown that packing considerations make it likely that α-helices of the same handedness would assume a coiled-coil configuration, i.e., a configuration in which the axes of the helices follow a helical course of very large pitch. Such a

---

* The γ-helix has not played an important role in subsequent developments and will therefore not be discussed.

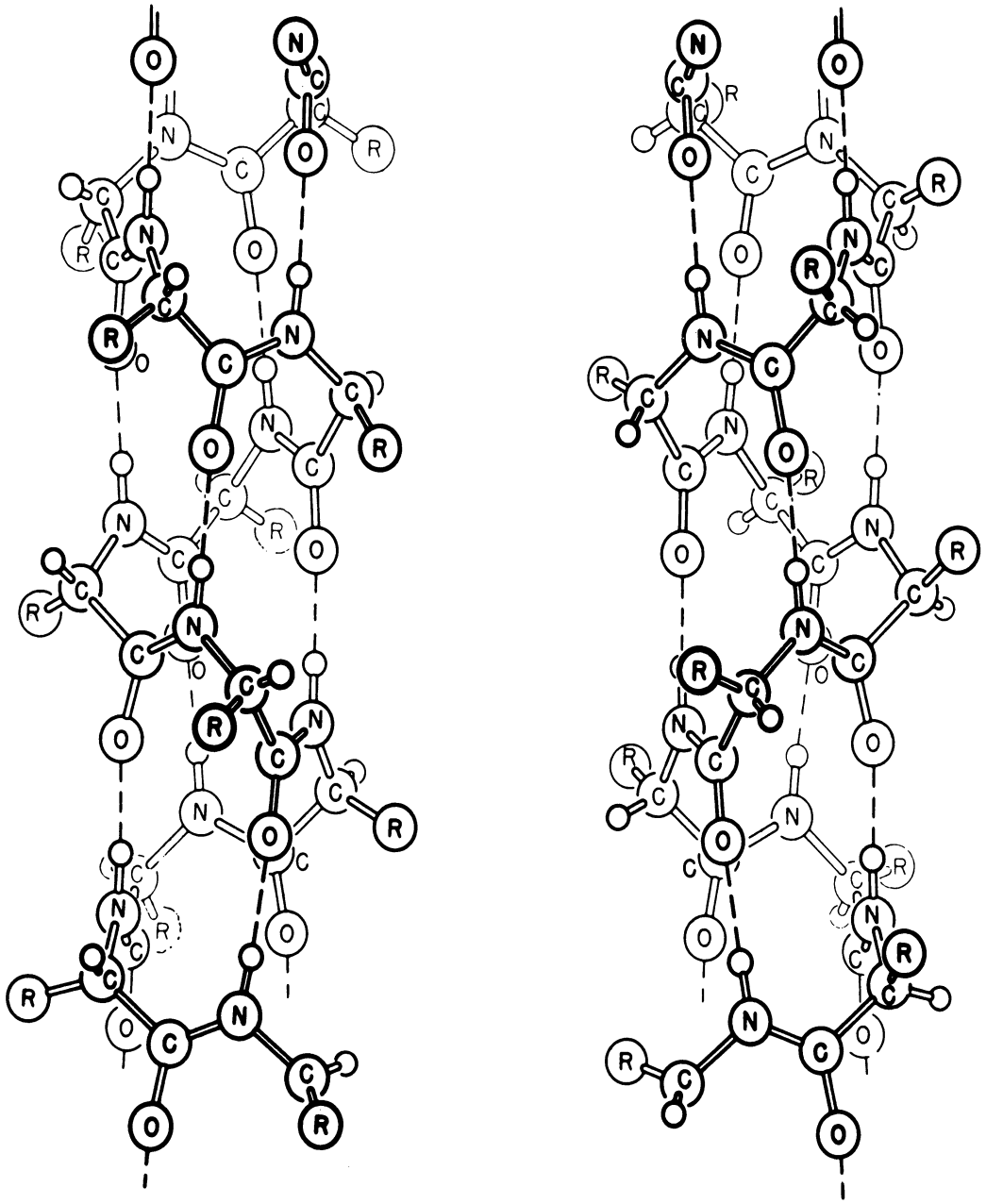

Figure 1-4 Drawings of left-handed and right-handed α-helices[2,25].

configuration would give rise to an α pattern having meridian reflections at both 5.1A and 1.5A. An alternate explanation for the formation of a coiled-coil, according to Pauling,[1] is that local variations of the hydrogen bond lengths along the helix will cause the helical axis to curve. The α-helix also explains the prominent 9.8A equatorial reflection and the density. If adjacent α-helices are packed hexagonally, an interaxial distance of about 10.6A will give a reasonable density of 1.3 grams per cubic centimeter and will give rise to a 9.2A equatorial spacing. The 9.8A equatorial spacing can be shown in well-resolved photographs to be split into two broad reflections, with one at 9.2A as required[2]. Additional evidence indicating the presence of the α-helix in the globular proteins has been obtained from the radial distribution studies of Riley and Arndt[32]. These authors concluded that the α-helix is the predominant chain configuration in the globular proteins.

The essentially different x-ray diffraction pattern of collagen indicates that its structure must be different from that of the α and β proteins. The strong meridional reflection at 2.86A is not observed in either the α or β diffraction patterns. In addition, the chemical composition of collagen is unusual in its high percentage of proline plus hydroxyproline (approximately 22%) and glycine (approximately 33%)[13]. Although the infrared spectrum of collagen exhibits perpendicular dichroism for both the CO and the NH stretching vibrations, the NH stretching frequency of 3330 cm^{-1} is significantly different from the 3300 cm^{-1} found in the α and β proteins[33]. Several sheet-like configurations for the collagen fibril have been proposed but all have one or more serious defects.

Pauling and Corey[33] proposed the first helical configuration for collagen in 1951. Their model, which contained two-thirds cis residues, has been abandoned. The γ-helix was considered by Bear[33] as a possible solution to the problem. This helix, however, would predict parallel dichroism in the infrared, which is the opposite of that observed. Ramachandran and Ambady[34] have shown that a helix containing ten residues in three turns could explain the wide-angle diffraction pattern of collagen. Difficulties arise when the packing of such units is considered, but Ramachandran and Kartha[35] have shown that if an additional twist is given to the chains, whereby a unit of three chains assumes a coiled-coil or approximately coiled-coil configuration, a "satisfactory" structure can be obtained. Crick and Rich[4] have been critical of some of the short van der Waals contacts in the Ramachandran-Kartha structure, but agree that the structure is essentially correct. The ideas of Crick and Rich arose from the work done on poly-L-proline[36] and poly-glycine II[37]. Groups of three chains can be extracted from the poly-glycine II lattice in two ways giving rise to collagen structures I and II. Structure I is stereochemically more satisfactory than structure II and its optical transform appears to be in rough agreement with the observed diffraction pattern. Huggins[38] has recently proposed a different solution to the collagen problem but no coordinates have been presented.

1.3 Review of Previous Work on Feather Keratin

The hard keratin structures of reptiles and birds (feathers, scales, beaks, claws etc.) give rise to x-ray diffraction patterns of the feather keratin type[39]. The reptilian and avian patterns have

most features in common but differ in detail. The patterns of the calamus and rachis of a feather are identical,* and are the subject of the subsequent discussion.

The feather keratin diffraction pattern was investigated as early as 1932 by Astbury and Marwick[40], who found that the quill of a feather gives rise to a well-defined x-ray fiber diagram quite different from that of animal hairs. They interpreted the observed 3.1A meridian reflection as arising from the axial projection of each amino acid residue in a slightly collapsed polypeptide chain. (This reflection is the outermost meridian reflection in Bear's photograph of sea gull quill shown in Figure 1-5.). The sample could be stretched continuously and reversibly by as much as 6% before rupturing, the 3.1A meridian spacing increasing to the approximately 3.3A meridian spacing which is observed in stretched hair. In particular, they noted the strength of 24.8A meridian reflection, and observed that it might arise from a periodicity of 24.8A in the polypeptide chain. The pattern was described as a "rather bewildering elaboration" of the type of photograph which is obtained from natural silk (fibroin) and the stretched form of hair (β-keratin), both of which correspond to polypeptide chains in a more or less fully extended state. The similarity of the side-chain spacings of the feather keratin and the β-keratin diffraction patterns was noted.

Astbury and Lomax[41], as a result of the analogy between the x-ray pattern of feather and the globular protein pepsin, suggested that the structure might arise from the aggregation of corpuscular units.

---

* The calamus or quill is the translucent portion of a feather which extends from the tip of the feather to approximately six centimeters from the tip at which point the rachis begins. The rachis is the distal part of the shaft of a feather which bears the barbs.

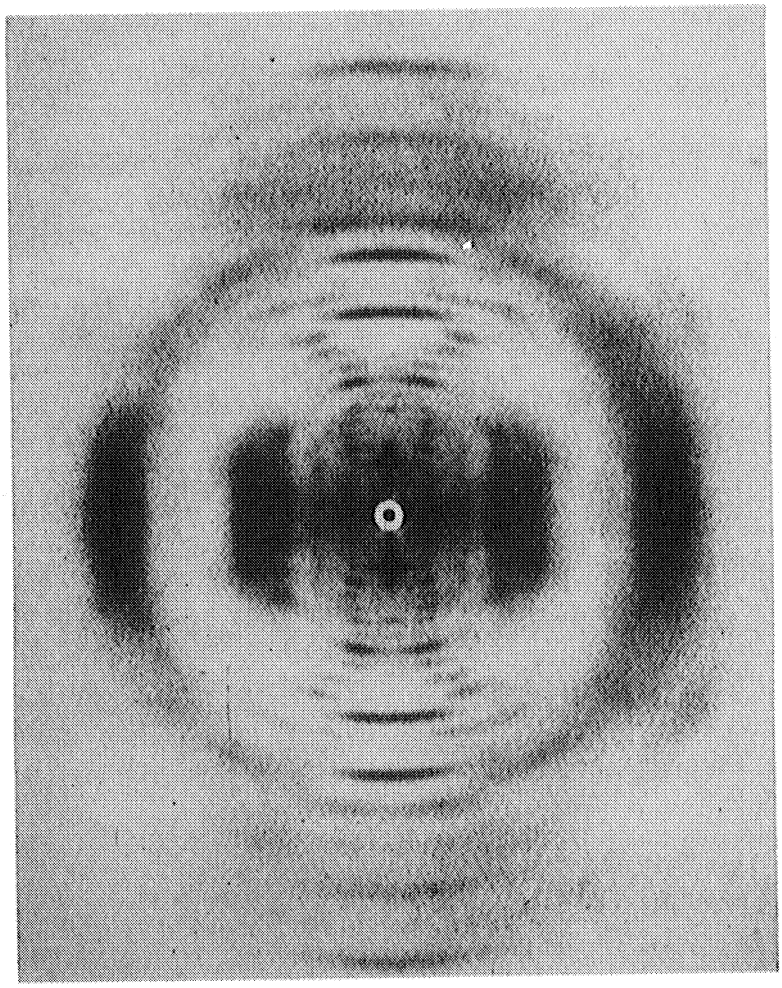

Figure 1-5. X-ray diffraction pattern of sea gull quill. After Bear and Rugo[13,14].

The studies of Corey and Wyckoff[42] demonstrated the presence of large lateral periodicities in the diffraction pattern. These authors concluded that although their data did not exclude the possibility of a protein such as feather keratin or collagen being chain-like in its nature, they could alternatively be considered as molecular crystals built up by the regular arrangement of large molecules. The investigations of Astbury and Bell[43] also showed the presence of a large fiber axis period. Bear,[44] in a comparative study of the diffraction pattern of feather, porcupine quill, and clam muscles, concluded that the meridian spacings of feather were all orders of 95A, and that the wide-angle diffraction pattern was of the β-keratin type. The prominence of the 34A row line was noted. In addition, Bear observed that the first three orders of 95A were very weak and that the long and short spacings "merged into each other". Astbury and co-workers [45] noted the similarity of the feather pattern to the F-actin pattern. The suggestion was made that the feather keratin diffraction pattern gave indications of originating in the end-to-end addition of originally corpuscular units. It was also suggested that the relationship of F-actin to myosin might be analogous to that of feather keratin to α-keratin. Cohen and Hanson[46] have recently obtained a more well-defined fiber diagram of F-actin which shows similarities to the feather pattern.

Bear and Rugo[14] studied the changes in the diffraction pattern of feather produced by heat, moisture and the sorption of small molecules. Throughout the heat-moisture treatment most of the reflections showed changes in intensities, but the very intense 23.6A meridian spacing and the essential features of the wide-angle diffraction pattern were unaltered. Photographs of specimens soaked in water showed that the 33.5A

equatorial reflection weakened to almost zero intensity while the 8.6A equatorial reflection increased somewhat in intensity. An increase in the intensity of the 11.9A meridian reflection was observed on photographs of specimens soaked in mercuric acetate[39]. Throughout Bear's experiments, the fiber axis identity period remained in the relatively narrow range of 94-97A. As a result of the treatment, a "net diagram" developed, which consisted of meridian reflections on the 4th, 8th, and 12th layer lines and off-meridian reflections, at the same R value ($\frac{1}{34}$ A^{-1}), on the 2nd, 6th, 10th, and sometimes 14th layer lines. On the basis of his data, Bear proposed a micelle-type structure for feather keratin with the globular particles arranged around "equivalent nodal points" of the net. The dimensions of the net are 34A in the horizontal or x direction and 95A in the vertical or z direction. With respect to the x, z coordinate axes, the centers of the particles in the unit cell are located at: (0,0), (0,1/2), (1/2,1/4), and (1/2,3/4). The particles are represented schematically as either prolate or oblate ellipsoids. The large spacings in the diffraction pattern were thought to arise from the arrangement of polypeptide chains within the globular particles. No proposal for a detailed structure was presented. It might be noted that due to the net-helix diffraction ambiguity[47] the data could equally well be interpreted on the basis of a helical distribution of sub-units.

In an effort to relate small-angle diffraction phenomena to specific molecular entities, Rougvie[48] studied the physical-chemical properties of solubilized feather keratin and recorded the x-ray diffraction patterns of reconstituted fibers. By employing appropriate solubilization techniques, he obtained a monomer (MW = 9,300 $\pm$ 700) in both the

reduced and oxidized forms and a dimer (MW = 19,300) in the oxidized cysteic-acid form.* The x-ray pattern of the reconstituted keratin showed some of the important features, but lacked much of the detail, of the native keratin. The reconstituted SH-keratin exhibited meridian reflections at 22.1A (strong), 16.1A (very weak), 6.20A (medium weak), 5.40A (weak) and 3.05A (weak). Equatorial reflections were observed at 33.5A, 9.48A, and 4.63A. Since the 33A equatorial reflection was absent on diagrams of reconstituted cysteic acid-keratin, it was concluded that lateral -S-S- linkages were present in the feather structure. The bulkier cysteic acid-side chains presumably prevented the lateral reaggregation in the reduced form. On the basis of the physical chemical measurements, the monomer could be described as a prolate ellipsoid of revolution with a major axis equal to 100A and a minor axis equal to 14.7A, while the dimer had the dimensions 220A and 14.2A respectively. As the monomer was thought to be produced from the dimer by breaking -S-S- bonds, the presence of longitudinal -S-S- bonds was also inferred. Using a molecular weight of 10,000, a mean residue weight of 116, a particle length of 95A, and an axial projection of 3.1A per residue, the conclusion was reached that the feather keratin molecule must be able to accomodate three β - polypeptide chains each of length 95A.

Pauling and Corey[49] attempted to explain the diffraction pattern by a composite model consisting of both α-helices and polar pleated-sheets of extended polypeptide chains. Three layers of protein formed an orthorhombic

---

* -S-S- bonds can be reduced to the -SH form or oxidized to the $-\overset{\overset{O}{\|}}{\underset{\underset{O}{\|}}{S}}-OH$ form.

unit cell of dimensions 95A by 34A by 9.5A. Calculation of the equatorial transform indicated some tentative agreement with the data, but later considerations showed the model to be unsatisfactory, and it has been superseded by a second model of Pauling and Corey consisting of ropes and cables of α-helices arranged in a coiled-coil configuration(1). Kraut(50) calculated the equatorial and near-equatorial diffraction pattern of this 2nd Pauling-Corey model. The agreement between the calculated and the observed intensities was extremely poor. In his work, Kraut obtained a density for feather keratin of 1.28 grams per cubic centimeter. He observed that the powder diagram of feather keratin gave a pattern which was in some respects similar to fibrinogen, an α-protein. In addition, an extremely weak and diffuse halo was found on oscillation photographs at 1.47A. On the basis of these observations, Kraut concluded that feather keratin was to be classified as an α protein. The possibility that the repeating distance was some multiple of 94.5A was noted.

1.4 Plan of the Present Work

At the beginning of the present research the situation with respect to the structure of feather keratin was very unclear. While the α-helix and the pleated-sheet configurations were thought to possess great generality, the Pauling-Corey model involving both α-helices and pleated-sheets remained to be proven correct. Even the classification of feather keratin as an α or a β protein was not certain. Although feather keratin has usually been classified as a β protein, the difficulty remains that the diffraction pattern does not contain a meridian reflection

at 1.1A, a characteristic of the diffraction patterns of silk and β-keratin[13]. Pauling and Corey have claimed that feather does give the 1.5A meridian spacing, but other investigators have failed to detect this key spacing

The considerations of the previous sections indicate four broad hypotheses for the structure of feather keratin:* 1) the wide-angle diffraction pattern is of the β type, but the low-angle diffraction pattern gives evidence for the existence of large micelle-type units (Bear-Rugo) 2) the structure is truly fibrous and both the wide-angle and the low-angle diffraction patterns are explainable on the basis of a combination of α-helices and pleated-sheets (Pauling-Corey model 1) 3) the structure consists entirely of coiled-coil configurations of α-helices (Pauling-Corey model 2) 4) the feather keratin structure is based on a configuration other than those that have been previously proposed.

As a result of a re-evaluation of the available x-ray, chemical, and infrared data, the validity of the second and third hypotheses seemed open to question. In particular, the x-ray diffraction patterns obtained in the present studies failed to indicate either the 1.5A meridional spacing or the 5.1A meridional spacing (or 5.4A layer-line spacing), which would be predicted on the basis of a model containing an appreciable proportion of the α-helical configuration. Further x-ray studies and the accumulation of additional chemical and infrared data also indicated

---

* The possibility of a similar molecular configuration for feather keratin and collagen was not originally considered. A recent paper by Ramachandran[51] suggests that both the structures of feather keratin and collagen are based on a cylindrical lattice. It will therefore be pertinent to discuss later the point of view that feather keratin and collagen possess similar configurations of the polypeptide chains.

that the α-helical configuration does not represent an appreciable component of the feather keratin structure.

While the data appeared to be consistent with the conclusion of Bear-Rugo that the feather keratin structure was based on extended or β-polypeptide chains, certain unique features of the x-ray diffraction pattern were not easily interpretable on the basis of the usual β models. A detailed analysis of the difficulties has led to the introduction of additional structural hypotheses. On the basis of these hypotheses, a new model for the feather keratin structure has been formulated. Predictions based on this model have been compared with the available data on feather keratin as a mean of testing the validity of the proposed structure.

CHAPTER II

X-RAY DATA

2.1 Introductory Remarks

In order to check and extend the available x-ray data on feather keratin, additional x-ray studies have been carried out: 1) studies were undertaken to determine the general characteristics of the diffraction pattern 2) the spacings in the diffraction pattern were determined 3) preliminary studies were made of the alterations in the diffraction pattern produced by physical and chemical treatment of the sample 4) the cylindrical Patterson function, which represents the weighted two-dimensional interatomic vector density distribution, was computed from the experimentally determined intensities. The results of these studies have proved helpful in formulating new structural hypotheses and ideas relevant to the feather keratin structure.

2.2 Experimental Techniques

A Norelco X-ray Diffraction Unit having a copper-target tube was used in the present work. All photographs were taken with the plate-voltage set at 30 kilovolts and the plate-current set at 20 milliamperes. A fairly monochromatic beam whose main intensity was confined to the $CuK_{\alpha 1}$ and $CuK_{\alpha 2}$ doublet (mean wave-length 1.542A) was obtained by using a nickel foil approximately 0.0007" thick as a filter. The beam was confined by a 0.25 mm collimator when it was desired to improve the resolution for a given photograph and by a 0.50 mm collimator when a shorter exposure time was the main factor. Specimens of turkey quill approximately

0.50 mm thick and 1 mm in length proved satisfactory. The specimens could be mounted in any desired position with respect to the beam by means of a Unicam Single Crystal Goniometer. Specimen-to-film distances of from 3 cm to 11.56 cm were employed and the diffraction pattern was recorded photographically. In such cases, the exposure times varied between 2 and 30 hours. In order to avoid the intense air-scattering at low angles, patterns were recorded with the camera mounted in a vacuum tank. In these instances, (specimen-to-film distance 11.56 cm) exposure times were of the order of 100-250 hours. In order to record very short spacings, the specimen was oscillated in the x-ray beam. Tipping experiments were performed for the purpose of determining whether a given reflection was on the meridian of reciprocal space.

2.3 Preliminary X-Ray Studies

Some preliminary x-ray studies were undertaken in an attempt to determine the general characteristics of the feather keratin diffraction pattern.

In order to determine which specimens exhibit the most crystalline and highly-oriented patterns, photographs of sea gull quill, turkey quill, and feathers from the birds king vulture, macaw and cockatoo were obtained. It was determined that sea gull quill and turkey quill give the most highly oriented and crystalline diffraction patterns.

In an attempt to determine whether the feather pattern is characteristic of all of the feather, photographs were taken from the tip of the quill up to a distance of 1.6 cm at 2 mm intervals. The pattern at the tip is disordered, having spacings 9.8A (medium intensity,

diffuse), 5.04A (medium), and 4.10A (medium). These spacings are not equal to any found in the normal feather pattern.* The 4.10A spacing corresponds to the most intense spacing in paraffins, and is probably caused by waxes in the tip of the feather. At 2 mm from the tip there is an almost fully developed feather pattern whose orientation is at right angles to the orientation found in the normal pattern. At 4 mm from the tip both orientations are present. At 6 mm or greater, the normal feather pattern is obtained. The orientation of the pattern improves with increasing distance from the tip. The diagram of feather rachis is the same as that of the quill. The barbs give a disordered pattern, indicating the existence of disordered material. There are sharp powder rings at 4.26A and 3.82A, possibly due to grease. The outlines of a feather pattern are barely observable.

In an attempt to determine if the calamus is homogeneous on a macroscopic level, x-ray patterns were taken of sections of the quill representing the outer, middle, and inner thirds of the thickness. As the differences between these photographs were small, feather may be presumed to be macroscopically homogeneous.

An examination was also made of the degree of orientation of the crystalline regions, in order to determine if any preferred orientation around the fiber axis existed. With the fiber axis vertical, the meridian and equatorial spacings are the same whether a photograph is taken with the beam perpendicular to the surface of the feather or parallel to the surface. In the view parallel to the surface, however, the

---

* The normal feather pattern is defined as the pattern obtained at distances of 6 mm or greater beyond the tip.

meridian arcs show a smaller angular spread than in the view perpendicular to the surface. In addition, the 11.2A and 8.6A equatorial reflections are much better resolved when the beam is parallel to the surface. Random orientation of the crystallites around the fiber axis was shown by a photograph taken with the beam parallel to the quill axis. The intensity around the rings, as estimated visually, is constant. The spacings are: 33.4A, 16.4A, 11.2A, 8.85A, 5.85A, 4.68A, and 3.37A, which correspond fairly well to the equatorial spacings obtained on the fiber diagram of feather.

If a higher degree of orientation could be introduced into the sample, i.e., uniquely orienting a given plane in addition to the fiber axis, a less ambiguous indexing of the reflections could be obtained. The technique of producing double-orientation by rolling the sample has been successfully applied in the case of silk fibroin, resulting in a significant simplification in the determination of its structure[17]. In the present case, attempts were made to press or roll the quill after it had been soaked in cool or hot water (rolling a dry specimen results in its breaking up). The resulting diffraction patterns showed diffuse spots and indicated disorientation. Although these preliminary results indicate that the feather structure is fairly rigid, the possibility that other methods will be found which will be successful in producing double-orientation should not be overlooked.

2.4 Spacings in the Feather Keratin Diffraction Pattern

The x-ray diffraction pattern of turkey calamus is shown in Figure 2-1; Figure 2-2 shows a reciprocal lattice diagram corresponding

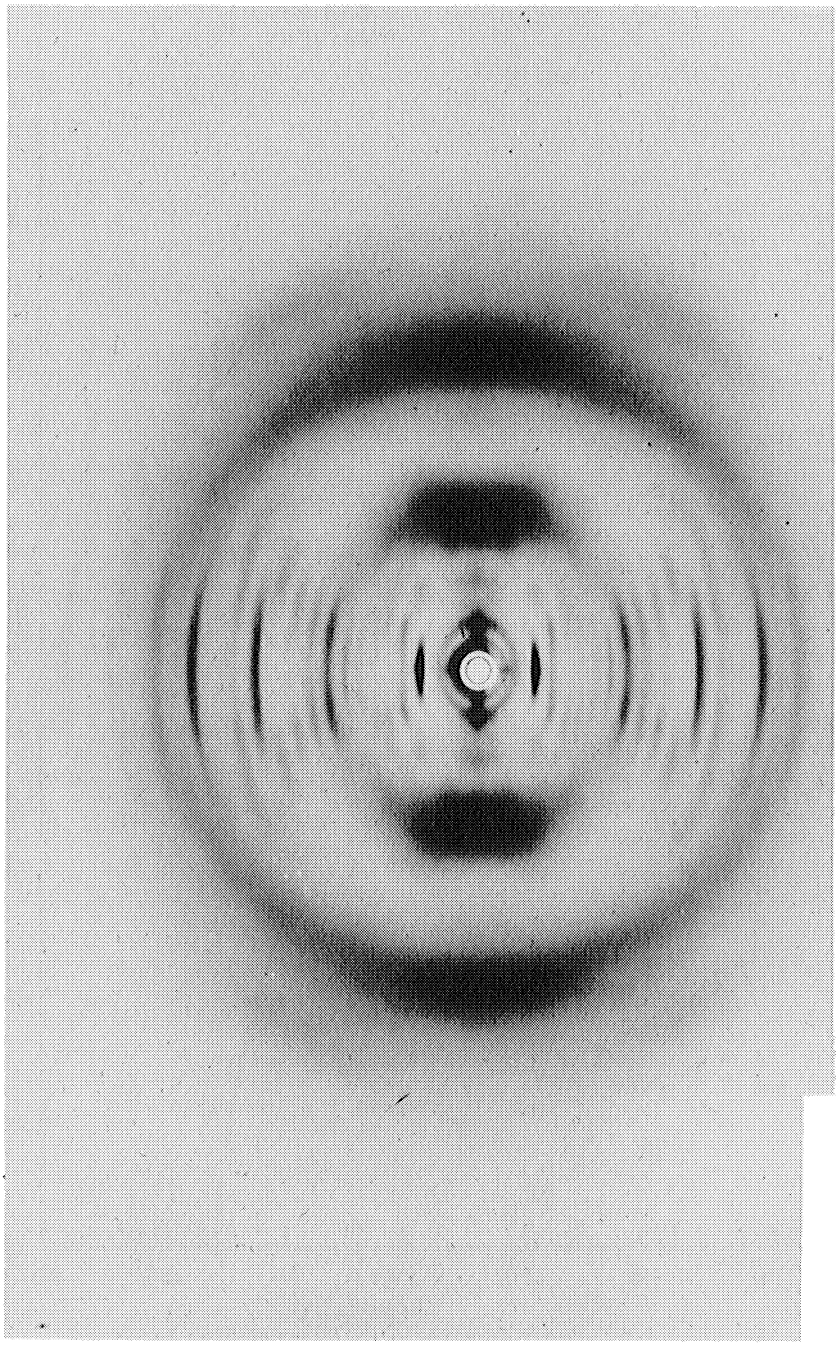

Figure 2-1. X-ray diffraction pattern of turkey calamus. CuK_{α} radiation, 11.56 cm half-cylindrical camera, taken in vacuum, beam parallel to surface, 250 hour exposure.

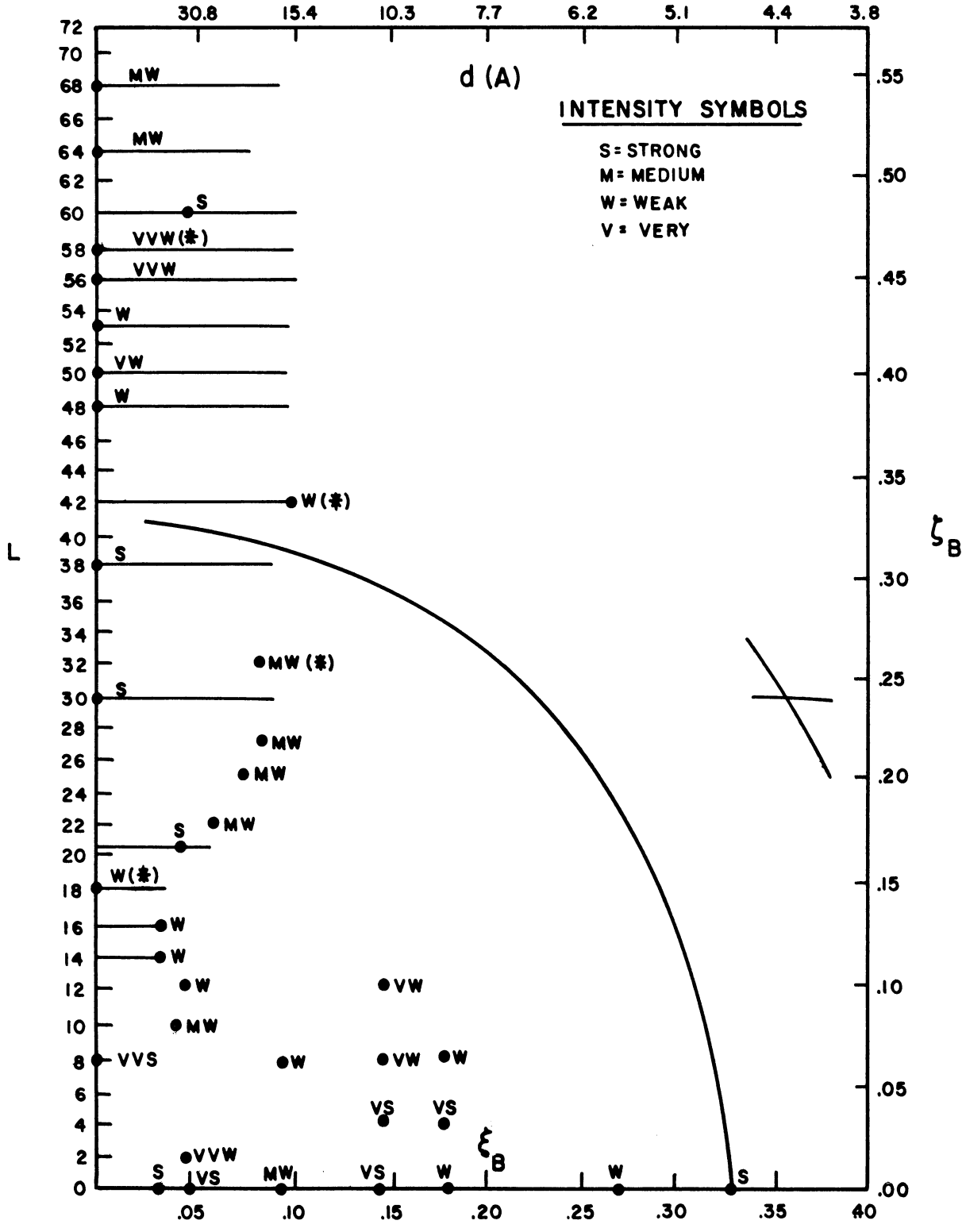

Figure 2-2 Reciprocal lattice representation of the diffraction pattern of turkey calamus. The horizontal lines indicate the approximate lateral extent of the reflections in reciprocal space. The circles indicate the maxima of the intensities of the reflections. A question mark denotes above average uncertainty in the estimation of the position of the maxima.

to the pattern. Tables II-I and II-II list the meridian and equatorial spacings of turkey calamus. The meridian spacings for sea gull quill are the same as for turkey but the equatorial spacings are about 3% larger. The main difference between the patterns of sea gull quill and turkey quill is that the former has a sharply developed row-line at about $R = 0.03A^{-1}$ while the latter does not exhibit a well-defined row line at this R value. With the exception of the diffuse equatorial spacing at approximately 4.67A, the equatorial spacings of the diffraction pattern obtained from a sample of carefully dried turkey calamus are consistently smaller than the corresponding spacings of the diffraction pattern obtained from a sample at room humidity.

The strong 5.1A meridian spacing which is characteristic of the α proteins is not present in the feather keratin diffraction pattern. In order to observe a truly meridional reflection (at a large Bragg angle) in a highly oriented fiber, it is necessary to oscillate the sample through an appropriate angular range around the Bragg angle. The strong 1.5A meridian reflection which could indicate the presence of α-helices, did not appear on the oscillation photographs designed to detect it. A possible weak reflection was observed at 1.49A but its intensity was orders of magnitude weaker than the corresponding reflection for the α-keratins. Oscillation photographs were also taken which would have detected reflections down to 0.92A. The reflection in the 1A meridian region which is characteristic of the β-keratins was not detected.[13]

In view of the diffuse nature of the pattern, the spacings obtained in the present work are in good agreement with those obtained by other investigators. We have, however, made some new experimental

TABLE II-I*

Meridian and Layer-Line Spacings in the Feather Keratin Diffraction Pattern									
This Study					Kraut (50)	Rudall (39)	Bear (44)	Corey & Wyckoff (42)	Astbury & Bell (43)
Spacings (A)		Int.	l	c_o					
M	L								
	95.1	vvw	2	190.2					
	49.5	vs	4	198.1	50.7		47.6		47
23.6_4		vvs	8	189.0	23.7	23.6	23.7	21.3	23.4
	18.6	mw	10	186.0	19.3		18.9		
	15.9	w	12	190.8			15.5		
	13.5	w	14	189.0			13.7		
	11.7_5	w	16	188.0	11.9	11.9	11.9		
10.4		w(?)	18	187.2	10.4	10.4_5	10.5		10.4
	9.38	s	20	187.7			9.52	9.08	9.1
	8.51	mw	22	187.2			8.61		
	7.60	mw	25	190.0	7.94		7.83		
	7.09	mw	27	191.3			7.24		
6.30		s	30	189.0	6.26	6.30	6.32	6.20	6.26
	5.89	mw	32	188.5	5.54	5.53	5.55		
4.97		s	38	189.0	4.96	4.98	4.99	4.90	4.93
	4.47	w	42	188.0	4.45	4.45	4.46	4.37	4.42
3.94		w	48	189.1	3.99			3.95	
3.80		vw	50	190.0	3.80				
3.57		w	53	189.2	3.57	3.54		3.52	3.54
3.37		vvw	56	188.9	3.40				
3.25		vvw	58	188.7	3.25	3.29		3.22	3.29
	3.15	s	60	189.2	3.09	3.08		3.07	3.08
2.96		mw	64	189.5	2.97	2.94			2.94
2.77		mw	68	188.3	2.75	2.74			2.74
					2.56				
2.39		vw	79	189.0	2.34				
2.25		vw	84	189.1					
2.10		vw	90	189.0	2.13				
					2.04				

* Intensity symbols are: s = strong, m = medium, w = weak, and v = very.

TABLE II-II*

Equatorial Spacings in the Feather Keratin Diffraction Pattern							
This Study				Kraut[50]	Rudall[39]	Corey & Wyckoff[42]	Astbury & Bell[43]
Spacings (A) room humidity	Int.	Spacings (A) dried in vacuum	Int.				
						115	115
						81.8	81.8
49.5	s	48.8	s	55		51	51
32.6	vs	31.2	vs	33.5	34	33.3	33.3
16.6	w	16.1	mw	17.3	17.6	17.1	17.6
11.2	mw	10.6	vs	11.2	11.3	11.0	11.3
~8.71	w(?)	~8.5	w(?)	8.84	8.8	8.56	8.8
~5.88	w	~5.7	w	5.82	5.8		5.8
				4.90			
~4.66 (diffuse)	s	~4.68 (diffuse) 4.35 (?)	s w	4.50	4.50	4.68	4.50
				3.90			
3.38	w			3.50			
				3.25			
				2.28			

* All patterns have been taken at room humidity unless otherwise indicated.

observations. While it had previously been concluded that the fiber axis identity period was 95A, the present studies show that the minimum possible identity period is about 190A. The 7.60, 7.09, 3.57, and 2.39A reflections would have close to half-integral layer line indices on the basis of the 94.5A repeat. The true repeat must therefore be some even multiple of 94.5A. The possibility of the repeat being some multiple of 95A was noted by Kraut[50]. The average c_o determined from Table II-I is 189A, in agreement, it might be noted, with that obtainable from the most accurately measureable meridian spots, those at 23.6$_4$, 6.30, and 4.97A.

It had previously been thought that 3.07-3.09A "meridian reflection" was to be indexed as the 31st order of an approximately 95A repeat [39,42,43,50]. It has been found in the present work, however, that the true maximum for the intensity of this reflection is not on the meridian. Figure 2-3 shows the diffraction pattern obtained from a specimen which had been tilted into the direction of the beam. The tilt angle chosen was appropriate to determine whether the 3.07A reflection was meridional.* It is possible to observe a definite thinning and weakening of this arc as the meridian is approached. The layer-line spacing for this reflection is 3.15A. The reflection must therefore be indexed as the 60th order of the 189A identity period. The true meridian arc at 2.96A is weaker in intensity and is to be indexed as the 64th order of the 189A identity period.

---

* In order to determine whether a given reflection is on the meridian it is necessary to take a photograph of a sample which has been tilted away from the vertical by an angle equal to the Bragg angle for the reflection.

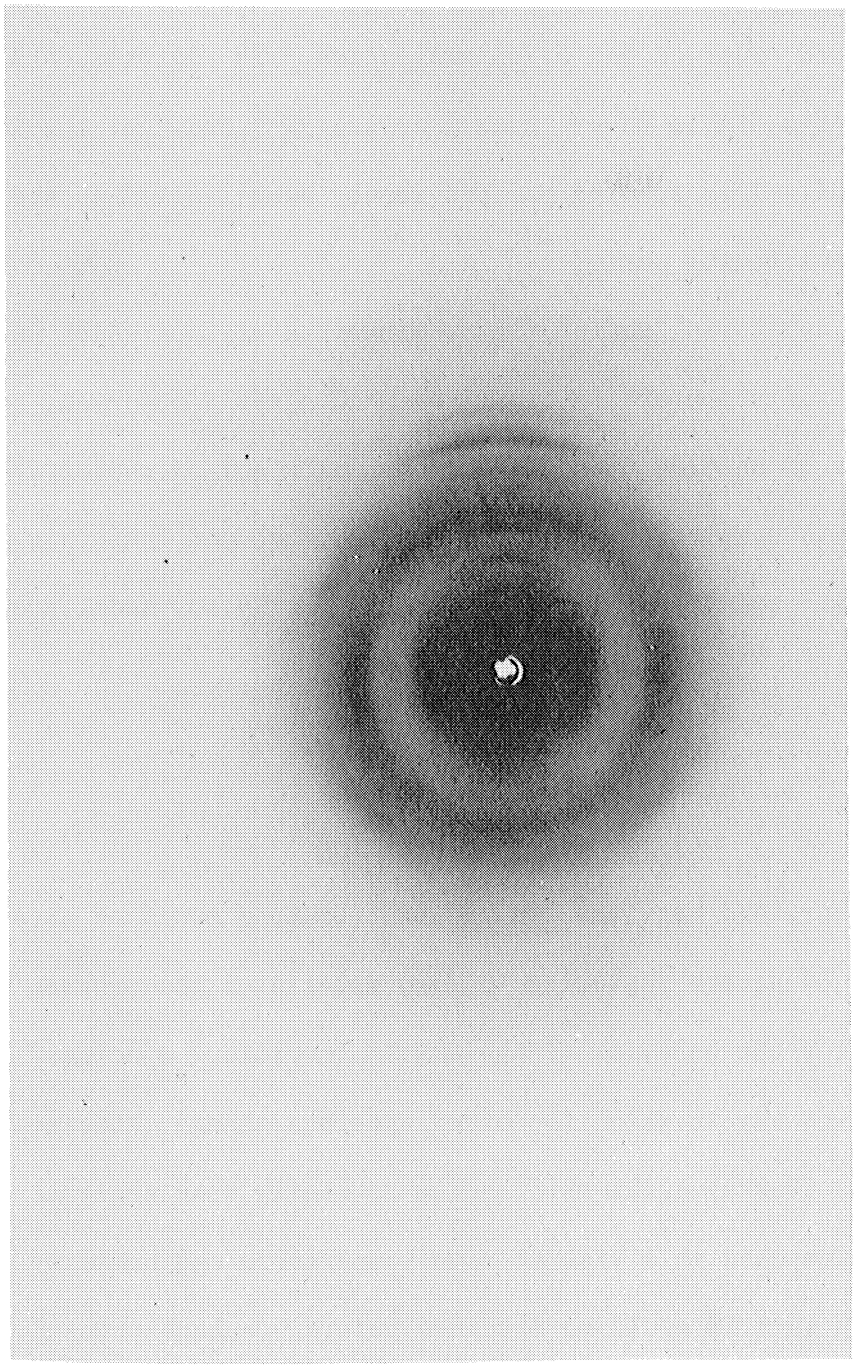

Figure 2-3. X-ray diffraction pattern of "tilted sample" of turkey calamus. CuK_{α} radiation, 5.69 cm half-cylindrical camera, sample tilted at 15° to the vertical.

Only a few reflections are odd orders of the new identity period, none of them being very intense. Therefore, 94.6A is a pseudo-identity period. With the new indexing, the 3.15A reflection becomes exactly a second order of the 6.30A reflection. In addition, the layer-line spacing at 5.89A is to be indexed as the 32nd order of the 189A identity period. This spacing had previously been indexed as the 17th order of a 95A identity period.[49]

The equatorial reflection at approximately 50A which Bear attributed to radiation artifacts[44] has been clearly observed, both on photographs of samples taken at room humidity and on photographs of thoroughly dried samples. We have therefore concluded that this reflection is real, and its existence must be accounted for by any model proposed for feather keratin.

2.5 Alterations in the Diffraction Pattern

Effects of Stretching

Astbury and Marwick[40] noted that feather could be stretched approximately 6% before rupturing, but no details of the process were given except for the behavior of the ~ 3.1A "meridian" spacing. In order to determine the way in which the other spacings change, specimens of turkey calamus (turkey quill stretches more easily than sea gull quill) were slowly stretched in a vise at room temperature and humidity. Extensions of up to 5.5% could be obtained before breakage occured. Table II-III shows the resulting changes of some of the prominent meridian spacings for a sample which was stretched approximately 5.5%. Figure 2-4 shows comparison photographs of the stretched sample and the unstretched sample. The percentage elongations for the spacings were all close to 5%. The most reasonable interpretation is that, within experimental

TABLE II-III*

Changes in Meridian Spacings in Feather Quill on Stretching 5.5%, 10 cm Photograph

d_o	d_s	% elongation
3.15A	3.30A	4.9 ± .7 (5cm photograph)
4.98	5.22	4.8 ± .4
6.30	6.62	5.1 ± .3
23.6	24.75	4.9 ± .4

* The 23.6A spacing could be measured to an accuracy of 0.1A while the maximum accuracy obtainable for the other specings was approximately 0.01A. The 3.15A spacing is, strictly speaking, a layer-line spacing.

X-ray diffraction pattern of turkey calamus, CuK_α radiation, "10 cm" flat plate camera, sample unstretched.

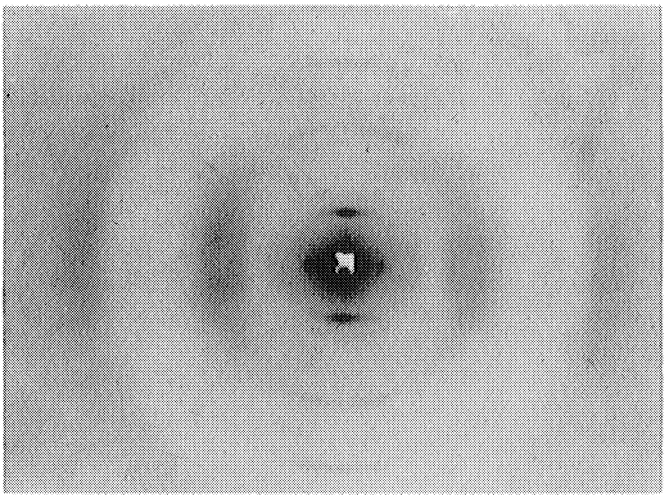

X-ray diffraction pattern of turkey calamus, "10 cm" flat plate camera, sample stretched approximately 5.5%.

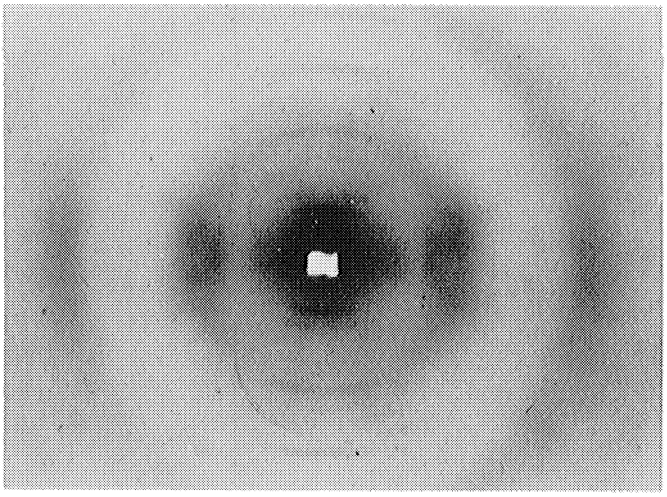

Figure 2-4. Comparison photographs of the diffraction patterns obtained from stretched and unstretched samples of turkey calamus.

error, the spacings all changed by the same percentage. No changes in the equatorial spacings were observed. These would have been detected if they were greater than 1%. The relative intensities of corresponding reflections in the stretched and unstretched patterns (judged visually) were identical. It is concluded that any proposed model for feather keratin should be able to account for the following facts: 1) the sample ruptures after being stretched approximately 5% 2) all of the fiber axis spacings change by the same percentage when the sample is stretched 5% 3) the relative intensities of corresponding reflections in the stretched and unstretched patterns are the same 4) the equatorial spacings of the stretched and unstretched patterns are the same.

Effects of Water and Chemical Reagents

The diffraction pattern of feather keratin can be altered as a result of soaking the sample in water or by treating the sample with chemical reagents prior to taking x-ray photographs. The changes in the positions and intensities of the reflections which are sensitive to such treatment provide additional information relative to the structure. Any proposed model for feather keratin must be able to explain these changes.

As has previously been observed, the diffraction pattern of a sample of turkey calamus taken at room humidity differs from the diffraction pattern of a thoroughly dried sample. The equatorial spacings of the pattern obtained from the dried sample are in general a few percent lower than the corresponding spacings obtained from a sample at room humidity. Examination of the photographs of sea gull quill taken by Bear and Rugo[14] shows that the diffraction pattern of a sample

taken at room humidity has equatorial spacings which are a few percent smaller than the corresponding spacings of the diffraction pattern obtained from a water-soaked sample. It is concluded that the feather keratin structure is capable of expanding at least a few percent in the lateral direction as a result of swelling in water.

The change in the intensity of the 32.6A equatorial reflection produced by soaking a specimen in water is striking.* Figure 2-5 shows photographs of the feather pattern obtained from a sample at room humidity and of the pattern obtained from a water-soaked sample. In the photographs taken at room humidity the approximately 32.6A equatorial reflection is very intense, but the intensity of this reflection is practically zero in the diffraction pattern obtained from the water-soaked sample. This effect, checked in the present work, was first noted by Bear and Rugo[14]. Upon drying the specimen, the intensity of the 32.6A equatorial reflection returns to normal. This remarkable intensity change must be accounted for by any proposed structure.

Samples of feather keratin have also been soaked in chemical reagents in the hope of breaking or weakening the -S-S- linkages or the hydrogen bonds. Photographs of specimens soaked in $NaHSO_3$ in the hope of breaking and/or weakening -S-S- linkages did not indicate any significant changes in the pattern other than that produced by water alone. A specimen soaked in 10M urea, a reagent which presumably disrupts hydrogen bonds, showed changes in its diffraction pattern comparable to the changes produced by soaking the specimen in water.

---

* The intensities of the other equatorial reflections do not change markedly upon soaking the specimen in water.

X-ray diffraction pattern of turkey calamus, CuK_α radiation, "10 cm" flat camera, room humidity.

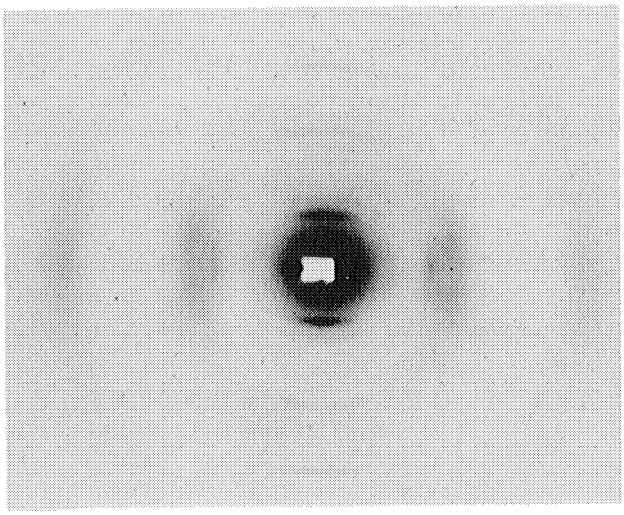

X-ray diffraction pattern of turkey calamus, CuK_α radiation, "10 cm" flat plate camera, sample in capillary filled with distilled water.

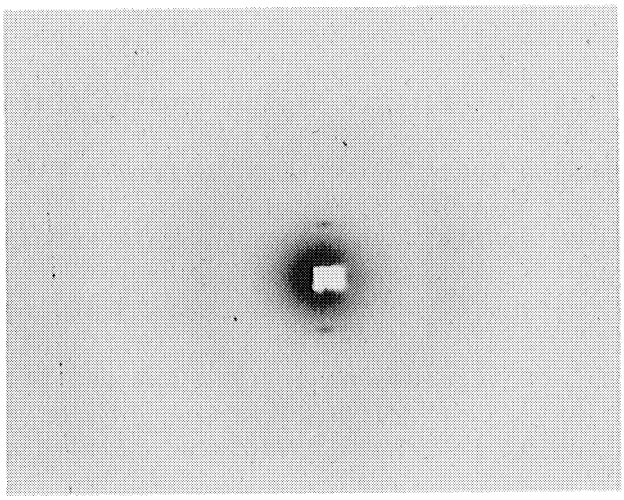

Figure 2-5. Comparison photographs of the x-ray diffraction pattern obtained from samples of turkey calamus at room humidity and from water-soaked samples.

Two attempts were made to introduce heavy atoms into the feather keratin structure. Rudall noted an increase in the intensity of the 11.9A meridian spacing on photographs of specimens which had been soaked in mercuric acetate[39]. The x-ray photographs obtained from specimens soaked in mercuric acetate, in the present work, failed to indicate any increase in the intensity of the 11.9A meridional reflection. The reason for the discrepancy is not known. A sample of turkey calamus was also soaked for eight days in a uraninum dye which had been used to insert a heavy atom into ribonuclease. No observable changes in the diffraction pattern were noted.

It should be emphasized that much more chemical work on feather keratin is needed. The effect of varying the pH, temperature, humidity etc. and of employing other chemical reagents in addition to those mentioned above requires more detailed investigation.

2.6 Cylindrical Patterson Function

Experimental Methods and Computational Techniques

The cylindrical Patterson function $P(r,z)$, which represents the weighted two-dimensional interatomic vector density distribution, contains all the information which is obtainable from a fiber diagram without the introduction of special assumptions. This information, although necessarily limited, serves a two-fold purpose: 1) it indicates what general types of chain configurations are present and provides information about the outstanding interatomic vectors 2) it can be used as a check on a proposed model. $P(r,z)$ is given by the intensity transform of a fiber diagram. Based on the assumption of periodicity of the chains

in the fiber axis direction and random orientation around the axis, MacGillavry and Bruins[52] derived the following relations for the Patterson function:

$$P(r,z) = \sum_{\ell} A_{\ell}(r) \cos\left(\frac{2\pi \ell z}{c}\right) \qquad (2\text{-}1)$$

$$A_{\ell}(r) = K \int_{0}^{\infty} H(\ell,\xi)\, J_0\,(2\pi\xi r)\, \xi d\xi \qquad (2\text{-}2)$$

where r represents the radial distance of a point from the fiber axis, c the fiber axis identity period, ξ the coordinate in reciprocal space perpendicular to the fiber axis, $H(\ell,\xi)$ the intensity distribution in reciprocal space on the ℓth layer line, $J_0(2\pi\xi r)$, the zero order Bessel function of the first kind, and K a constant of proportionality. Vineyard[53] has subsequently generalized these relations to include the case in which the chains are not assumed to be periodic along the fiber axis direction. Since feather keratin has a periodicity along the fiber axis direction, the simpler treatment of MacGillavry and Bruins has been followed.

Two photographs of feather keratin were obtained on which the appropriate intensity measurements were made. The 11.56 cm half-cylindrical camera was employed to increase the accuracy of measuring the Bernal coordinates. The intense air scattering at low angles was eliminated by enclosing the camera in an especially constructed chamber which was evacuated prior to taking the x-ray photographs. The samples of turkey quill (approximately 0.5 mm in thickness) were mounted with the fiber axis vertical and perpendicular to the beam, and with the beam parallel to the surface of the quill. Since the 0.25 mm collimator was

employed, in order to increase the resolution in the photographs, the relatively long exposure times of 100 and 250 hours respectively were necessitated. Two films (one placed in back of the other) were used for each exposure in order to be able to measure the intensity of both the weakest and the strongest reflections in the pattern. In the region of optical densities from 0.25 to 1.00, the film (No-Screen Medical X-Ray Film) obeys the reciprocity law[54], i.e., intensity x time is a constant. The average deviation from linearity in the range of optical densities between 0.25 and 1.50 is about 6%, in the range between 0.25 and 1.75 about 9%, and in the range between 0.25 and 2.00 about 13%. Developing and fixing were performed at room temperature employing Kodak Liquid X-Ray Developer and Kodak Liquid X-Ray Fixer.

The intensity distribution along the layer lines was measured by means of a Knorr Albers Recording Microphotometer. We have employed the previously accepted fiber axis identity period and indexing. Based on 94.5A for the fiber axis identity period, the following indices were assigned to the observed layer lines: 0,2,4,5,6,7,8,9,10,11,12.5,13,5, 15,16,19,21,24,27,31 (if both the indices and the repeat are doubled to eliminate the half-integral assignments, the Patterson function remains unchanged). Microphotometer traces were taken along all the layer lines with the exception of the 31st whose intensity was not recorded on these photographs. The intensity on the 31st layer line is confined to regions very close to the meridian of reciprocal space and was estimated visually from other photographs. Layer lines higher than the 31st were excluded because the spots which are confined to small ξ

values,* are very weak and would not be expected to contribute significantly to the Patterson function. It was found in practice that the first film of the photograph exposed for 100 hours was sufficient to make all the required measurements, but for completeness an additional set of measurements were taken on the 1st film of the photograph that had received the 250 hour exposure. The Bernal coordinates of the reflections were obtained from the appropriate distances on the microphotometer traces according to the formula given in Bunn(55). The plate speed of the microphotometer was quoted as 10 mm/minute and the paper speed as 2"/minute yielding a ratio for $\frac{\text{paper speed}}{\text{plate speed}}$ of approximately 5.08/1. The actual ratio employed was 5.23/1 based on a calibration of the equatorial reflections of a single crystal of hexamethylene diproprionamide. The discrepancy was rectified by measuring the paper speed as 2.06 $\pm$ .01 inches per minute. The densitometer slits were masked so that the length of the slit in the vertical direction was comparable to the breadth of the layer lines. Background was estimated by drawing a "smooth line" through the minima of the peaks in such a way that the background was zero for large ξ values. The correction for the "Lorentz factor" (a purely geometrical factor and not a velocity factor as in the case of single crystals) was computed as less than 5% and was neglected. No effort was made to correct for the non-linearity in the response of the film or for the polarization factor, as these corrections also are small compared to the corrections employed to take into account the unknown temperature factor and the unknown amount of amorphous scattering in the 4.66A region. For CuK_α with $\lambda = 1.542$, the

* From equation (2-2), it is evident that the value $\xi H_\ell(\xi)$ is the effective factor determining $A_\ell(r)$.

average value of the polarization factor, $(\frac{1 + \cos^2 2\theta}{2})$ is approximately 0.90. Yakel[56] used a temperature factor of $e^{-1.5R^2}$ for collagen which exhibits a "highly disoriented" x-ray diffraction pattern. Bunn and Garner[57] have employed a temperature factor of $e^{-1.25R^2}$ for the "highly oriented" nylon pattern. As the feather keratin pattern exhibits an intermediate degree of orientation, we have employed a temperature factor of $e^{-7.5R^2}$.

An inspection of the x-ray pattern of feather keratin indicates that there is a considerable component of amorphous material in the feather keratin structure. Parker's[58] dichroic infrared measurements, which showed an increase in the dichroism of the N-H stretching band from about 1.8/1 to 4.8/1 upon deuteration (presumably preferentially of the amorphous material), also indicate a large component of amorphous material in the feather structure. In order to make an effort at evaluating the large uncertainties in the corrected intensities, five different Patterson functions were computed. Patterson_1 was based on the uncorrected relative intensities multiplied by $e^{+7.5R^2}$, i.e, the inverse of the temperature factor. Patterson_2 is identical with Patterson_1 except that the 4.66A reflection* was cut down by a factor of 1/2 on the equatorial layer line and was diminished monotonically until it was zero at about the ninth layer line. In Patterson_3, the 4.66A reflection was cut down to 1/4 of its value on the equatorial layer line and was diminished monotonically until it was zero at about the eighth

* A large part of the intensity in the ring of scattering in the 4.66A region arises from the contribution of amorphous material. In fact, the intensity in this ring, for layer lines higher than the 8th or 9th, is probably due entirely to amorphous scattering.

layer line. In Patterson_4, the same intensities were used as in Patterson_3 but no temperature factor was applied. In Patterson_5 the same intensities were used as in Patterson_3 but a correction factor of $e^{-8.35R^2}$ was applied in order to avoid series termination errors[59].

The numerical calculations were performed on MIDAC (Michigan Digital Automatic Computer). The function P(r,z) was evaluated in the range 0-34A for r and 0-28A for z. The grid interval for both r and z was 1A. For completeness, one function was calculated up to r values of 34A and z values of 95A. The calculations were checked on a desk calculator.

The One-Dimensional Patterson Projection P(r)

As a preliminary to the calculation of the cylindrical Patterson function, the one-dimensional Patterson projection P(r) was computed. This function gives the density of interatomic vectors whose radial component is r. Since P(r) represents the projection of P(r,z) on a plane perpendicular to the fiber axis, it is obtainable by integrating P(r,z) over the interval from z = 0 to z = P where P is the fiber axis identity period. The result is:

$$P(r) = \int_0^P \sum A_\ell(r)\cos\left(\frac{2\pi \ell z}{P}\right) dz = PA_0(r) = \int_0^\infty H(0,\xi)J_0(2\pi\xi r)\xi d\xi \qquad (2\text{-}3)$$

Figure 2-6 and 2-7 show curves of the optical density above background versus the Bernal coordinate ξ for the equatorial layer line. The data were obtained from measurements made on the 100 hour exposure photograph of feather keratin and the 250 hour exposure photograph respectively. The optical densities were multiplied by $e^{7.5R^2}$ (the inverse of the assumed temperature factor) and the curves for P(r) shown

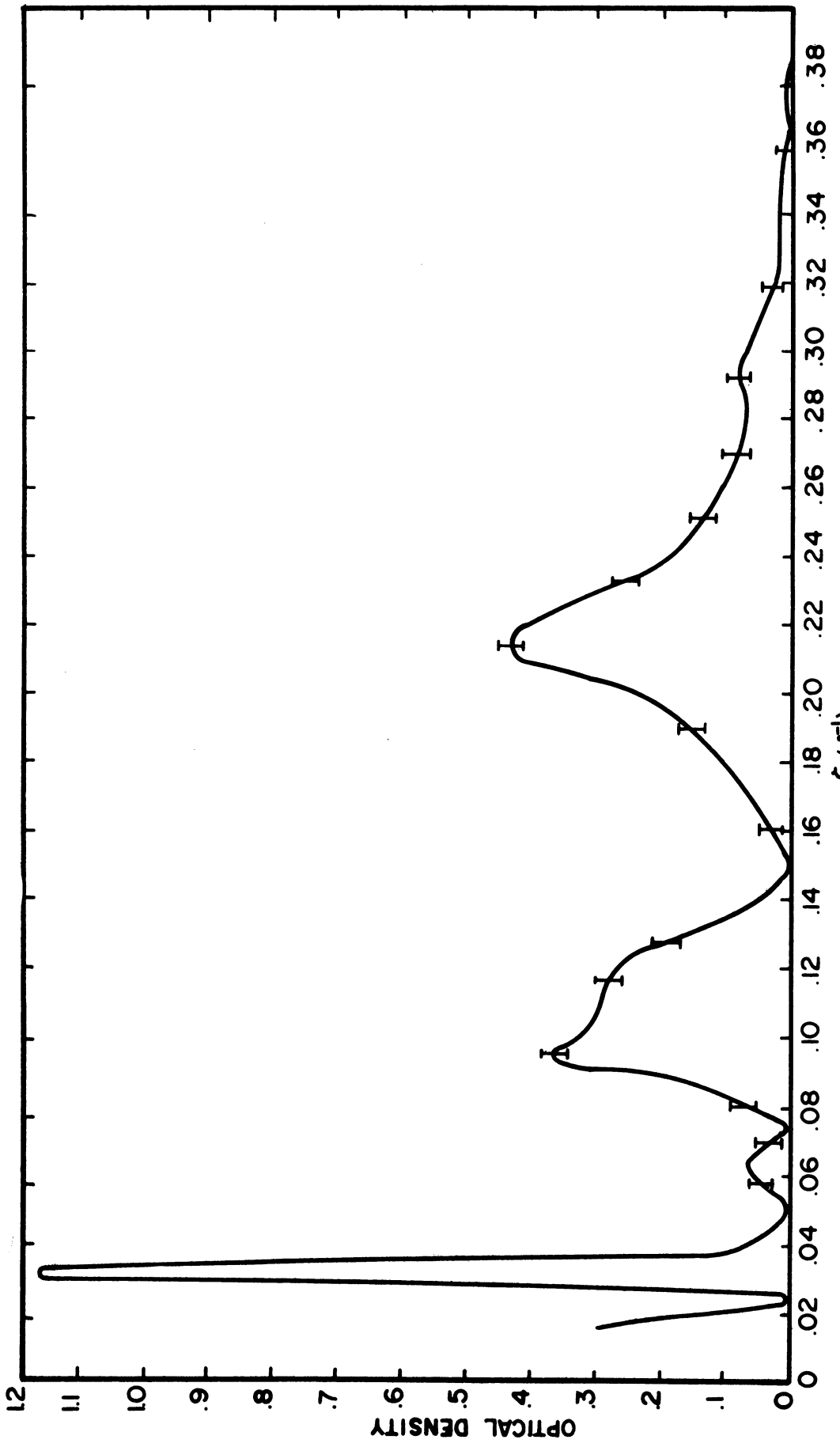

Figure 2-6

Figure 2-6 Optical density on equatorial layer line for 100 hour exposure photograph of turkey calamus. Vertical lines on curve indicate the estimated experimental error.

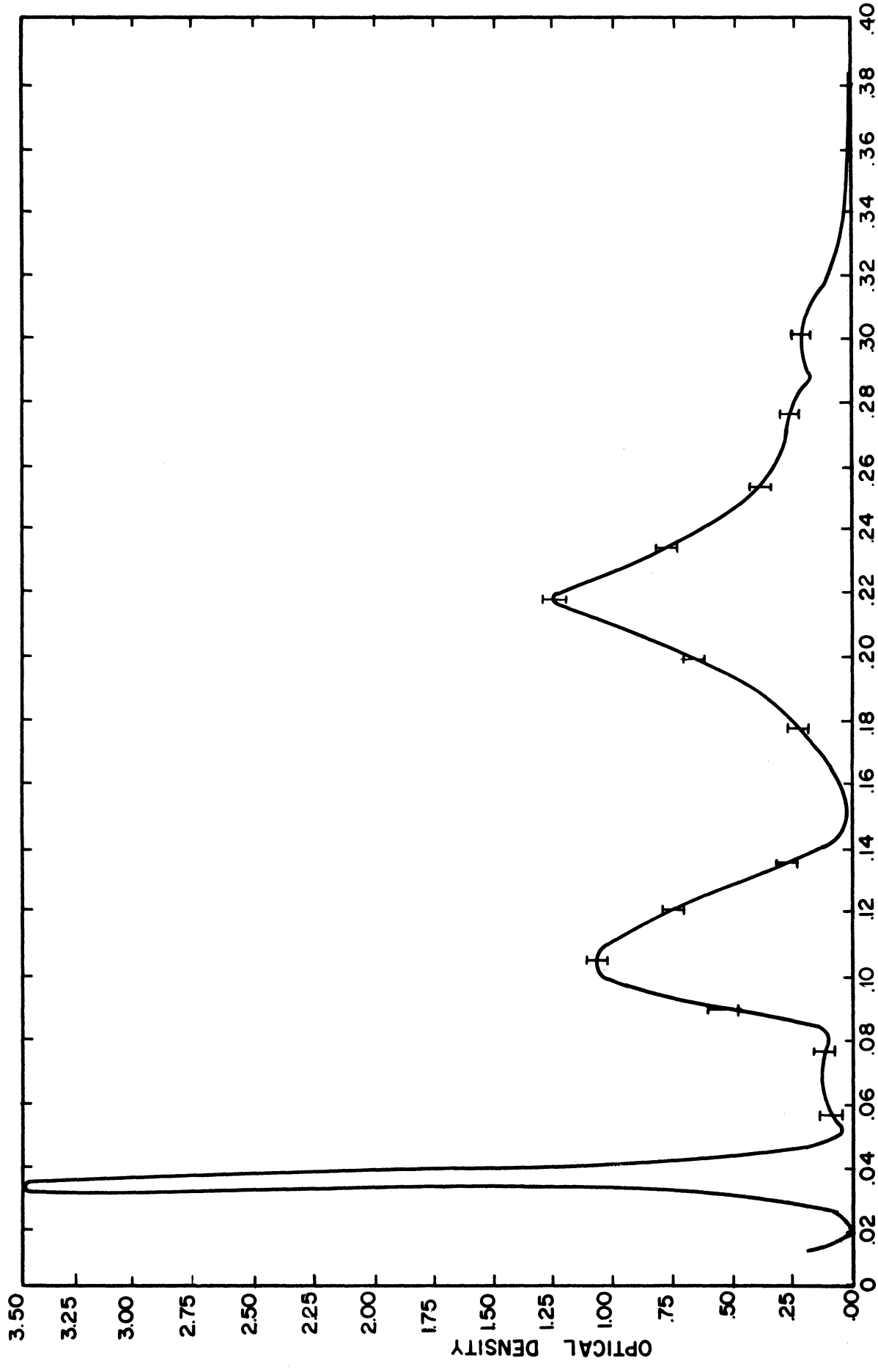

Figure 2-7

Figure 2-7 Optical density on equatorial layer line for 250 hour exposure photograph of turkey calamus. Vertical lines on curve indicates the estimated experimental error.

in Figures 2-8 and 2-9 were obtained. The main features of P(r) for feather keratin are peaks at about 5A and 10A and a minimum at about 3A. In an effort to determine whether the features of P(r) would be preserved if the reflections were treated as discrete, the intensities were considered to be localized at the ξ coordinates $0.030A^{-1}$, $0.090A^{-1}$ $0.116A^{-1}$, and $0.214A^{-1}$ and given the weights 2.25, 2.75, 2.40, and 10.00 respectively (based on a visual intensity estimate). The resulting curve for P(r) is shown in Figure 2-10. It may be concluded that the function P(r) is not very sensitive to small variations in the intensities or to the method of treating the intensities.

It is of interest to compare P(r) for feather keratin with the functions P(r) obtained from a structure based on the α-helix, from a structure based on extended or β polypeptide chains, and from the collagen structure. The difference between P(r) for feather keratin and that expected for an α-helix is striking. Whereas P(r) for feather keratin has a minimum at about 3A, the theoretical P(r) for the 3.60 residue per turn α-helix and the P(r) determined from the equatorial reflections of poly-γ-methyl-L-glutamate both have maxima at about 3A[56]. This difference suggests that α-helices with their axes parallel or nearly parallel to the fiber axis are not a major component of the feather structure. For purposes of comparison, P(r) for silk fibroin, a β protein, was calculated from the data of Marsh, Pauling, and Corey[17] and is shown in Figure 2-11. The similarity of the function P(r) for feather keratin and P(r) for silk fibroin is evident. Since the function P(r) is a weak condition on a structure, it is not

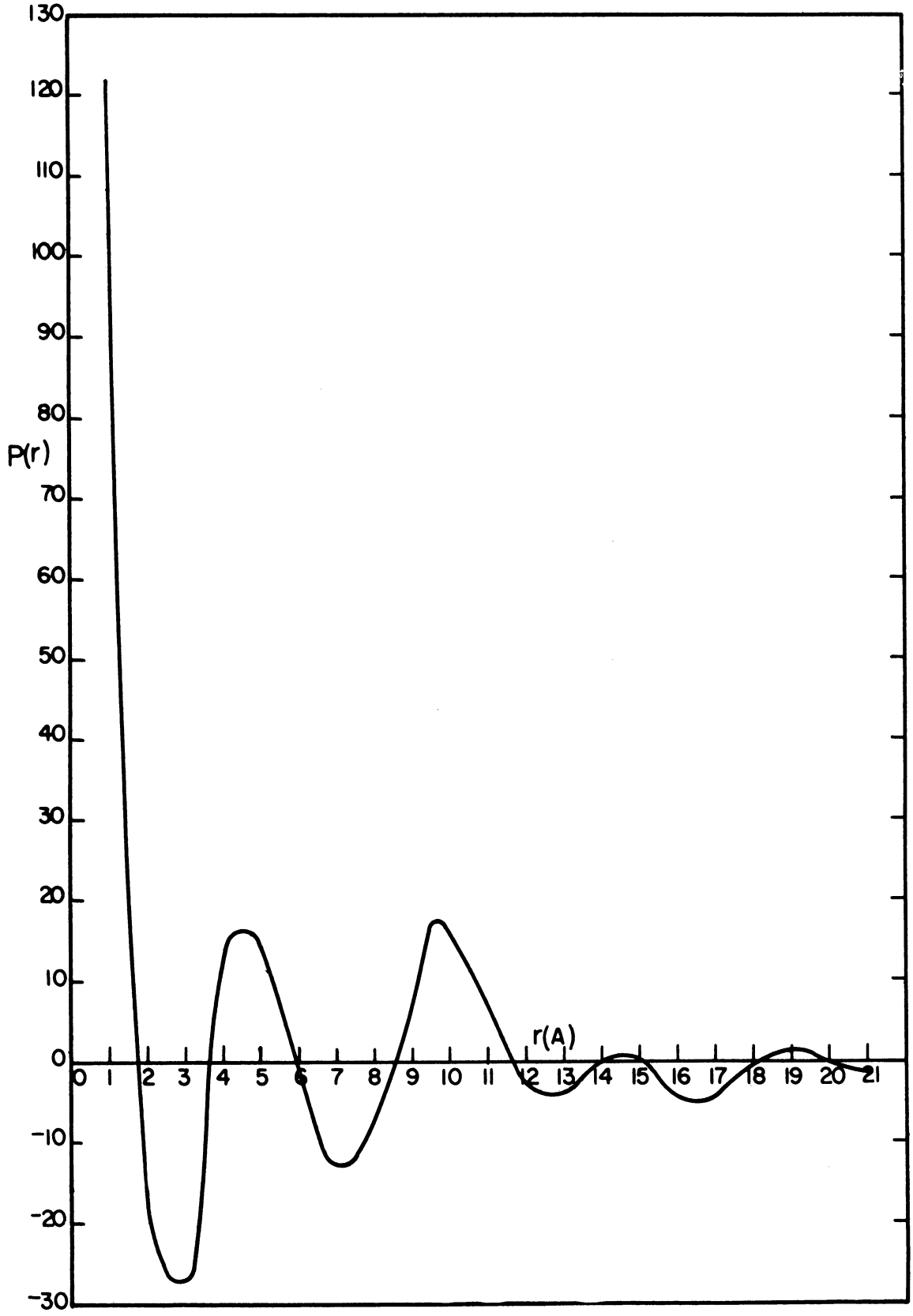

Figure 2-8 P(r) turkey calamus calculated from data obtained from the 100 hour exposure photograph.

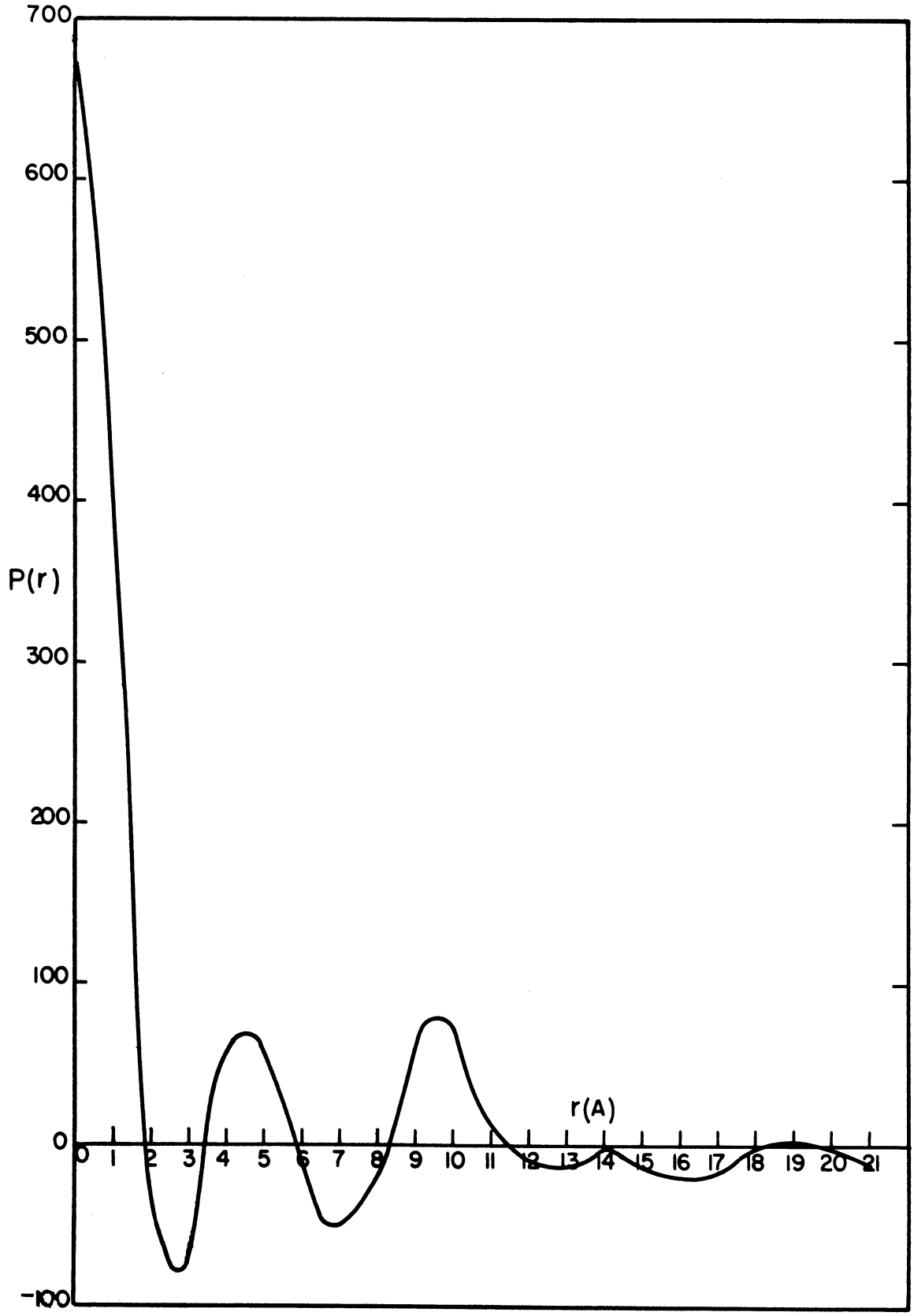

Figure 2-9 P(r) turkey calamus calculated from data obtained from the 250 hour exposure photograph.

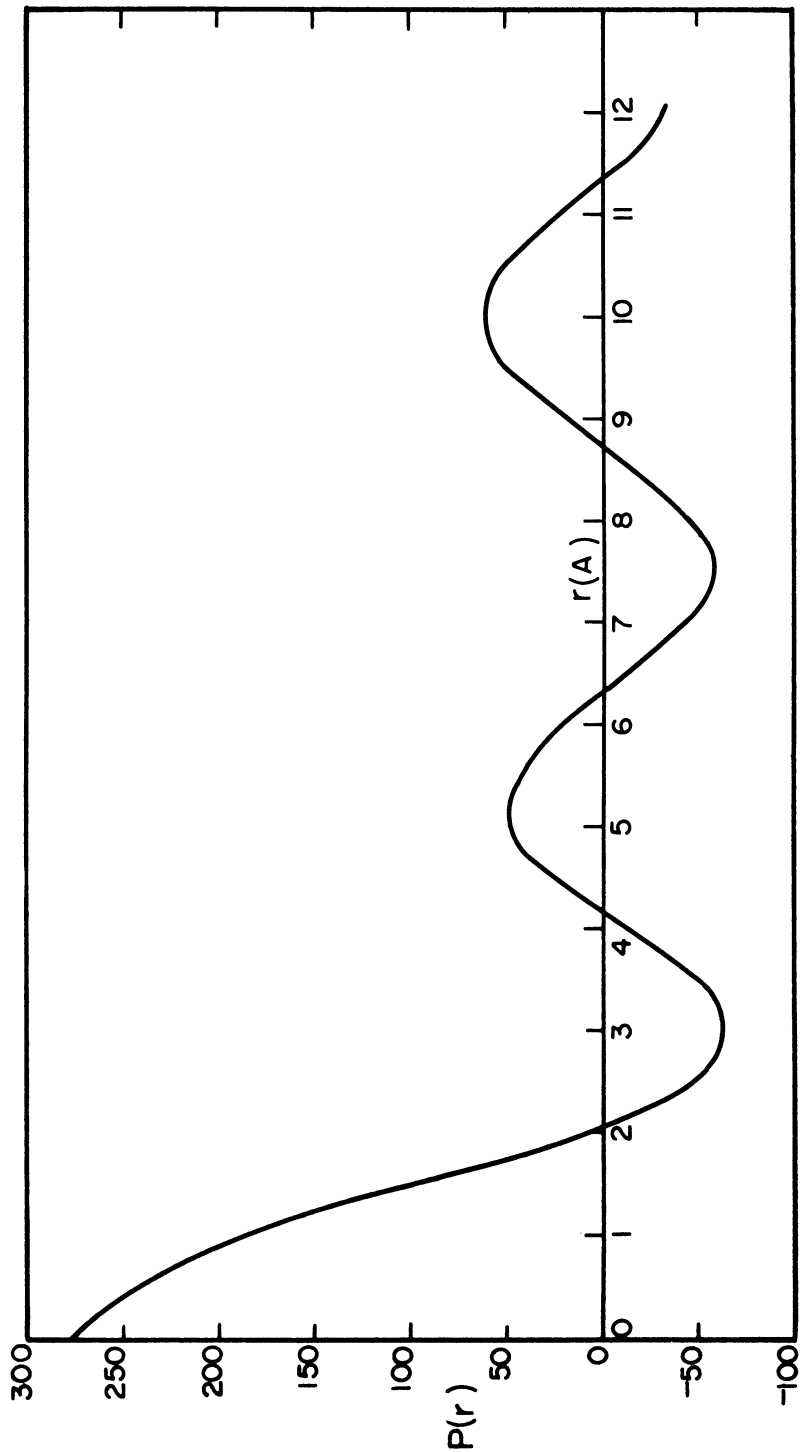

Figure 2-10 P(r) turkey calamus calculated by treating reflections as discrete.

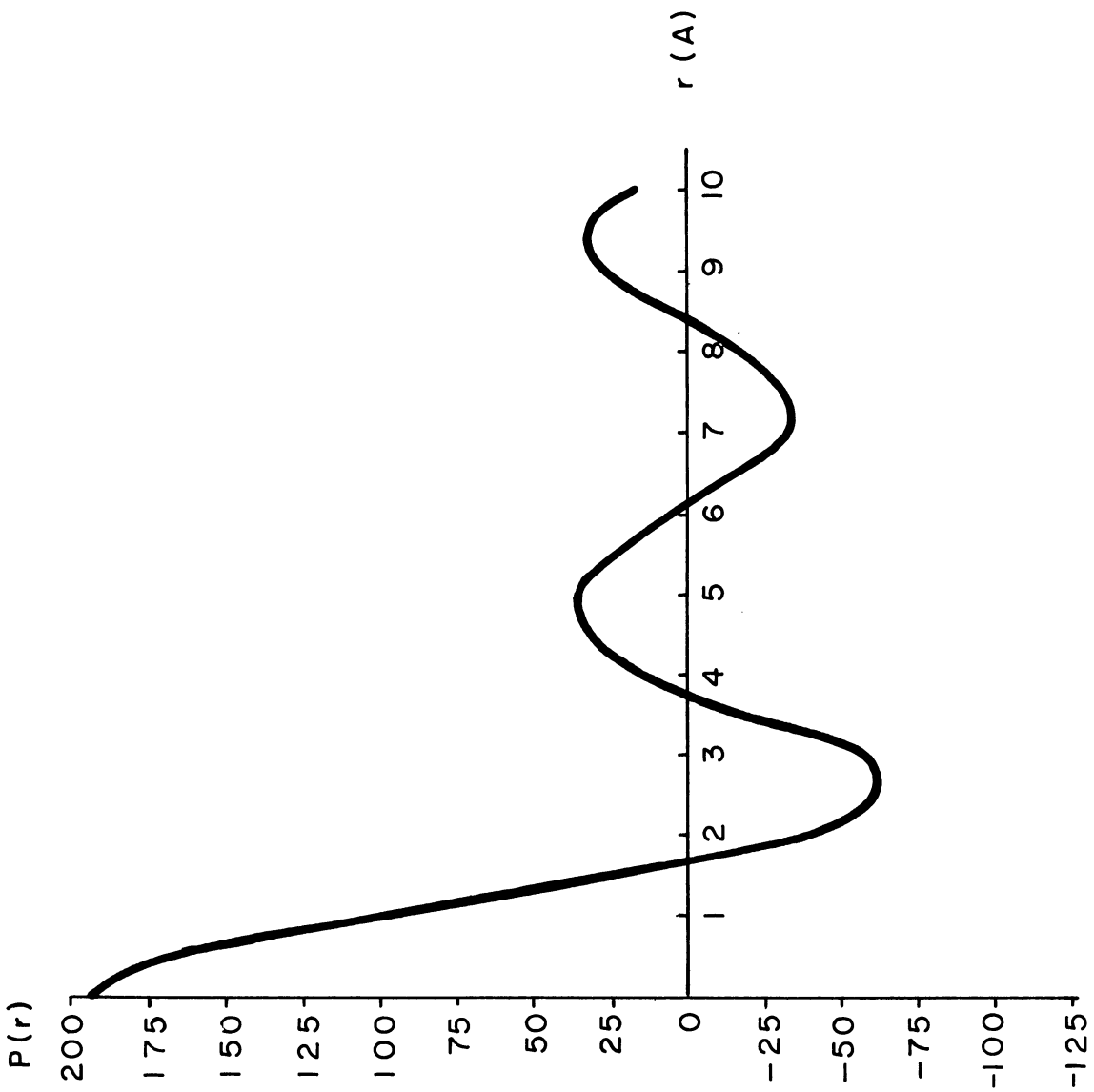

Figure 2-11 - P(r) silk fibroin calculated from the data of Pauling, Corey, and Marsh.

legitimate to conclude that two structures having similar projected Patterson functions such as silk fibroin and feather keratin are based on exactly the same type of long range lateral order. It is reasonable, however, to assume that the 5A peak in the function P(r) for feather represents, in a manner analogous to that of silk fibroin, the lateral distance between adjacent polypeptide chains. While it is true that there is a 5A peak in the function P(r) for collagen[56], the functions P(r) for feather keratin and collagen are not quite as similar as are the functions P(r) for feather and silk fibroin.

The Cylindrical Patterson Function

Portions of the five cylindrical Patterson functions are shown in Figures 2-12 through 2-16. The outer contour has been chosen in each case as the 100 contour. Since the scale is not absolute, the maps can only be used to indicate the peaks in the two-dimensional interatomic vector density distribution. For Pattersons 1 and 2 the contour interval has been chosen as 100, for Patterson 3 as 75, while for Pattersons 4 and 5 the interval has been chosen as 50.

In general, the resolution of the cylindrical Patterson function for feather keratin is poor and it is only possible to draw very general conclusions from it. The poor resolution is probably due to the "poor" quality of the diffraction data obtainable from a fibrous system in comparison to that obtainable from a single crystal. At this stage, the primary value of the Patterson function is to provide additional evidence against the presence of the α-helix in the feather structure and to indicate the existence of a few prominent interatomic

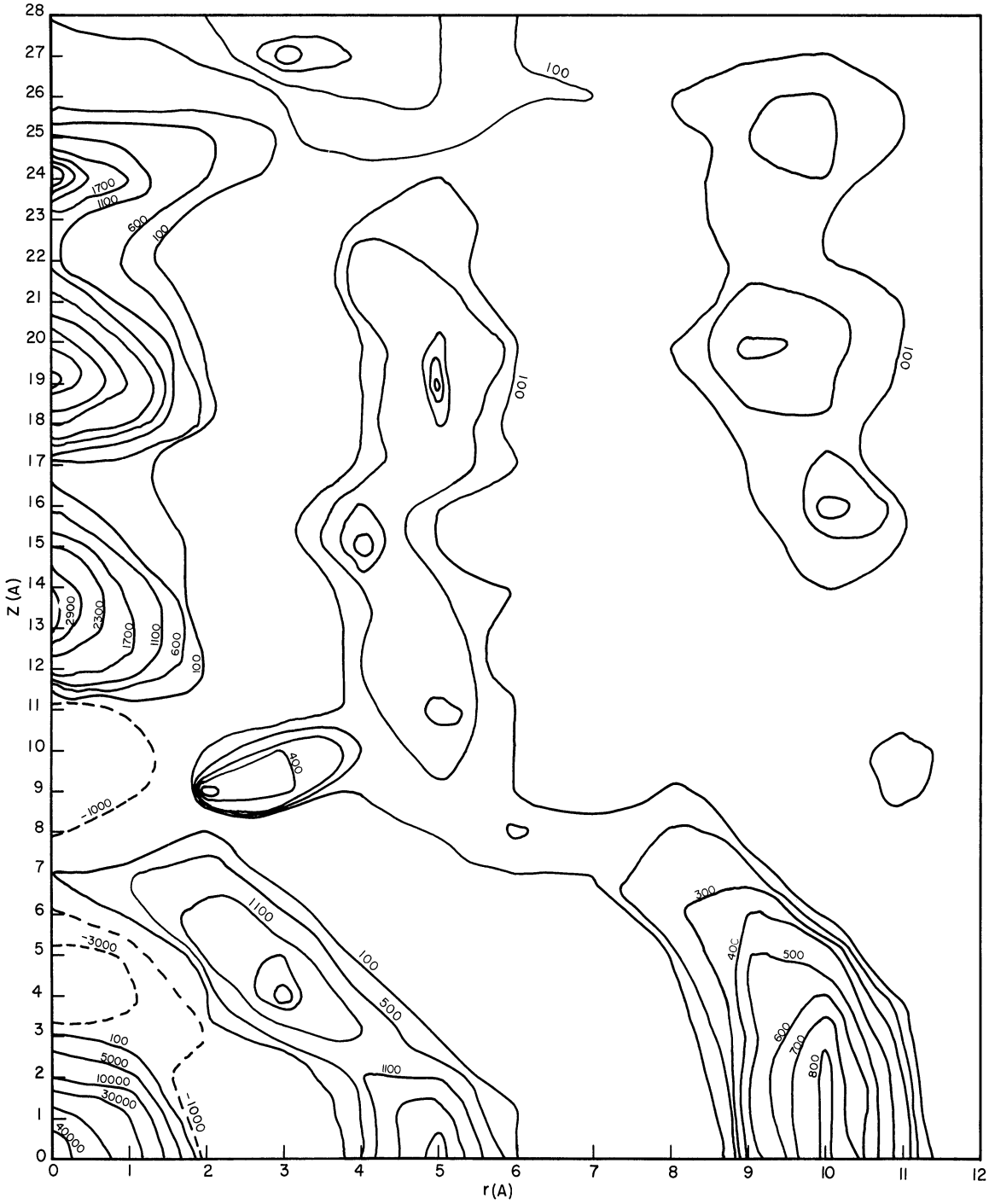

Figure 2-12 - Cylindrical Patterson Function (1).

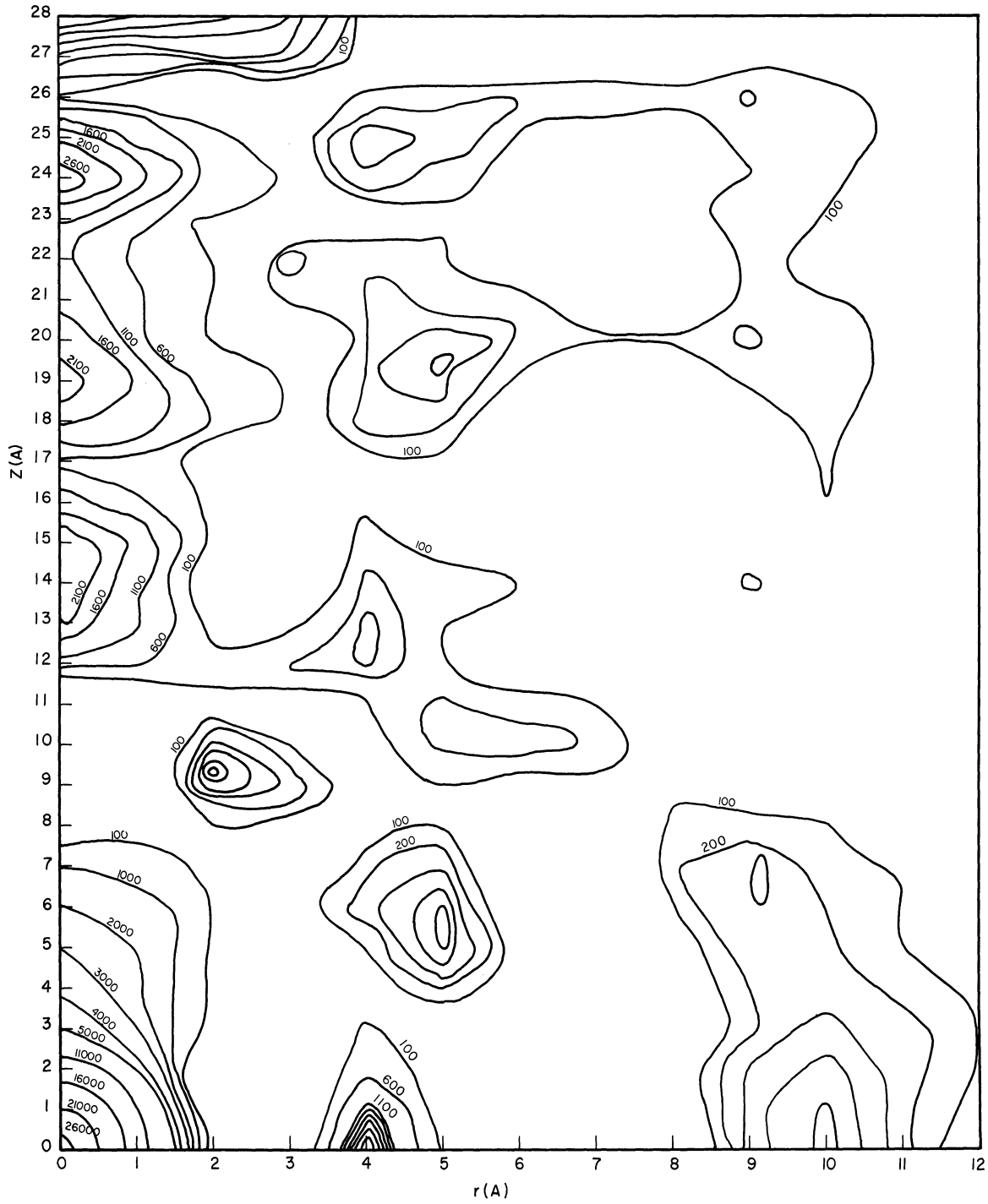

Figure 2-13 - Cylindrical Patterson Function (2).

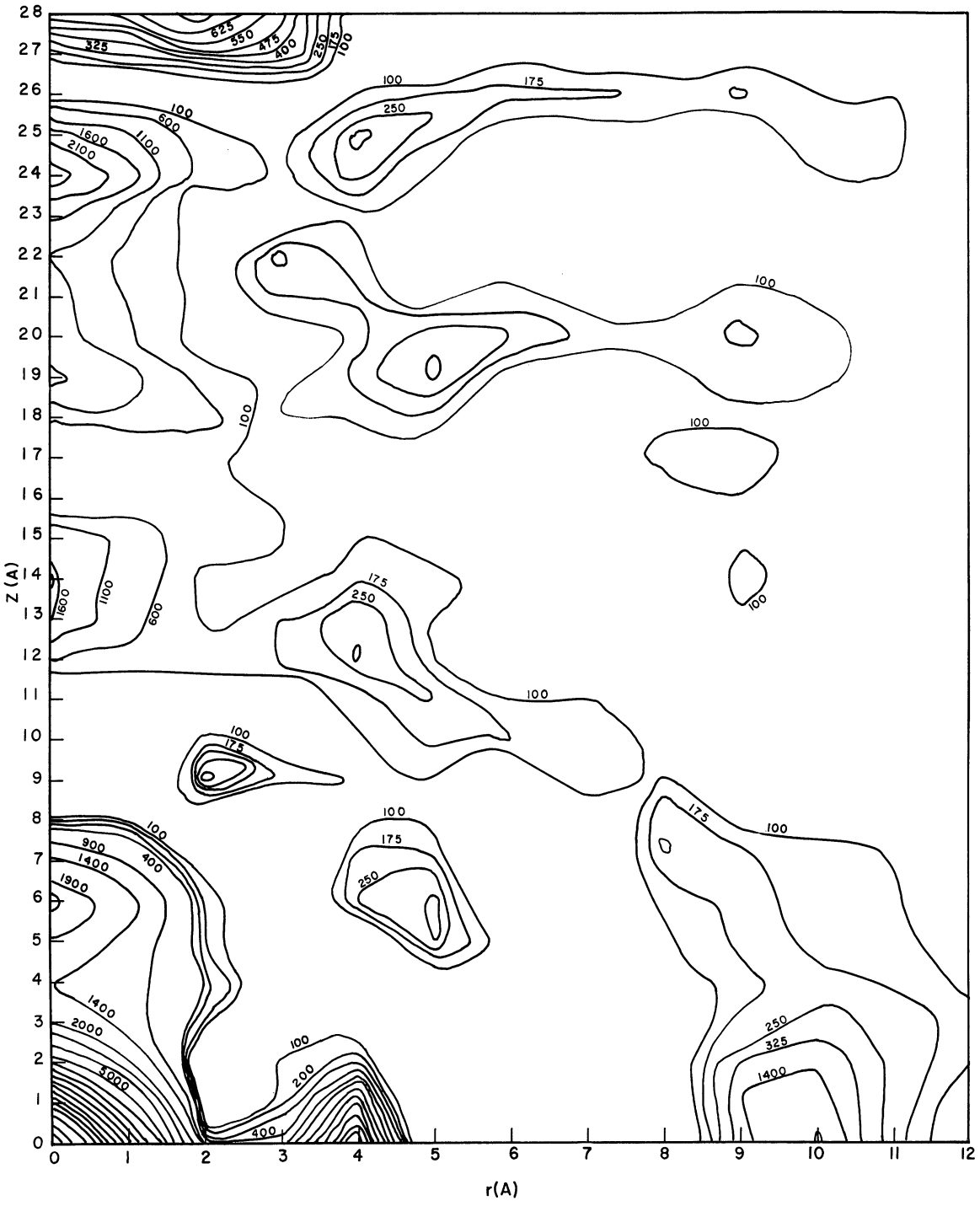

Figure 2-14 - Cylindrical Patterson Function (3).

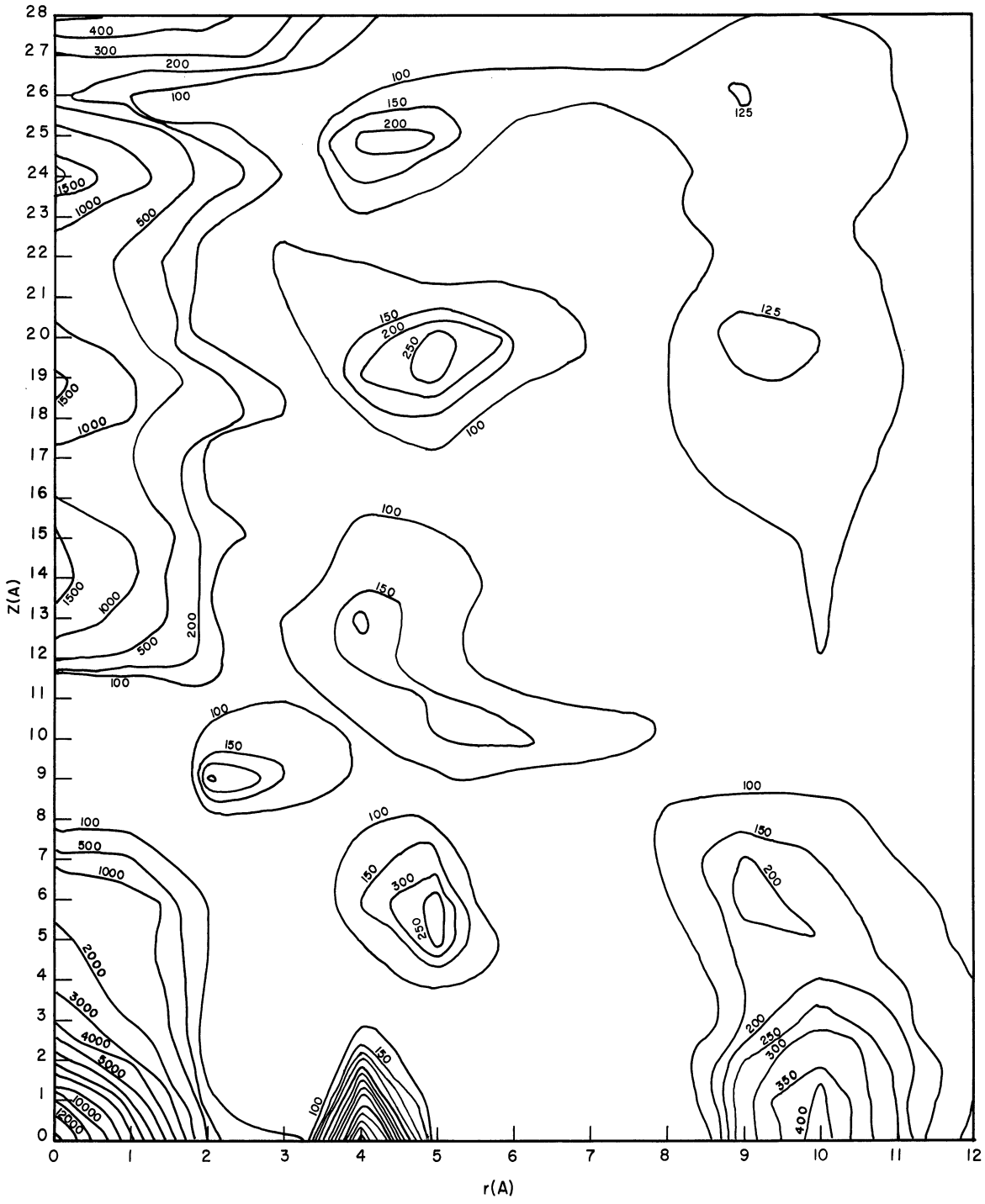

Figure 2-15 - Cylindrical Patterson Function (4).

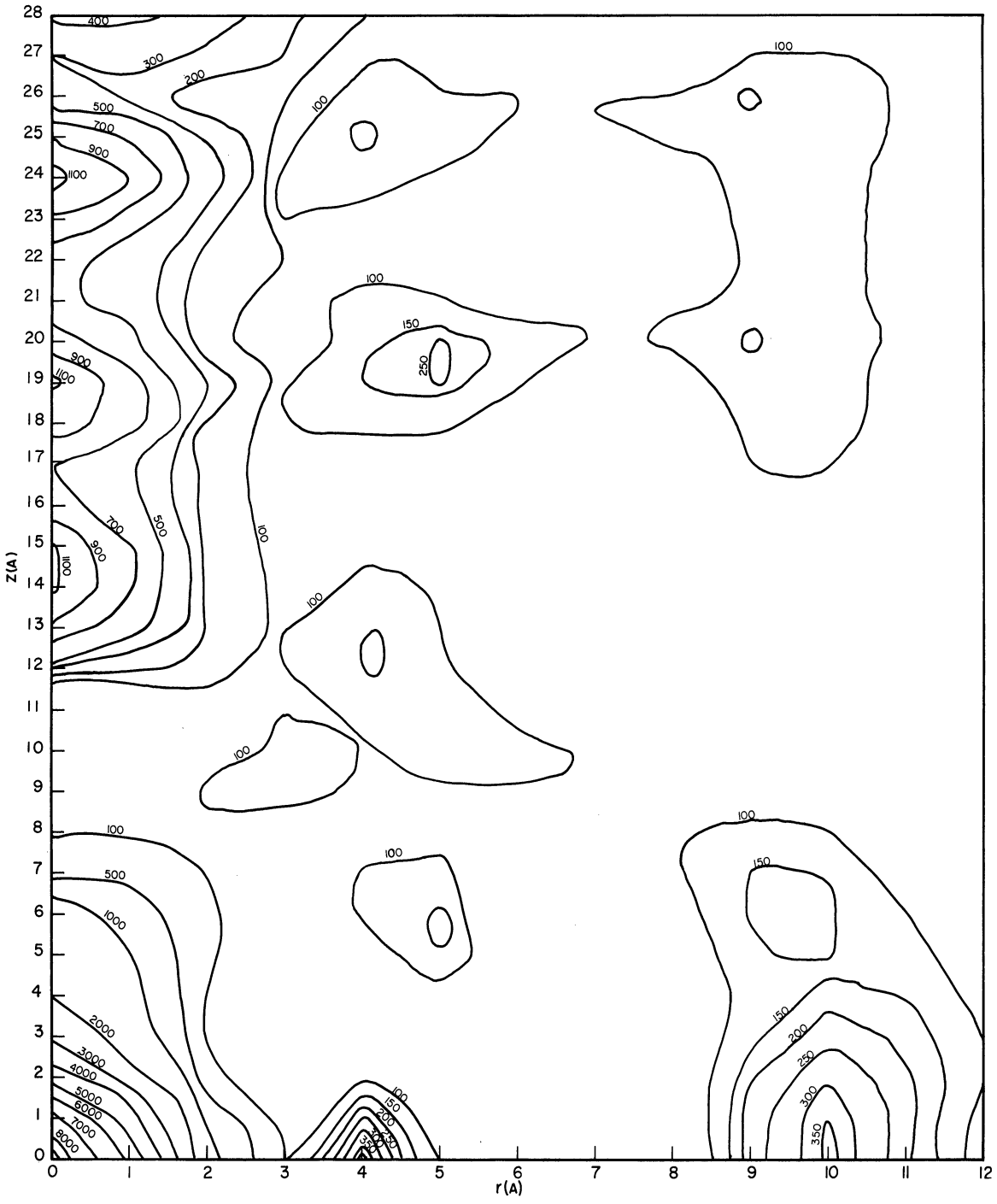

Figure 2-16 - Cylindrical Patterson Function (5).

vectors. For example, the cylindrical Patterson function for poly-γ-methyl-L-glutamate (presumably based on the α-helix) exhibits a series of peaks in the region r $\cong$ 3A[56]. These peaks are located at approximately P(3,2), P(3,5), P(3,8), and P(3,12). There are no peaks in the region r = 4-5A. The dissimilarity to the data for feather keratin suggests that α-helices are not a major component of the feather structure.

It is also of interest to compare the cylindrical Patterson function of feather keratin with that of collagen. The cylindrical Patterson function for collagen exhibits peaks at P(5,0) and P(5,12)[56]. As the function was not calculated beyond r = 8A or z = 14A it is not known whether there are peaks in the r = 9-10A region. Feather keratin has, in addition to peaks near P(5,0) and P(5,12), a peak at P(2,9) but there is no peak in the function for collagen at P(2,9). Primarily due to the limited data, it is not possible to conclude, from the consideration of the cylindrical Patterson function alone, whether feather keratin and collagen have similar structures.

The peaks in the cylindrical Patterson function for feather keratin will now be considered. The features of the Patterson function which remain relatively constant as a result of taking different approximations to the corrected intensities are of particular importance. Along the line P(0,z), which represents interatomic vectors having no lateral component, large peaks at P(0,19) and P(0,24) are common to all five Patterson functions. In addition there are somewhat less sharply localized peaks at P(0,6-7) and P(0,13-15). The function P(r,0), which represents interatomic vectors having no axial component, exhibits large peaks at P(4-5,0) and P(9-10,0). The exact position of these peaks is

somewhat uncertain due to the large grid size. Smaller peaks located at P(2,9), P(5,19-20), and P(9,20) are common to all of the maps. The peak at P(4,15) in Patterson 1 has shifted to P(4,13) in Pattersons 2-4 and to P(4-12) in Patterson 5. Pattersons 2-5 have peaks at P(4-25).

An interpretation of the peaks in the Patterson function in terms of detailed polypeptide chain configurations is not simple. It is of interest to note at this point, however, that many of the peaks fall in the intervals r = 4-5A, r = 9-10A, z = 19-20A and z = 24-25A. The existence of large peaks in the r = 4-5A and r = 9-10A regions is consistent with the assumption that feather keratin is a β protein; the peaks in the z = 19-20A region and the z = 24-25A region suggest the possibility that there is an 8-fold and a 10-fold pseudo-division of the 189A fiber axis identity period.

CHAPTER III

CHEMICAL AND INFRARED STUDIES

3.1 Introductory Remarks

In addition to the x-ray data, chemical and infrared studies provide significant structural information relative to the configuration of the polypeptide chains in a protein. The chemical work on feather keratin consists of amino acid composition studies, amino acid sequence studies (incomplete), and physical-chemical studies on solubilized preparations of feather keratin. The infrared studies provide important structural information particularly about the nature and orientation of the hydrogen bonds.

3.2 The Amino Acid Composition of Feather Keratin

The amino acid analysis of a protein represents the first stage in the determination of its chemical structure. Table III-I summarizes the results of the most recent amino acid composition studies on turkey calamus[60]. 95.5% of the total weight, 93.5% of the nitrogen and 86.4% of the sulfur were recovered. The results are accurate to $\pm$ 2 or 3%. The average residue weight is 101. The percentages of nitrogen, sulfur, moisture, and ash in turkey calamus are: 17.39, 2.64, 8.10, and 1.84 respectively. Technical difficulties made the estimation of methionine, threonine, and serine somewhat uncertain.

A comparison of the amino acids recovered from various parts of white turkey feather showed that the percentage of aspartic acid, phenylalanine, proline, arginine, methionine, serine, and valine are identical in the barbs, medulla, calamus, and rachis. On the other hand,

alanine, cystine, glutamic acid, glycine, isoleucine, tyrosine, histidine, lysine, and leucine show variations. Cystine is more prevalent in the barbs than in the calamus, medulla or rachis. Species variation in amino

TABLE III-I

Amino Acid Composition of the Calamus of White Turkey Feathers*

Amino Acid	Grams/100 Grams Protein	Residue%
Alanine	7.12	8.8
Arginine	6.69	4.2
Aspartic Acid	7.09	5.8
Cystine	8.29	3.8
Glutamic Acid	8.74	6.5
Glycine	9.60	14.0
Histidine	0.59	0.4
Ileucine	3.94	3.3
Leucine	8.85	7.4
Lysine	0.98	0.7
Methionine	0.34	0.3
Phenylalanine	5.76	3.8
Proline	10.98	10.5
Serine	15.09	15.7
Threonine	4.73	4.4
Tyrosine	3.97	2.4
Valine	8.43	7.9
Total	111.19	99.9

acid content were also investigated. Turkey feather barbs contain less cystine and tyrosine and more phenylalanine than goose feather barbs or goose down.

About 10% of the residues are proline. The percentage of proline is constant among the various parts of white turkey feathers and in different species. The proline content in the soluble portions

* Values are in terms of grams of amino acid per 100 grams of moisture and ash free material. More than 100 grams of amino acids are recovered since the weight of the amino acids analyzed includes the weight of the water of hydrolysis.

of the feather may be as high as 13%[61]. The small residues of glycine, alanine, and serine, comprise approximately 40% of the total. Serine and threonine, with their polar side chains, constitute 20% of the residues. Aspartic and glutamic acid account for 12.3%, while the basic residues histidine, lysine, and arginine comprise only 5.4% of the amino acids. Phenylalanine is the only aromatic residue.

The amino acid composition of solubilized feather keratin will be discussed later.

3.3 Amino Acid Sequence Studies

The determination of the amino acid sequences in the constituent polypeptide chains of a protein is one of the most difficult and important tasks in the elucidation of its chemical structure. Schroeder[62] has isolated and identified 59 peptides from the partial acidic hydrolysates of unoxidized and oxidized white turkey feather calamus. The only significant conclusions from these incomplete amino acid sequence studies are: 1) in a sequence such as x-proline, x tends to be an amino acid with a relatively small side chain; glycine-proline and threonine-proline-(i)leucine are predominant, 2) no proline-proline sequences have been identified, 3) cystine has glutamic acid, serine, and proline as close neighbors.

3.4 Solution Studies

By employing special techniques, it is possible to solubilize feather keratin. Several experiments have been performed in order to characterize solubilized preparations of feather keratin. The following features of the solubilization studies are of particular importance for

structural work: 1) the molecular weight of the resulting monomeric unit, 2) the size and shape of the feather keratin monomer, 3) end-group determinations on solubilized preparations of feather keratin, 4) the amino acid composition of solubilized feather keratin.

The first studies on feather keratin in solution were made by Ward, High, and Lundgren[63], who investigated a soluble keratin-detergent complex. This complex was prepared by digesting whole feathers in a solution containing $NaHSO_3$ and Nacconol NRSF.* The particle weight of the protein portion of the complex was estimated as being between 34,000 and 40,000. The preparation however was polydisperse, and thus no firm structural conclusions can be drawn from these early studies.

Using a urea-bisulfite system as solvent, Woodin[64] solubilized 80-85% of whole feathers and obtained an electrophoretically homogeneous material. Oxidation of the reduced or SH-keratin with performic acid resulted in the formation of cysteic acid-keratin. The measurements of osmotic pressure, sedimentation rate, and viscosity showed that in infinitely dilute solution both SH-keratin and cysteic acid-keratin have a molecular weight (number-average) of approximately 10,000. The accuracy of the molecular weight determination was about $\pm$ 7%. The weight-average molecular weight of the SH-keratin as determined by light-scattering measurements is 11,000 $\pm$ 1,000. Woodin concluded that the weight-average and the number-average molecular weights were sufficiently close to preclude the possibility of a large distribution of particle weights. The specific viscosity of both the SH-keratin and the cysteic acid-keratin extrapolate to the same value of 0.15 at zero concentration (intrinsic

---

* Nacconol NRSF is a commerical mixture of solium alkylbenzene sulfonates.

viscosity). On the assumption that the particle could be treated as an unhydrated prolate ellipsoid of revolution, an axial ratio of 13.2 was obtained from the intrinsic viscosity of 0.15. No molecular dimensions were calculated.

Rougvie[48] reported similar studies on a monomer and dimer of feather keratin. By reduction of whole feathers by thioglycol, the -S-S- bonds were broken and preparations of SH-keratin were obtained. These preparations however were not sufficiently stable for obtaining physical-chemical data.* A more stable form of protein was obtained by oxidizing the -SH groups to $-SO_3H$ groups through reaction with peracetic acid. Both a monomer and dimer of cysteic acid-keratin were obtained. Table III-II lists the important properties of the cysteic acid-keratin monomer.

TABLE III-II

Summary of Physical Chemical Properties for Feather Keratin Monomer

S^{o}_{20}	Sedimentation constant	1.06 ± .03 Svedberg Units
$\bar{V}$	Partial specific volume	0.725
M	Molecular weight	9,300 ± 700
a/b	Axial Ratio prolate assumption (from sedimentation-diffusion data)	9.74 (zero hydration) 6.83 (30% hydration)
$[\eta]$	Intrinsic viscosity	0.135
a/b	Axial ratio prolate assumption (from viscosity measurements)	12.3 (zero hydration) 9.77 (30% hydration)
$(\bar{r}^2)^{1/2}$	Effective length, random coil	85A
a/b	Axial ratio prolate assumption (from Scherage-Mandelkern theory)	22

* Preparations of SH keratin however were satisfactory for use in the reconstitution experiments discussed in Chapter I.

Rougvie attributed the difference of his intrinsic viscosity measurement (0.135) and Woodin's (0.15) to the possibility of the binding of urea to the keratin in Woodin's experiments.

The data concerning the dimer of cysteic acid-keratin are more limited. The molecular weight of the dimer was estimated to be 19,300 on the basis of the sedimentation-diffusion data. The axial ratio (prolate assumption, 30% hydration) is 15.5. (The partial specific volume of the monomer was used in the calculation.) No viscosity data for the dimer were reported.

Rougvie attempted to derive the molecular dimensions of the feather keratin monomer and dimer from these data. The classical anhydrous volume of the monomer $\frac{M\bar{V}}{N}$ is 11,200 cubic angstroms. For an axial ratio of 6.83/1, (no reason was given for choosing 6.83 as the "most favoured" axial ratio), the prolate ellipsoid of revolution which describes the molecule is 100A by 14.7A. Using a molecular weight of 19,300 and an axial ratio of 15.5, the corresponding dimensions for the dimer are 220A and 14.2A respectively, i.e., approximately double the length and the same width as the monomer.

A comparison of the results of Woodin and Rougvie indicate agreement on two important points: 1) the feather keratin monomer in solution has a molecular weight of approximately 10,000, 2) the axial ratio for the monomer, on the basis of the assumption of a prolate ellipsoid of revolution, is considerably greater than unity. The measurements of the axial ratio, however, cannot yet be taken as quantitatively correct. In particular, the agreement between the axial ratio as determined by sedimentation-diffusion studies and by viscosity

studies is not quantitatively satisfactory. Thus the exact relationship Rougvie obtained between the dimensions of the monomer and the dimensions of the dimer, on the basis of an axial ratio of 6.83/1, cannot yet be considered an unambiguous result. In fact, as will be shown later, the assumption that the shape of the monomer in solution can be approximated by a prolate ellipsoid of revolution is highly questionable.

A study of the end-groups of a protein can indicate whether the chains are branched or unbranched, cyclic or open, as well as the minimum number of component chains in the molecule. Woodin[65] in a preliminary study of soluble cysteic acid-keratin obtained only 0.1 equivalents of α-dinitrophenyl amino acids per mole of protein by reaction with 1-fluro-2:4 dinitrobenzene. The amount of ε-lysine detected was between 0.1 and 0.15 moles per mole of protein. In a more detailed study[66], Woodin confirmed the observation that only 0.1 equivalents of α-dinitrophenyl amino acids and 0.125 equivalents of ε-DNP lysine are obtained by reaction with flurodinitrobenzene. The absorption peak of DNP cysteic acid-keratin was studied between 240 mμ and 400 mμ. As no peak was observed at 390 mμ, Woodin concluded that N-terminal proline was not present. The absorption spectrum of the phenylthiohydantoins derived from phenylthiocarbamate derivatives of cysteic acid-keratin was studied between 240 mμ and 350 mμ. The peak at 267 mμ is characteristic of a phenylthiohydantoin of an amino acid. The optical density at 267 mμ, if due to a phenylthiohydantoin of an amino acid with a molar extinction coefficient of 16,000 corresponds to 0.1 equivalents of N-terminal amino acids per mole of protein. In addition, the reaction of soluble feather

keratin with carboxypeptidase and with hydroxyl ions was interpreted as evidence for the absence of a molar proportion of α-carboxyl groups. On the basis of his data, Woodin concluded that the feather keratin monomer is an unbranched cyclic peptide.

In the same study, Woodin also determined the amino acid composition of cysteic acid-keratin. The only important result relevant to the present studies is the fact that about 13% of the residues are proline

3.5 Infrared Studies

The infrared studies on feather keratin provide important structural information particularly about the orientation of the hydrogen bonds.

The CO stretching mode (1650 cm^{-1}) and the NH stretching mode (3315 cm^{-1}) both show perpendicular dichroism. The initial quantitative measurements gave low values for the perpendicular dichroism of the NH stretching band: from about 1.3/1[67] to 1.8/1[58]. Parker[58] has subsequently shown that a large part of the absorption arises from non-oriented OH or NH groups. If these groups are removed by exchanging with D_2O, the residual NH stretching band has a perpendicular dichroism of 4.8/1. These facts are consistent with feather keratin being a β protein.

Ambrose and co-workers[68,69] have proposed, on the basis of an empirical correlation, that the value of the CO stretching frequency is characteristic of the fold of the polypeptide chains. According to this point of view, a value for the stretching frequency near 1660 cm^{-1} is characteristic of the α form while a value near 1640 cm^{-1} is characteristic

of the β form. The fact that the CO stretching frequency in feather keratin has a double peak has been interpreted by them as evidence for the admixture of some α form. The intensities of the two components of the CO peak are comparable, which would indicate that the amount of α form is approximately equal to the amount of β form. It should be noted, however, that no explanation for the frequency criterion has been given. The frequency shift may be due to other factors besides the over-all chain configuration. In particular, Krimm[70] has suggested the possibility that the frequency shift may be due to angular effects, i.e., the frequency for the CO stretching mode may be a function of the angle between the CO and NH hydrogen-bonded vectors, which is only secondarily related to the chain configuration.

Angell[71] has examined the infrared spectra of unoriented specimens of reconstituted soluble keratin in both the reduced (SH-keratin) and oxidized (cysteic acid-keratin) forms. The SH-keratin has, like the native material, two bands of approximately equal intensity, at about 1632 cm^{-1} and 1655 cm^{-1}. In the cysteic acid-keratin, these bands have shifted to 1620 cm^{-1} and 1650 cm^{-1} respectively. The higher frequency component is slightly less intense compared to the SH-keratin. The origin of these effects is not known.

CHAPTER IV

THE β-HELIX HYPOTHESIS

4.1 Introductory Remarks

In this chapter, an attempt will be made to develop a new hypothesis relative to the configuration of the polypeptide chains in the feather keratin structure. An analysis of the x-ray diffraction pattern suggests that the existing configurations for the polypeptide chain are not adequate to explain the data. Although feather keratin can be classified as a β protein, some deviation from a simple extended chain model seems to be required. Therefore, it is necessary to introduce additional assumptions relative to the chain configuration. An analysis of the data suggests that the following assumptions are reasonable: 1) there is a regular sequence of proline resudues along the β-polypeptide chain, 2) the chain assumes a helical configuration of pitch 189A (fiber axis identity period).* A detailed analysis has led to the conclusion that only one structure satisfying these conditions is stereochemically feasible. The reasons for rejecting the existing chain configurations, for introducing the assumptions stated above, and the stereochemical arguments that have led to a new model for the feather keratin structure will now be discussed.

4.2 Inadequacy of the Existing Configurations

The inadequacy of the existing configurations of the polypeptide chain in accounting for the structure of feather keratin must be established

---

* The number of residues per turn of the helix was determined by the x-ray data. The requirement of forming satisfactory hydrogen bonds between two adjacent coaxial helical polypeptide chains aided in the determination of the other parameters of the helix.

in order to demonstrate the necessity for introducing additional structural assumptions. The configurations under consideration are the α-helix[25], the three-stranded collagen structure[4] and the various forms of extended or β-polypeptide chains[18,72,73]. Many other configurations have been discussed in the literature[13,27], but have not been as successful in explaining the data relative to the fibrous proteins. In the formulation of these earlier configurations of the polypeptide chain a less rigid set of atomic dimensions were employed than those used in the α-helix, the extended chain structures, and in the recent models of collagen. Some new helical configurations, in addition to the α-helix, have been proposed[28]. These configurations, although based on the most recent values for the bond angles and distances in the polypeptide chain, are unstable. Semi-quantitative estimates of the instability of these helical configurations have been made in terms of the deviation of the residues from planarity, the deformation of bond angles, and the orientations (of the atoms attached to the α-carbons) around the C-N and C-C' bonds. The α_{II} ribbon structure and the π-helix have the minimum instability. On the basis of the α_{II} ribbon structure, which has an axial translation of 2.75A per residue, a strong meridional reflection at 2.75A would be expected. (There is a medium-weak meridional reflection at 2.77A in the feather keratin diffraction pattern.) This structure, however, could not explain the medium-weak meridional reflection at 2.96A which is the most important feature of the wide-angle diffraction pattern of feather keratin. In addition, the α-II ribbon structure, would predict parallel dichroism in the infrared for the NH and CO stretching frequencies, which are not observed. Since the π-helix and the α-helix are topologically very

similar an essentially similar set of arguments can be used for both these helices. We shall therefore restrict our attention to the α-helix, the three-stranded collagen structure, and the extended chain structures.

The absence of the 1.5A and the 5.1A meridian spacings (or 5.4A layer-line spacing) from the diffraction pattern of feather keratin is a strong argument against the existence of α-helices in the feather keratin structure. A comparison of the one-dimensional Patterson projection P(r) for feather keratin and that expected for an α-helices also suggests, as has been just observed, the α-helices with their axes parallel or nearly parallel to the fiber axis are not present to any significant extent. In addition, the incorporation of a proline ring into a left-handed α-helix completely disrupts the chain configuration, while the introduction of a proline ring into a right-handed α-helix causes minor discontinuities and loss of hydrogen-bonding[2]. Since feather keratin has a proline content of about 10-13%, the α-helical configuration is not an energetically favorable one. From the infrared point of view, the α-helix is expected to exhibit parallel dichroism for the NH stretching mode[27]. Hence, the residual perpendicular dichroism of 4.8/1 found for this vibration is another argument against the α-helical configuration representing a significant part of the feather structure. It is also of interest to note that Kraut's calculation of the intensities of the equatorial and near-equatorial reflections of the Pauling-Corey model 2 (an all α model) indicated very poor agreement between the calculated and the observed intensities. The strongest evidence for the existence of α-helices in the feather keratin structure would be the acceptance of the Ambrose-Elliott frequency criterion. This criterion, however, as has been mentioned

previously, does not give unambiguous information about the over-all chain configuration. Thus, the bulk of the evidence strongly suggests that the α-helical configuration is not a major component of the feather keratin structure.

A comparison of the x-ray, chemical, and infrared data also indicates that it is unlikely that the structures of feather keratin and collagen are based on similar configurations of the polypeptide chain. The x-ray diffraction patterns of feather keratin and collagen, although indicating some similarities, also exhibit many significant differences. The only meridional reflection in the wide-angle pattern of stretched collagen is the strong meridional reflection at 2.86A[33]. The wide-angle diffraction pattern of feather keratin, on the other hand, exhibits a medium-weak meridional reflection at 2.96A as well as strong meridional reflections at 6·30A and 4.97A. In addition, the mechanical properties (extensibility) of feather keratin and collagen as revealed by x-ray diffraction studies are strikingly different[2,74] (Section 5.6). The proline content of feather keratin (~10%) compares with a proline plus hydroxyproline content of approximately 22% in collagen[13]. The glycine content of collagen is 34%, while the glycine content of feather keratin is only 14%. The glycine content of collagen is structurally significant, the recent model for collagen formulated by Crick and Rich[4] requiring that every third residue be glycine. Glycine-proline-hydroxyproline sequences are common in collagen[4] but no proline-proline sequences have been observed in feather keratin. Furthermore, the infrared spectrum of collagen differs from that of feather keratin. The NH stretching frequency for feather keratin is

observed at 3315 cm^{-1} while the NH stretching frequency for collagen is observed at 3330 cm^{-1}.[33] The significance of this difference is not yet fully understood. It is therefore concluded that feather keratin and collagen are not based on similar configurations of the polypeptide chain.

The relationship of the extended chain configurations to the feather keratin structure will now be discussed. The wide-angle diffraction pattern of feather keratin is of the β type[14]. The infrared spectrum exhibits perpendicular dichroism for both the CO and NH stretching modes, which is expected for a β protein. In order to confirm the identification of feather keratin as a β protein, the one-dimensional Patterson projection for silk fibroin (a β protein) has been calculated from the data of Marsh, Pauling, and Corey. A comparison of the function P(r) for feather keratin and P(r) for silk fibroin shows, as has been discussed, that the main features of both functions are similar, i.e., both functions exhibit peaks at approximately 5A and 10A as well as a minimum at about 3A. In addition, the cylindrical Patterson function P(r,z) for feather keratin exhibits many peaks in the 4-5A region and in the 9-10A region, which is expected for a β protein. Thus, the conclusion of Bear-Rugo that the feather keratin structure is based on extended or β-polypeptide chains appears to be in agreement with the data.

There are, however, several features of the diffraction pattern which indicate a deviation from the usual extended chain model: 1) the short meridian spacing at 2.96A, 2) the absence of any spacing in the 1A meridian region, 3) the long fiber axis identity period of 189A, 4) the intense equatorial spacing at about 33A, 5) the very intense 23.64A

meridian spacing. The minimum residue length for the extended chain structures is about 3.1A (polar pleated-sheet configuration). Hence, if the 2.96A meridian spacing in the feather keratin diffraction pattern is interpreted as the axial projection of an amino acid residue along the chain, the residues in an extended chain must be tipped with respect to the fiber axis. In the usual extended chain models, the chain axis is vertical. The only other mechanism for shortening the projected residue length in an extended polypeptide chain is to employ cis residues. The experimental evidence indicates that cis residues do not occur in a polypeptide chain[3] and we will therefore assume that they are not present in the feather keratin structure. The 1.1A meridian spacing, in the usual extended chain model is due to an approximately regular sequence of atoms along the backbone of the polypeptide chain whose z separation is about 1.1A. This regularity in the feather keratin structure is not indicated by the diffraction pattern. On the basis of the usual β model, the long fiber axis repeat of 189A would have to be explained by a periodicity of 189A in the side chains. Such a periodicity implies a regular sequence of 64 amino acid residues and is a priori unlikely. The lateral dimensions for a sheet-structure, on the basis of the usual extended chain model, are about 5A for the inter-chain distance (within a given sheet) and about 10A for the inter-sheet distance. It would therefore be very difficult to explain the existence of the intense 33A equatorial reflection on the basis of a sheet model. In addition, the intense 23.6$_4$A meridian spacing implies a regularity other than that which would be expected to arise from the average side group.

The question arises: can an extended polypeptide chain be modified in a natural manner to account for these facts?

4.3 Assumption of a Regular Sequence of Proline Residues

The high percentage of the imino acid proline in feather keratin, viz. 10-13% (Section 3.2), and the persistence of the intense 23.6_4A meridian spacing during the course of the heat-moisture treatment are two important features of the data. A possible connection between these facts can be demonstrated if a regular sequence of proline residues along the polypeptide chains is assumed. The only reflection in the diffraction pattern which could represent the axial projection of an amino acid residue in an extended chain configuration is the 2.96A meridian reflection. This reflection implies that there are 64 amino acid residues in the 189A identity period. Thus, according to the above hypothesis, the number of residues between successive prolines would be restricted to: 1,3,7,15,31, or 63. The corresponding proline percentages to be expected are: 50,25,12.5,6.25,3.13, and 1.56. Since the percentage of proline found is 10-13%, the hypothesis is self-consistent and it can be concluded that there are seven amino acid residues between successive prolines. It is noteworthy that in the amino acid sequences which have been observed proline either occurs once or is absent, which would be expected if the hypothesis that every eighth amino acid residue is a proline is correct. In addition, the proline content of different parts of white turkey feathers and different species of birds is constant, which indicates a possible structural significance for the proline residues. If the conclusion is tentatively accepted that successive proline residues

are separated by seven amino acid residues, the 189A repeat is divided axially into eight equal parts by the prolines. This offers a reasonable explanation for the (strong and persistent) 23.6$_4$A meridian reflection. It is important to note that the three CH_2 groups in the side chain of proline are in a fixed spatial configuration and should therefore scatter more coherently than the atoms in the side chains of the other amino acids (with the exception of hydroxyproline). In addition, it is likely that water molecules would form hydrogen-bonds to the free CO groups on the prolines, thus adding 10 electrons in a relatively fixed spatial configuration.

The assumption of a regular sequence of proline residues along a given β-polypeptide chain has further desirable structural implications. It is now possible that neighboring chains are aligned with their proline residues all at the same z level. Proline, being an imino acid has no hydrogen atom attached to its nitrogen atom, and an examination of a molecular model shows that its carbonyl oxygen atom is in an unfavorable position for the formation of a hydrogen bond. Therefore, if a proline residue is opposite another amino acid residue a hydrogen bond will not be formed. The maximum number of hydrogen bonds will be formed when all the prolines are at the same z level. Model building (Section 4.6) shows that two proline residues at the same z level can pack together satisfactorily as well as form good hydrogen bonds along the non-proline regions of the chain.

It will now be shown that the configuration of the non-proline residues of the chain is severely restricted. If the residues on chain 1

are labeled proline-residue$_1$.....residue$_7$ - proline and the residues on chain 2 are labeled in a similar manner, the bonding is between residues of equal subscripts. Using a z repeat between successive prolines of 23.64A, the fold of the non-proline part of the chain is determined, as will be shown by the following considerations. A residue of an extended polypeptide chain must be tipped with respect to the fiber axis in order to have a projected residue length of 2.96A. The presently known extended chain configurations are: 1) the parallel chain configuration [18], 2) the anti-parallel chain configuration [18], 3) the polar chain configuration [72]. The repeat distance of the parallel-chain configuration cannot be lowered much beyond 6.50A without making the CO bonds skew, resulting in a loss of hydrogen bonding. Parallel-chains must be tipped at an angle of approximately 25° with respect to the fiber axis in order to attain an axial projection of 2.96A per residue. This would be incompatible with the observed infrared dichroism (Section 5.7). The same argument applies with greater force to the anti-parallel configuration, whose repeating distance is approximately 7.00A. These objections do not hold for a polar pleated sheet whose repeat is approximately 6.14A. In this case, a tipping angle of about 15° would bring the axial projection per residue down to the required value. Therefore, for trans residues, the residues between successive prolines must either be in the polar pleated-sheet configuration or in a configuration which is some small modification of the polar pleated-sheet configuration.

4.4 β-Helix Structure for Feather Keratin

The data do not permit an unequivocal decision relative to the configuration of the polypeptide chain in the feather keratin structure; the previously proposed configurations are not adequate. The most serious difficulties of a sheet-like structure, as has been remarked, are that such a structure could not provide a natural explanation for the existence of the short 2.96A meridian reflection, the intense 33A equatorial reflection, and the long fiber axis identity period of 189A. The following considerations indicate that it is likely that the polypeptide chains assume helical configurations:* 1) In the absence of strong non-periodic forces exerted on the main chain atoms by the side chains a helical structure should result; Crane[75] has noted that any structure built from identical units which are linked together in the same way will be a helix. In the present case, the proline residues are expected to exert a strong periodic influence on the chain configuration and it is even more likely that a helical structure will result. 2) The fact that the long and short spacings change by the same percentage upon stretching, without alterations in the relative intensities of the reflections, is to be expected on the basis of a helical structure (Section 5.6).3) The short 2.96A meridian spacing requires that the residues of an extended polypeptide chain be tipped with respect to the fiber axis; such a tipping is incorporated naturally into a helix model. It will therefore be assumed that the structure of feather keratin is based on a β-helix [76]. In such a helical structure, a number of coaxial polypeptide chains would be joined together by hydrogen bonds, with the side chains projecting

* Strictly speaking, a polypeptide chain in a sheet-like structure may be considered as being a degenerate helix, with the helix operation consisting only of a translation.

alternately into and out of the cylinder formed by the main chains. On the assumption of a regular sequence of prolines, the assymetric unit for the helix consists of eight amino acid residues, i.e., proline-residue$_1$.....residue$_7$.

The previous considerations do not permit a unique determination of the parameters of the β-helix. We shall restrict our attention to a β-helix whose pitch is 189A (fiber axis identity period). This choice seems reasonable on physical grounds and the consequences of restricting the class of β-helices to those having a pitch of 189A will be investigated. Let us consider a pure β-helix (no prolines). The assymetric unit of structure in this case is two amino acid residues. The following relationships exist between the pitch P, the radius r, the pitch angle θ (the angle between the tangent vector to the helix and the helix axis), the amino acid residue length l, the number of chains n, the hydrogen bonding distance between adjacent chains d, and the number of residues per turn of the helix g:

$$P = 2\pi r \cos\theta \qquad (4\text{-}1)$$

$$P/g = \ell \cos\theta \qquad (4\text{-}2)$$

$$d \cong \frac{2\pi r \cos\theta}{n} \qquad (4\text{-}3)$$

Taking 64 as the number of residues per turn, 189A as the pitch, and 4.75A as the hydrogen bonding distance between chains [72], θ, l, and r have been computed for a range of n. The results are shown in Table IV-I. The most recent values for the bond angles and distances in the polypeptide chain[77] eliminate the cases of n = 8 and n = 12, the former having too short and the latter too large a value for the residue length

TABLE IV-I

Pitch Angle, Residue Length, and Radius of the Helix as a Function of the Number of Chains			
n	θ	l	r
8	11.60°	3.02(A)	6.19A
9	13.08°	3.04	7.00
10	14.54°	3.06	7.83
11	16.06°	3.08	8.67
12	17.55°	3.10	9.34

of a hydrogen-bonded polar chain configuration. The case of n = 11 is on the borderline as far as its residue length is concerned, and is probably not feasible. Considerations of both bond parameters and infrared dichroism show that the cases n = 9 and n = 10 are possible. The case of n = 10 has been chosen since a ten chain model would be expected to give rise to an enhancement in the x-ray diffraction pattern of the 10th, 20th, 30th.....orders of the 189A identity period while a nine chain model would give rise to an enhancement of the 9th, 18th, 27th orders. Table II-I shows that this condition is more nearly satisfied for the case of n = 10. The plausibility of the choice n = 10 is supported by the fact that the cylindrical Patterson function P(r,z) suggests a ten-fold periodicity along z. In addition, the analysis of Section 5.4 shows that the radius of the postulated unit of structure should be about 8A.

4.5 Uniqueness of the Helical Structure

It is of considerable interest to determine if the assumptions that have been introduced lead to a unique configuration of the polypeptide

chain. In order to study this problem, a set of scale models of the polypeptide chain is required. We have constructed, from 3/16" diameter steel rods, a set of such molecular models to a scale of 5 cm/A. The connectors were made in such a manner that the rotation angles around single bonds could be varied while keeping the distance between bonded atoms fixed. The dimensions of the models are based on the latest values of bond angles and distances within the polypeptide chain [77]. There are three types of fundamental units involved: 1) planar peptide groups, 2) tetrahedral carbon atoms, 3) proline residues. The planar peptide groups are in the trans configuration and have the following dimensions: N-C' = 1.32A, C'-C_α = 1.53A, N-H = 1.01A, C_α-N = 1.47A, and C' = O = 1.24A. The angles are: N-H-C' = 123°, H-N-C_α = 114°, C_α-N-C' = 123°, N-C'-C_α = 114°, N-C'-O = 125°, and O-C'-C_α = 121°. The angles at the tetrahedral carbon atom are all 109.5°; the C-H distance is 1.09A (methane) while the C-C distance is 1.54A (diamond). The residues are in the L-configuration [78]. The precise coordinates for poly-L-proline are not yet known [36]. As a first approximation, the five-membered ring is assumed to be planar and to have the dimensions of a regular pentagon of side 1.52A. Actually, the γ-carbon atom on the proline ring can be about $\pm$ 0.4A above or below the ring. [79] A planar nitrogen is used. The hydrogen atoms are located symmetrically above and below the proline rings such that the H-C-H angle is 109.5° and the C-H distance is 1.09A. A set of space-filling LaPine models, scale 1.5 cm/A, was useful for studying the steric hindrance aspect of the structure. In order to measure coordinates as accurately as possible, an aluminum grid was constructed. Marks were scribed on the grid around complete concentric circles at angular intervals of 1°.

The radii of the circles extended from approximately 1A to 10A in intervals of 0.1A. Rods were attached to a central pole (about 6' tall). The models were fixed in position by means of clamps connected to the end of the rods.

The problem must now be defined more precisely. For a given sequence of atoms along the polypeptide chain, e.g., -CO-NH-CHR- , there are four possible pure β-helices (no proline residues). The helix is either left-handed or right-handed and the CO groups in the polar chain point either to the left or the right as viewed from the outside of the cylindrical surface. The 4 helices are: 1) right-handed with the CO bonds pointing to the right, 2) right-handed with the CO bonds pointing to the left, 3) left-handed with the CO bonds pointing to the right, 4) left-handed with the CO bonds pointing to the left. These four helices are not interconvertible by any rotation and/or translation. If optimum hydrogen bonding is required,* as well as corresponding amino acid residues on neighboring chains at the same z level (in order to have prolines at the same level), structures 1 and 4 are eliminated (Figure 4-1). Structure 1 corresponds to Figure 4-1 (c) and is eliminated as the hydrogen bonding is not optimum. A similar consideration eliminates structure 4.

Before discussing structures 2 and 3, it should be noted that the Pauling-Corey polar pleated-sheet configuration has to be modified in order to form a helix with the best possible hydrogen bonding. In the polar pleated sheet structure, the CO bonds make an angle of approximately 8.5° with respect to the chain axis, and good hydrogen bonds are

* The hydrogen bonds should be as close to linear as possible[17].

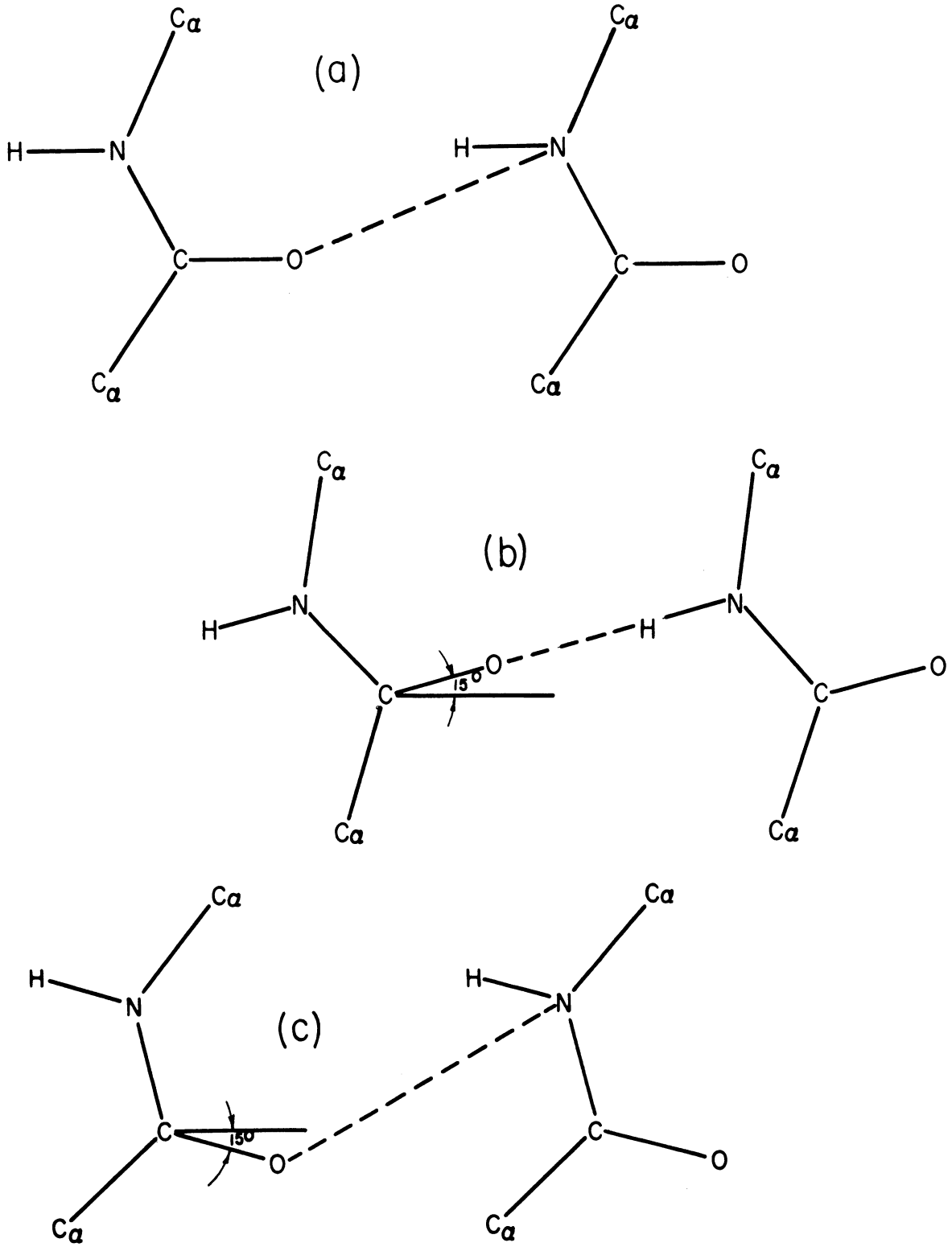

Figure 4-1 Hydrogen-bonding scheme (a) scale drawing (1.5 cm./A) of two amide groups on same vertical level placed 4.85A apart. (b) If the groups are rotated 15° counter-clockwise an almost co-linear hydrogen bond results while if the chains are rotated 15° clockwise (c) an unsatisfactory hydrogen bond results. If the CO bonds had pointed to the "left", a 15° counter-clockwise rotation would have resulted in an unsatisfactory hydrogen bond while a 15° clockwise rotation would have resulted in a more nearly co-linear bond.

formed to neighboring chains, with corresponding amino acids at the same z level, when the chain axis is vertical. It is, however, possible to construct with the models a closely related configuration in which the CO bonds make a right angle with respect to the chain axis. In this case, in order to get good hydrogen bonding with corresponding amino acids at the same z level, it is necessary to tilt the chain axis away from the vertical by about 15°. Figure 4-2 shows a schematic diagram of a Pauling-Corey extended polar polypeptide chain in which all the carbonyl groups and all the imino groups are similarly oriented. The difference between the Pauling-Corey configuration and the structure in which the CO groups make a right angle with respect to the chain axis may be described as follows: 1) in the Pauling-Corey structure the $C_{\alpha 1}$-$C_{\beta 1}$ bond is approximately coplanar with the previous N-H bond and the $C_{\alpha 2}$-H_2 bond is approximately coplanar with the previous N-H bond, 2) in the present configuration, the $C_{\alpha 1}$-$C_{\beta 1}$ bond is approximately 10° below (beneath the plane of the drawing) the $(CO_1\text{-}N_1H)_1$ plane while the $C_{\alpha 2}$-H_2 bond is approximately 10° above the $(CO_2\text{-}N_2H)_2$ plane.

We now require that proline residues be introduced into the modified Pauling-Corey configuration at every eighth amino acid residue. Figure 4-2 shows that there are two configurationally different amino acid residues in the chain repeat, i.e., the $C_{\alpha 1}$-$C_{\beta 1}$ bond is approximately cis to the preceding N-H bond, while the $C_{\alpha 2}$-$C_{\beta 2}$ bond is approximately trans to the preceding N-H bond. It might be thought that the proline residues could be placed in either of these two positions. From Figure 4-2 it can be seen, however, that the proline disrupts the chain configuration least when inserted at $C_{\alpha 1}$ and most when inserted at $C_{\alpha 2}$. (It can be thought that the proline residue is a three carbon ring from C_{β}

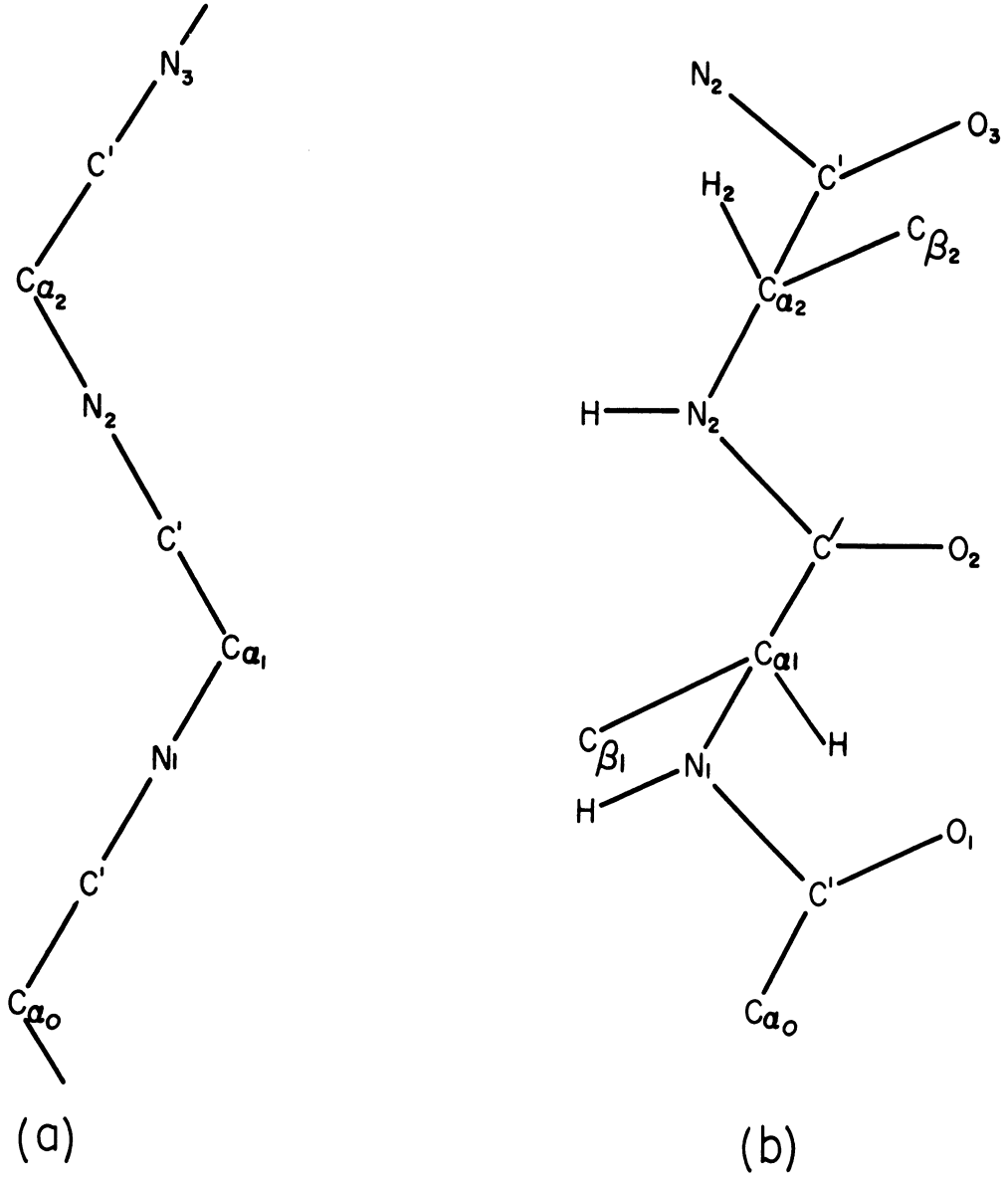

Figure 4-2 Schematic diagram of a Pauling-Corey extended polar polypeptide chain (72). The side view is indicated by (a) and the front view by (b).

to N with C_δ replacing H.) In fact, the chain makes an approximately right angle bend when the proline is inserted at $C_{\alpha 2}$. If the proline is inserted at the $C_{\alpha 1}$ atom, the plane of the amide group before the proline residue can be made almost parallel to the plane of the amide group after the proline residue. When the correct position for the insertion of the proline residues is chosen, the proline rings are on the inside of the cylinder formed by helix 2 and on the outside of the cylinder formed by helix 3.

Before considering the attempts to construct helices 2 and 3, it is necessary to introduce some data concerning the van der Waals radii of carbon and hydrogen. Various values for the van der Waals radius of hydrogen have been quoted in the literature; Stuart quotes a value of less than 0.90A, Briegleb a value of 0.95A, and Pauling a value of 1.2A[80].* The value for the van der Waals radius of an aliphatic carbon atom (σ-electrons) is 1.35A according to Stuart and 1.5A according to Briegleb. The sum of the van der Waals radii of carbon and hydrogen cannot be much less than about 2A. Thus, it seems reasonable that if a carbon-hydrogen contact is less than about 2A instability will result.

Attempts to construct helix 3 were unsuccessful due to a short van der Waals contact between the $C_\alpha C_\beta H$ atoms on the first amide groups after the proline rings. If the corresponding groups on two neighboring chains are labeled $C_{\alpha 1}C_{\beta 1}H_1$ and $C'_{\alpha 1}C'_{\beta 1}H'_1$ respectively, the short contact is between $C_{\beta 1}$ and H'_1 (Figure 4-3). It was not possible to

* In the values quoted by Stuart and Briegleb, the thermal motion of the atoms has been taken into account.

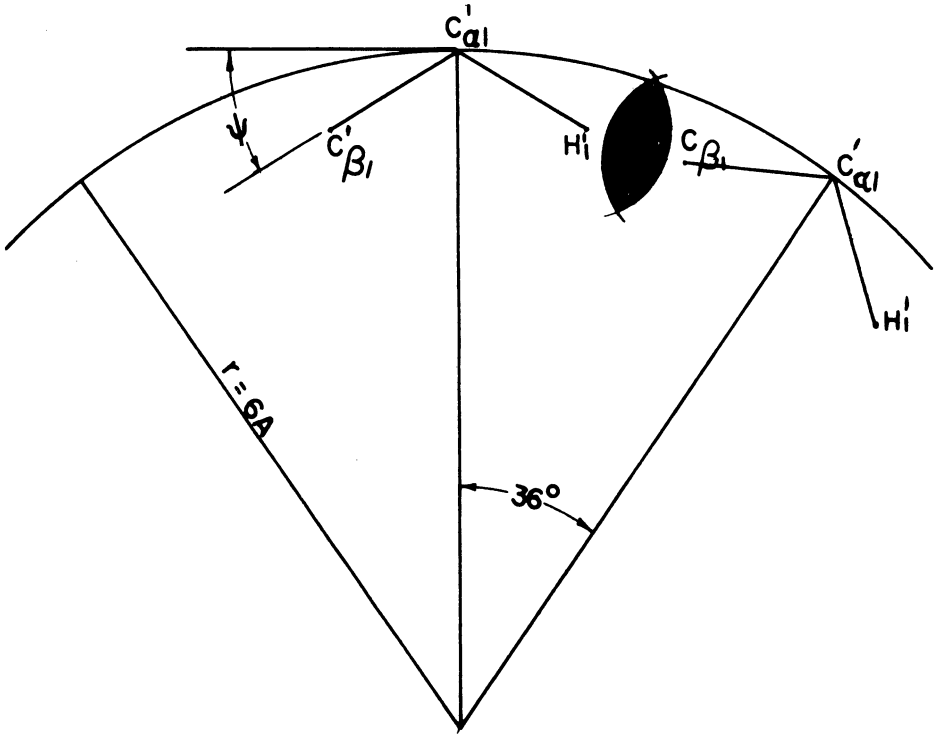

Figure 4-3 Diagrammatic representation of short van der Waals contact. The short contact is indicated by darkened area representing the overlapping of the van der Waals spheres of H_1' and $C_{\beta 1}$.

increase this contact to a value greater than 2A and still maintain the modified polar pleated-sheet configuration. Most of the attempts to construct helix 3 resulted in a smaller value than 2A for this contact. In fact, the hydrogen bonding between chains had deteriorated seriously by the time the contact was up to 1.8A. The reasons for the short contact are twofold: 1) the α-carbon atoms under consideration are located at approximately 6A radius (a decrease of approximately 3A from the set of α-carbon atoms located at the 9A radius occurs due to the "pleating" of the chains), 2) when the chains are tipped to form the left-handed helix it can be seen by using molecular models that the $C_\alpha C_\beta H$ groups form a plane which makes only a small angle with the horizontal. If we assume that the α-carbon atoms lie at a radius of 6A and that the $C_\alpha C_\beta H$ groups are horizontal, than a graphical calculation of the $C_{\beta 1} - H_1'$ contact can easily be made as a function of the angle ψ between the $C_\alpha - C_\beta$ direction and the tangent vector (Figure 4-3). The results are shown in Table IV-II.

TABLE IV-II

$C_{\beta 1}H_1'$ Contact as a Function of the Angle ψ	
ψ (degrees)	$C_{\beta 1}$-H_1' (distance in A units)
0	2.0
10	1.7
20	1.4
30	1.2
40	1.2
50	1.5
60	1.8
70	2.3
80	2.7
90	3.0

It is evident that the only way to increase the van der Waals contact beyond 2.0A is to use angles from 70-90°. But when the C_α-C_β bond points in the radial (or approximately radial direction), model building shows that the configuration of the chain approaches the parallel-chain or the anti-parallel chain pleated sheet configurations, i.e., the anti-polar configurations. According to the considerations of Section 4.3, these configurations must be ruled out. Hence, it is not possible to construct helix 3.

Helix 2 is the only remaining possibility. The uniqueness of the solution (if it exists) has been demonstrated. To recapitulate: of the four possible helices which could form regular structures, 1 and 4 have been eliminated on the basis of forming poor hydrogen bonds, and 3 has been eliminated on the basis of a too short van der Waals contact. The possibility of building helix 2 must now be considered.

4.6 Construction of a Molecular Model

We consider first the conditions that an acceptable structure should satisfy: 1) conditions involving hydrogen bond lengths and angles, 2) conditions involving van der Waals contacts.

Most of the observed NH....O hydrogen bond lengths in crystal structures (the lengths between the nitrogen atom and the hydrogen-bonded oxygen atom) fall in the range 2.7A to 2.9A[81]. The angles between the NH and NO vectors are variable but it is reasonable to require that the vector from the nitrogen atom to the hydrogen-bonded oxygen atom lie not more than 30° from the NH direction.[25] In

considering the problem of constructing helix 2, these criteria have been accepted.

The second set of conditions a structure must satisfy involve the van der Waals contacts. As has been mentioned the van der Waals radius for carbon (σ-electrons) is about 1.3A. According to Pauling[82], the van der Waals radius of an oxygen atom is 1.4A. It is therefore required that a carbon-carbon contact should be no less than 2.6A and that a carbon-oxygen contact should be no less than 2.7A. "Short" carbon-hydrogen contacts introduce considerably less strain energy into a structure than short carbon-carbon contacts or short carbon-oxygen contacts. If we accept Pauling's value of 1.2A for the van der Waals radius of hydrogen, a carbon hydrogen contact should be no less than 2.5A. It can be shown, however, that a value for a carbon-hydrogen contact of as low as 2A would not be likely to introduce serious instability into a structure. We now wish to make a semi-quantitative estimate of the amount of strain energy introduced into a structure by a hydrogen-carbon contact of 2A. In this case, the "effective value" for the radius of the hydrogen atom is 0.7A. Using the empirical equation quoted in Stuart[83] for the intermolecular potential between two methane molecules, it can easily be calculated that the amount of strain energy involved in bringing the molecules to a distance of 3.56A apart is about 1.3kcal/mole while for an intermolecular distance of 3.36A the strain energy is about 3.35kcal mole. Breaking up the intermolecular distance into two C-H distances (1.18A) plus double the effective radius of the hydrogen atoms, a value for

this radius of 0.7A is obtained for an intermolecular distance of 3.56A while a value of 0.6A is obtained for an intermolecular distance 3.36A. The strain energy of 1.3kcal/mole obtained for an intermolecular distance of 3.56A is low compared to the estimated energy of a hydrogen bond of about 8 k cal/mole.[25] Pauling[82] has quoted a value for the radius of a methyl group of about 2A as determined from crystal structure determinations. The diameter of methane in the gaseous state is 3.08A as determined from Sutherland's model, 3.28A as determined from viscosity data, and 3.23A as determined from the van der Waals coefficient b.[84] Thus, it can be inferred that the effective diameter of a methyl group depends on the state of a system. It is therefore reasonable to assume that in a hydrogen-bonded fibrous system, where the attractive forces of the hydrogen bonds play an important role, the "effective radius" for a hydrogen atom involved in a carbon-hydrogen contact may be somewhat smaller than the radius as determined from crystal structures. In particular, it is concluded that an effective radius for hydrogen of about 0.7A can be employed and that a C-H contact of about 2.0A will not introduce serious instability into a fibrous structure.

We now consider the problem of constructing helix 2 (the right-handed helix with the prolines on the inside of the cylindrical surface and the CO bonds pointing to the left). As has been remarked, the asymmetric unit of structure for this β-helix consists of eight amino acid residues, i.e., proline-residue$_1$.....residue$_7$. The additional requirement imposed by the helix is that every eighth residue in the structure be related by a rotation of 45° around the helix

axis and a translation of 23.6_4A along the helix axis. In order for the proline rings to pack at the same vertical level, corresponding residues on adjacent chains are related by a 10-fold rotation axis. As has been noted, the non-proline residues are required to be in a polar configuration with the CO bonds all similarly oriented and the NH bonds having the opposite orientation. The hydrogen bonding is between corresponding residues on adjacent chains.

The analytical geometry involved in solving this problem is very complex as the number of residues (eight) in the assymetric unit of structure is large. For example, in the case of the α-helix there is only one residue in the assymetric unit. In addition, the proline residues introduce discontinuities into the chain configuration. In order to obtain a preliminary idea of the stereochemical feasibility of the proposed structure, the simpler problem of a pure β-helix having no proline residues was considered first. In this case, the number of residues in the assymetric unit of structure is reduced to 2 and it is not necessary to introduce discontinuities into the chain configuration. The problem is therefore susceptible to a direct attack by the methods of analytical geometry. The results of the calculations indicate that it is possible to construct pure β-helices of the type proposed (see Appendix B).

When the prolines are introduced into the chain, the large number of undetermined parameters in the system make the problem too difficult to attack by methods of analytical geometry

alone. An attempt was therefore made to obtain a solution by the use of molecular models. Due to the large number of unknown parameters, the exact starting point was not clear. There was, however, one important clue. Since the prolines are not expected to introduce serious discontinuities into the chain configuration, the problem was considered as a "perturbation calculation" with some of the important parameters being approximately determined from the case of a pure β-helix. By choosing reasonable variations in the important parameters of the system, such as the orientation of the proline rings, the rotation angles in the proline unit,* and the value for the radius of the first carbonyl oxygen atom before the ring, the range of the hydrogen bond lengths and angles and of the van der Waals contacts was investigated. Before discussing the results, it should be mentioned that in order to insure the formation of a helix the oxygen atom on the seventh amide group after the proline was fixed in a position which was rotated 45° and translated 23.6_4A with respect to the oxygen atom on the amide group before the proline. The angle of the normal to the plane of the amide group before the proline with respect to the helix axis was made equal (within a few degrees) to the angle of the normal to the plane of the seventh amide group after the proline with respect to the helix axis. It should also be noted that it is only necessary to consider the problem for two chains and for a z distance of 23.6_4A as the rest of the structure is determined by symmetry.

*The proline unit is defined as extending from one amide group before the proline to one amide group after the proline.

As a result of the model building, it was determined that the hydrogen bond lengths were in the range 2.7A to 2.9A. The angles between the vectors from the nitrogen atoms to the hydrogen-bonded oxygen atoms were always less than 30°. Thus, the criteria for forming good hydrogen bonds was satisfied.

The carbon-oxygen van der Waals contacts were all equal to or greater than 2.7A as required. The contacts between the β-carbon atoms on chain 2 and the hydrogen atoms on the α-carbon atoms on chain 1 for the three out of eight side chains which point toward the inside of the cylinder varied from about 1.9A to 2.1A. The remaining contacts involve those on the proline rings. If a planar proline ring were employed, the contact between the α-carbon atom on chain 1 to the hydrogen atom on the γ-carbon atom on chain 2 would be short by about 0.3A. The γ-carbon atom, however, can be 0.4A below the ring (Section 4.5). For this position of the γ-carbon atom, the contact between the α-carbon atom on chain 1 and the γ-carbon atom on chain 2 was at least 2.6A. A contact between a H atom on C_α (chain 1) to a H atom on C_γ (chain 2) was about 1.4A and a contact between a hydrogen atom on C_β (chain 1) to a hydrogen atom on C_γ (chain 2) was also about 1.4A. If it were possible to use flexible models which, for example, could introduce measurable and reasonable distortions at the tetrahedral carbon angle, the contacts between the hydrogens and the β-carbons of about 1.9A to 2.1A could almost certainly be made 2A or greater. In addition, the bond angles in the polypeptide chain itself may vary somewhat from the ones which have been employed. The

configuration around the proline ring is not yet known with certainty and also may vary slightly from the configuration which we have used. It is concluded that the proposed structure satisfies the criteria of forming acceptable van der Waals contacts which have been discussed previously.

One general feature of the proposed model is that the axial projections of the proline residues and the residues near the prolines are somewhat shorter than the axial projections of the remaining residues. Thus, the proposed structure deviates from the usual β-structures in not possessing as much regularity in the z direction. The general x-ray consequences of this deviation will be discussed in Section 5.3.

Figure 4-4 shows a photograph of two chains of the proposed model. Eight amino acid residues, one of which is a proline, are shown on each chain.

A preliminary attempt to obtain a set of coordinates has been made (see Appendix C). This attempt was based on using the measured values of the coordinates of the α-carbon atoms as determined from the model. A generalization of the methods discussed in Appendix B was employed but resulted in a fairly large cumulative error. Better coordinates can be obtained from direct measurements on the model. Due to experimental difficulties, the final coordinates as determined from model building will be accurate to no more than $\pm$0.1A.

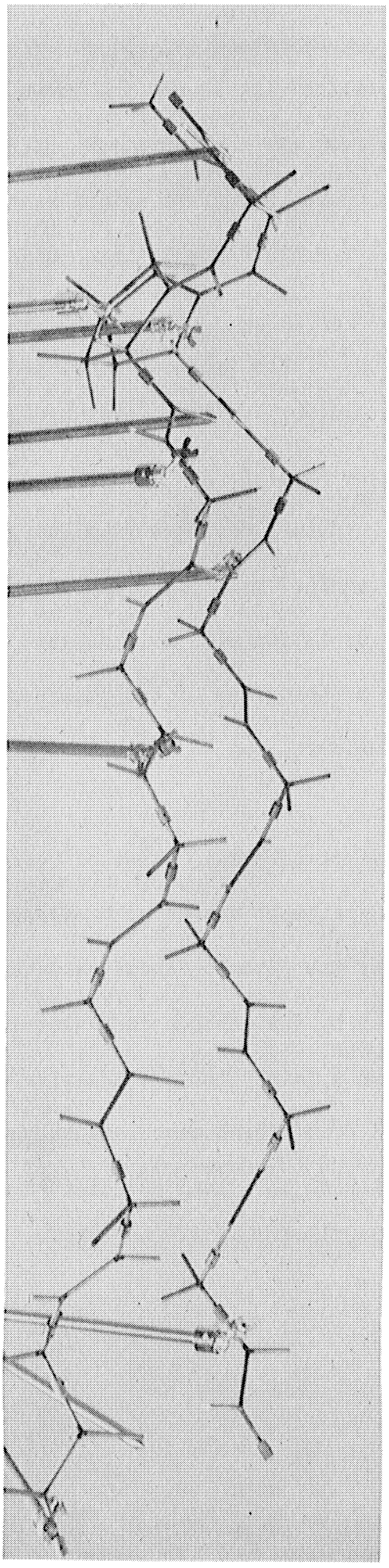

Figure 4-4 - Photograph of molecular model of proposed feather structure.

CHAPTER V

EVALUATION OF THE β-HELIX HYPOTHESIS

5.1 Introductory Remarks

As we have just seen, the β-helix hypothesis has led to a unique unit of structure for feather keratin. It is now necessary to evaluate the extent of agreement between the proposed model and the data.

The x-ray data will be considered first. The following points will be discussed: 1) an attempt to determine whether a reasonable packing arrangement of the cylindrical molecules will be in agreement with the equatorial diffraction pattern, 2) a preliminary attempt to explain the meridional and near-meridional diffraction pattern, 3) an independent attempt, by means of a radial Fourier analysis, to estimate the mean radius of the postulated cylindrical unit of structure, 4) an evaluation of the extent of agreement of the model with the cylindrical Patterson function, and 5) an attempt to explain the alterations in the x-ray diffraction pattern produced by physical and chemical treatment of the sample.

The infrared, chemical, and density data will then be considered. The following points relevant to the infrared data will be discussed: The agreement of the proposed model with the measured dichroism of the NH stretching band, and the question of whether a doubling of the CO stretching frequency in the infrared necessarily implies the presence of a component of α protein in the structure. From the chemical point of view, the agreement of the model with the observed proline content of feather keratin was the starting point of the present work. The main independent facts which must be accounted for are the following: 1) upon solubilizing feather keratin,

a homogeneous particle whose molecular weight is about 10,000 is obtained, 2) the axial ratio of this particle, on the basis of the assumption of a prolate ellipsoid of revolution, is at least 5/1, 3) the particle apparently has no end-groups. Definitive knowledge concerning the details of partial hydrolysis, cyclization, end-group determinations etc. is not available. We will therefore only attempt to suggest a reasonable mechanism which could explain the main features of the solution data. The density of the proposed model is lower than the measured density of feather keratin. This discrepancy is discussed in relation to the available data on the density of fibrous proteins, and the possibilities for explaining the discrepancy are noted.

5.2 Equatorial Diffraction Pattern

In order to calculate the equatorial diffraction pattern of the proposed model it is necessary to know the molecular packing arrangement. The most natural possibility would be for the cylindrical molecules to pack in a hexagonal or pseudo-hexagonal manner. Primarily due to the incomplete nature of the data, it has not been possible to deduce unambiguously the exact form of the packing. For example, the reality of the 115A (medium), 81.8A (medium), and the 51.0A (faint) equatorial reflections measured by Corey and Wyckoff[42] has been questioned by Bear[44], who attributed them to radiation artifacts. In the present studies, the approximately 50A equatorial reflection has been observed clearly on some photographs, but the final resolution of the existence of the long equatorial spacings must be decided by more detailed low-angle scattering experiments. We will, however, tentatively assume the reality of at least the "50A"

equatorial reflection.

Despite the uncertainties involved, it is possible to examine various packing schemes for their plausibility and agreement with the data. The first condition a packing arrangement must satisfy is to predict a very intense equatorial spacing in the region of 31-34A. Assuming that alternate side chains extend approximately 3.2A beyond the main chain radius of 8A, the diameter of the proposed cylindrical unit is about 22.4A. Since the 100 reflection from an assumed hexagonal cell with a_0 = 22.4A is 19.4A, the unit cell, if it exists, must contain more than one cylindrical unit.

Aggregation of cylindrical molecules into larger structures, due to the presence of -S-S- and salt linkages, is a well known phenomenon in fibrous proteins.[85] In the present case, the first possibility is that the cylindrical molecules tend to form stable aggregates of 3-unit groups. The independent scattering from 3-unit groups, i.e., with no long range side-to-side order, would not be expected to give a strong 33.5A equatorial reflection, since the only inter-cylinder distance is 22.4A. Stable aggregates of 3-unit groups may pack hexagonally as shown in Figure 5-1. If the diameter of an individual cylinder is 22.4A, the value of a_0 for the hexagonal unit cell is 38.7A. With respect to the x,y coordinate axes, the centers of the cylinders are located at: (0,0), (1/3,2/3),(2/3,1/3).* The structure factor for a set of unit scatterers located at these points is given by: $G_{hko} = \left[1 + e^{i2\pi(\frac{h+2k}{3})} + e^{i2\pi(\frac{2h+k}{3})}\right]$. The spacings d_{hk0} for a hexagonal lattice of unit cell length a_o are: $d_{hk0} \frac{a_o}{\sqrt{4/3(h^2+hk+k^2=1)}}$. From this it will be seen that the 100 and $1\bar{1}0$ reflections, which correspond

* The coordinates are expressed in fractional parts of the unit cell lengths.

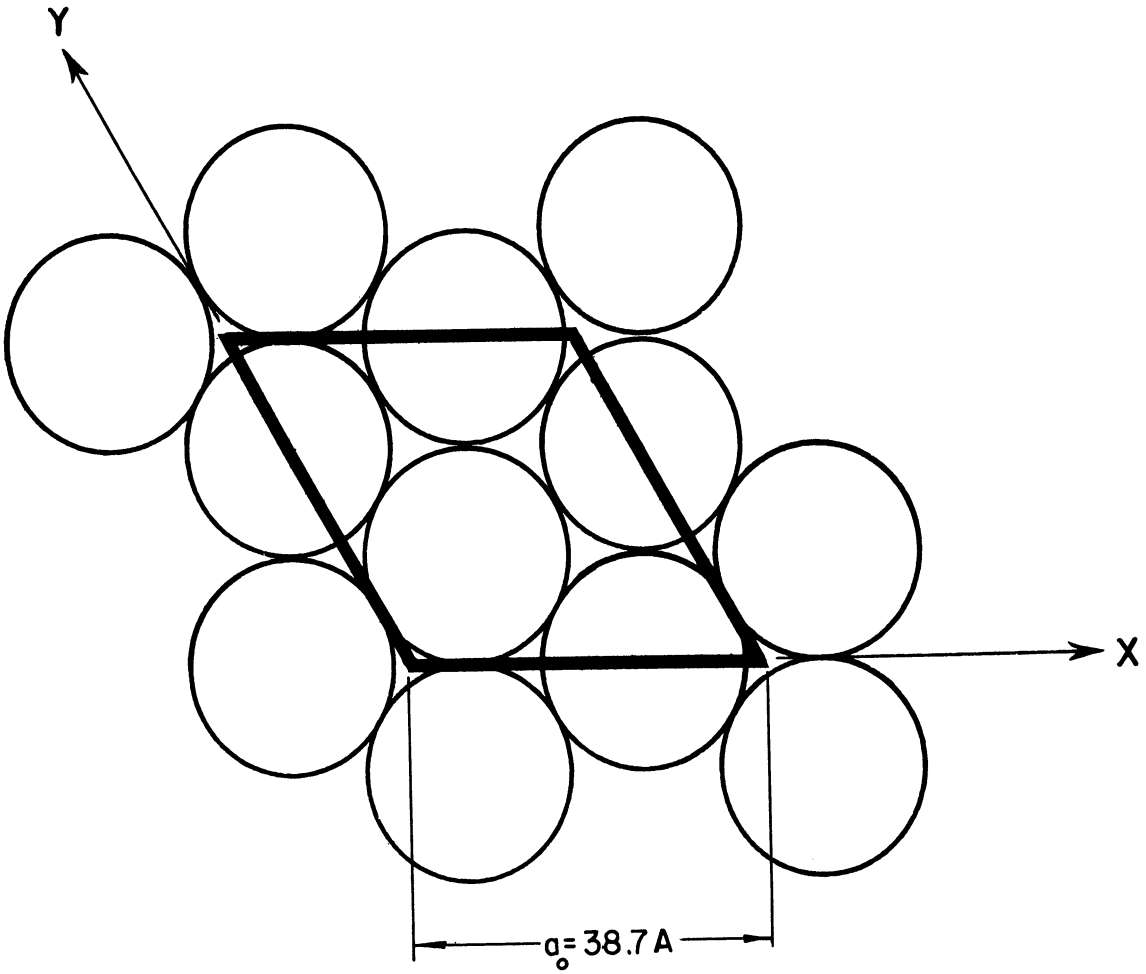

Figure 5-1 Hexagonal packing arrangement of three-unit groups.

to a spacing of 33.5A, would be predicted to have zero intensity. (It has been verified that the transform of the individual cylindrical unit is very strong at $R = 1/33.5A^{-1}$.) Finally, it would be impossible, on the basis of the packing proposed above, to account for the existence of spacings greater than 33.5A. The possibility of lattice expansion relative to the 3-unit groups was examined, but very little improvement was noted.

Another possibility involving the packing of 3-unit groups is the orthorhombic arrangement shown in Figure 5-2. If a diameter of 22.4A is assumed for the individual cylinder, $a = 3\ d = 67.2A$, $b = \sqrt{3}\ d = 38.8A$. With respect to the x,y coordinate axes, the centers of the cylinders are located at: (0,0), (1/6,1/2), (1/3,0), (2/3,0), (1/2,1/2), and (5/6,1/2). The spacings d_{hk0} are given by: $d_{hk0} = \frac{1}{\sqrt{h^2/a^2 + k^2/b^2}} = \frac{67.2A}{\sqrt{h^2 + 3k^2}}$. The 200 and 110 reflections correspond to a spacing of 33.6A. Their calculated structure factor is zero. Furthermore, this lattice does not predict a spacing in the 50A region. The possibility of lattice expansion relative to the 3-unit groups was examined but, as in the previous case, little improvement was noted.

The aggregation into isolated units of seven cylinders was considered as the next most plausible packing arrangement. Figure 5-3 shows a 7-cylinder unit. The intensity of scattering from the 7-cylinder unit was obtained by multiplying the intensity transform for a 7-point "lattice" (whose points are located at the centers of the cylinders) by the intensity transform for an individual cylindrical unit. The individual cylindrical unit was assumed to consist of a hollow cylinder of electron density at r = 8A, weighted 1/2 (representing the main chains), and a uniform shell of electron density from r = 3A to r = 11.2A, weighted 1/2 (representing

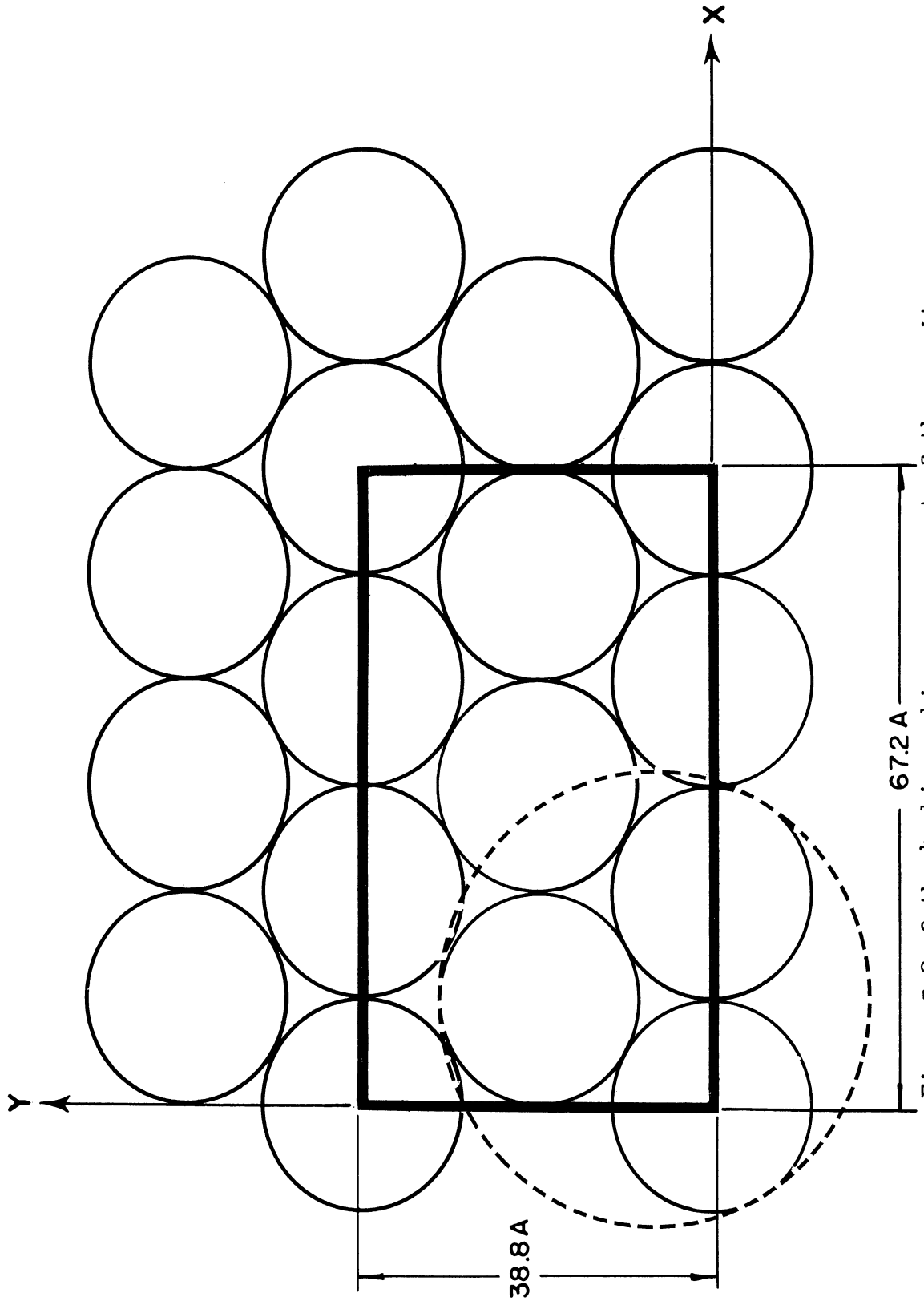

Figure 5-2 Orthorhombic packing arrangement of three-unit groups.

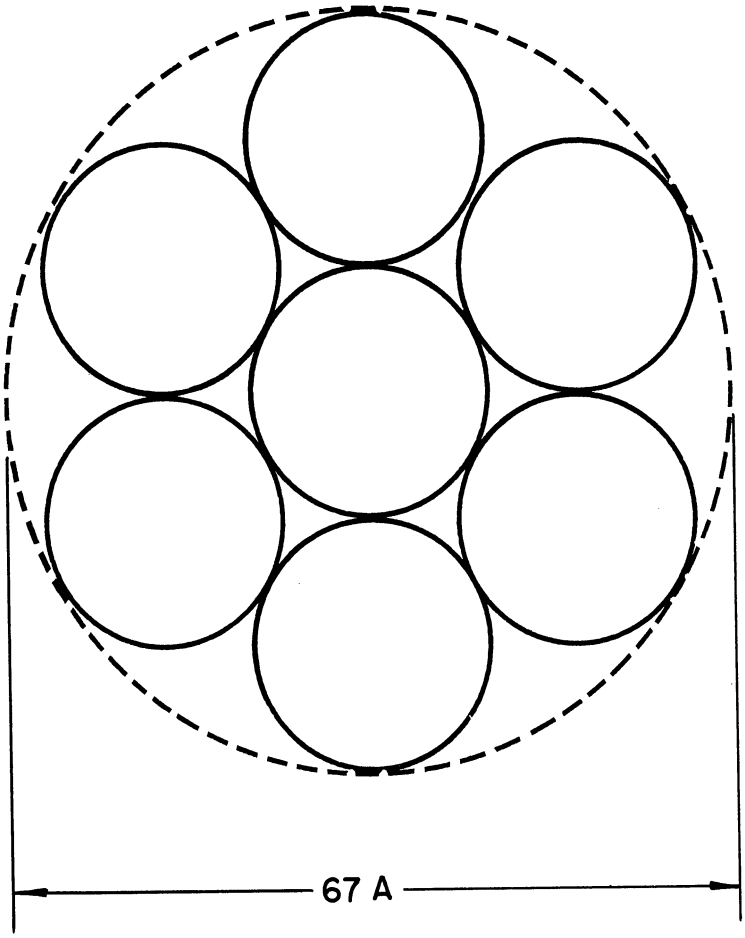

Figure 5-3 Seven cylinder unit.

the side chains). It should be noted that this is an approximation to the projected electron density of the cylindrical unit. The calculations were performed before the coordinates of the atoms in the main chains had been determined. We have observed, however, that many different reasonable approximations to the projection on a horizontal plane of the cylindrical unit of structure give approximately the same result for many of the features of the equatorial scattering.

The normalized intensity of n points in central hexagonal arrangement is given by:[86]

$$P_n = \frac{1}{n^2} \sum_p \sum_q J_0 (2\pi R s_{pq}) \qquad (5\text{-}1)$$

where the centers of the pth and q^{th} points are at a distance s_{pq} apart. The transform of a hollow cylinder of radius r is given by:

$$F = J_0 (2\pi r R)^* \qquad (5\text{-}2)$$

where R is the radial coordinate in reciprocal space. The transform of a uniform shell of electron density whose inner radius is r_1 and whose outer radius is r_2 is given by:

$$F = 2 \left[\frac{(2\pi r_2 R) J_1 (2\pi r_2 R) - (2\pi r_1 R) J_1 (2\pi r_1 R)}{(2\pi r_2 R)^2 \left(1 - \left(\frac{r_1}{r_2}\right)^2\right)} \right] \qquad (5\text{-}3)$$

---

* The formulas apply to the scattering per unit area.

Hence, the transform of the cylindrical unit described above is:

$$F_c = \left[\tfrac{1}{2} J_0(50.2R) + \frac{70.4RJ_1(70.4R) - 18.8RJ_1(18.8R)}{(.928)(4950)R^2}\right] \quad (5\text{-}4)$$

The scattering for the unit is as usual proportional to F^2. We finally obtain the intensity of scattering from the 7-cylinder unit for an inter-cylinder distance of 22.4A

$$I_7 = \tfrac{1}{49} F_c^2 \left[7 + 24 J_0(141R) + 6 J_0(182R) + 12 J_0(244R)\right] \quad (5\text{-}5)$$

The intensity transform of the 7-cylinder unit is shown in Figure 5-4. The scattering begins to show agreement with certain of the significant features of the experimental data. In particular, a strong peak is predicted near 33A. The intensity is also high near 11A. This unit, however, does not give complete agreement with other features of the equatorial diffraction pattern. For example, whereas feather keratin exhibits a strong equatorial reflection at about 50A (Table II-II), the intensity in the 50A region predicted by the isolated 7-cylinder unit is very low. In addition, the reflection at about 33A arises only as a diffraction effect of the total unit, and in fact the predicted spacing is closer to about 40A.

In an effort to determine the effect on the equatorial scattering of increasing the number of cylinders in the unit, the intensity transform of a 19-cylinder unit was calculated. The 19-cylinder unit is unacceptable, as it predicts practically zero intensity for the very strong 33A equatorial reflection.

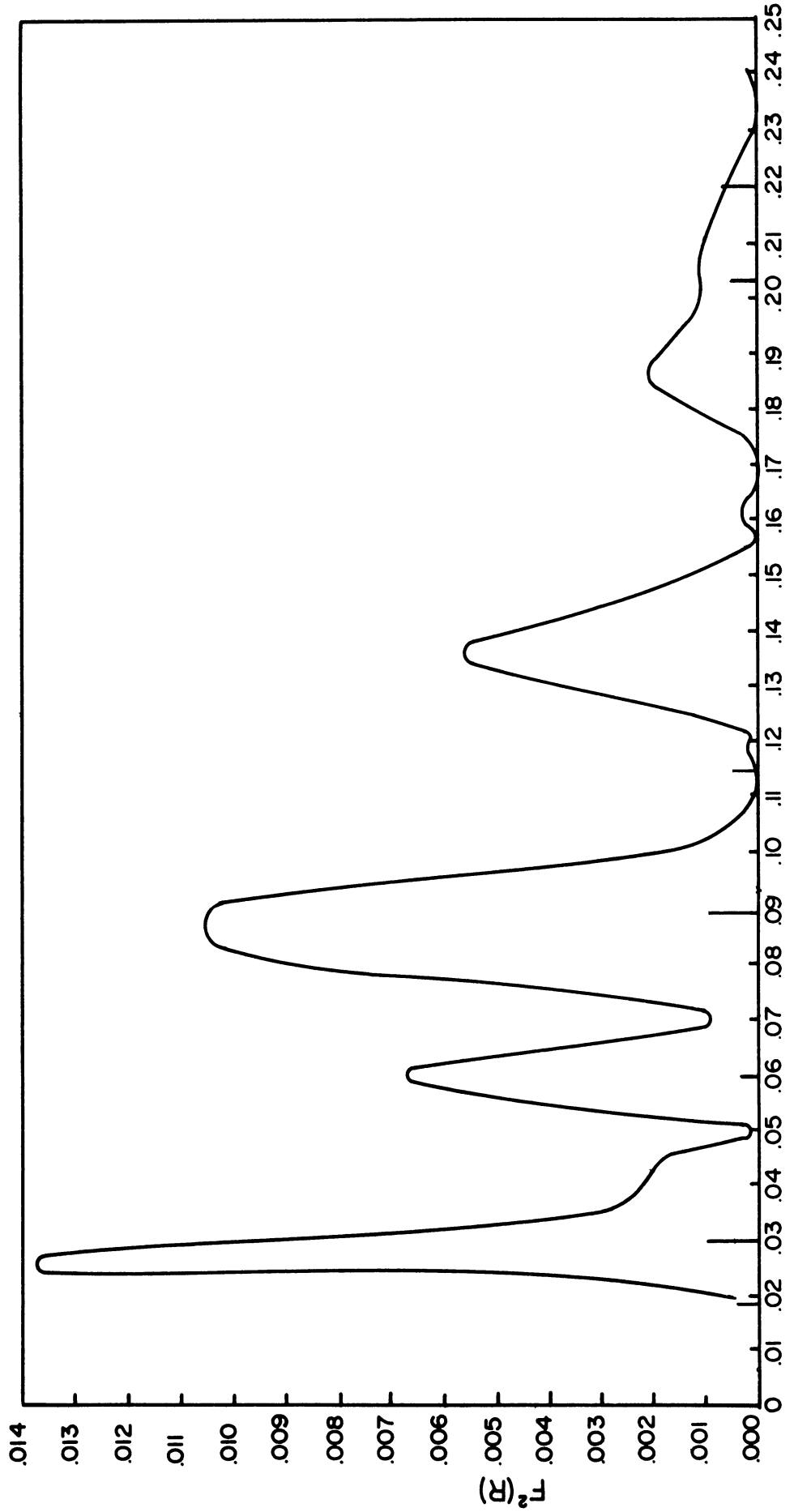

Figure 5-4 Equatorial scattering of the seven cylinder unit. The vertical lines indicate the relative intensities of the equatorial reflections in the feather keratin diffraction pattern.

The packing of the 7-cylinder units in a hexagonal lattice was examined next. This is a likely way in which such units would pack. Figure 5-5 shows a possible packing arrangement for the feather keratin molecules. In this case, two different approximations were used for the projected electron density of the cylindrical unit. Structure 1 approximates the projected electron density of the cylindrical unit by a hollow cylinder of radius 7.83A weighted 1/2 to represent the main chains, and three hollow cylinders of radii 3A, 5A, and 10A weighted 1/8, 1/8, and 1/4 respectively, to represent the side chains. Structu 2 approximates the cylindrical unit by a hollow cylinder of radius 8A weighted 1/2 to represent the main chains and two hollow cylinders of radii 5A and 10A, each weighted 1/4 to represent the side chains. In addition, 5% of the scattering power for structure 2 was assumed to be water and was located at $r = 3A$. Figure 5-6 shows the transforms of the two cylindrical units which were calculated according to the methods described previously. The intensity transform of the packing arrangement shown in Figure 5-5 was then determined by a usual structure factor calculation. The centers of the cylinders in the unit cell are located at: (0,0), (1/3,0), (2/3,0), (1/3,1/3), (2/3,2/3), (0,1/3) and (0,2/3). The structure factor for a set of unit scatterers located at these points is given by:

$$G_{hko} = \left[1 + e^{\frac{i2\pi h}{3}} + e^{\frac{i4\pi h}{3}} + e^{\frac{i2\pi(h+k)}{3}} + e^{\frac{i4\pi(h+k)}{3}} + e^{\frac{i2\pi k}{3}} + e^{\frac{i4\pi k}{3}}\right] \quad (5\text{-}6)$$

The structure factor for the 7-cylinder unit placed in the hexagonal

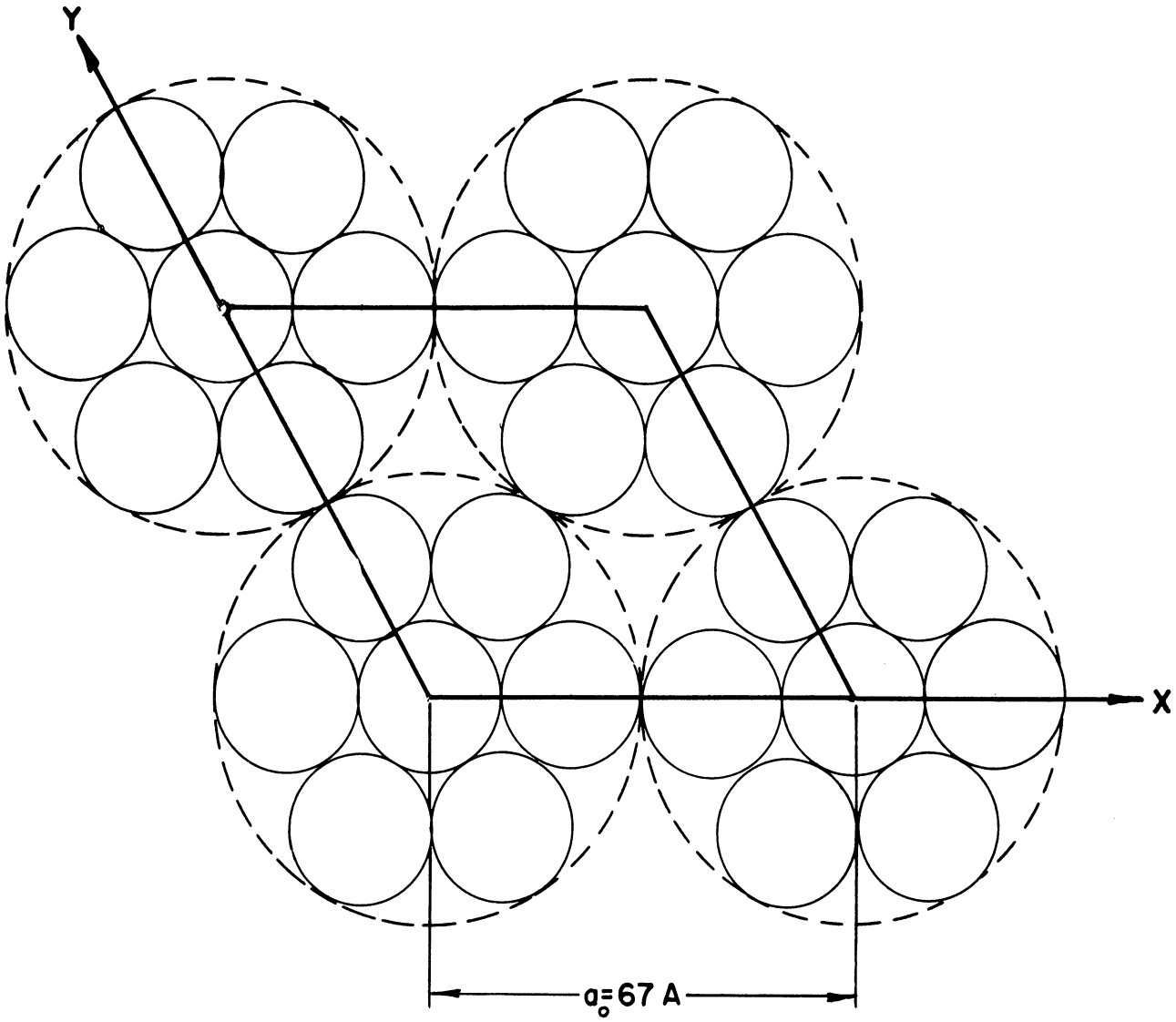

Figure 5-5 Hexagonal packing of seven cylinder units. The dotted circles represent the cross-sectional view of the molecular envelopes of the cylindrical units.

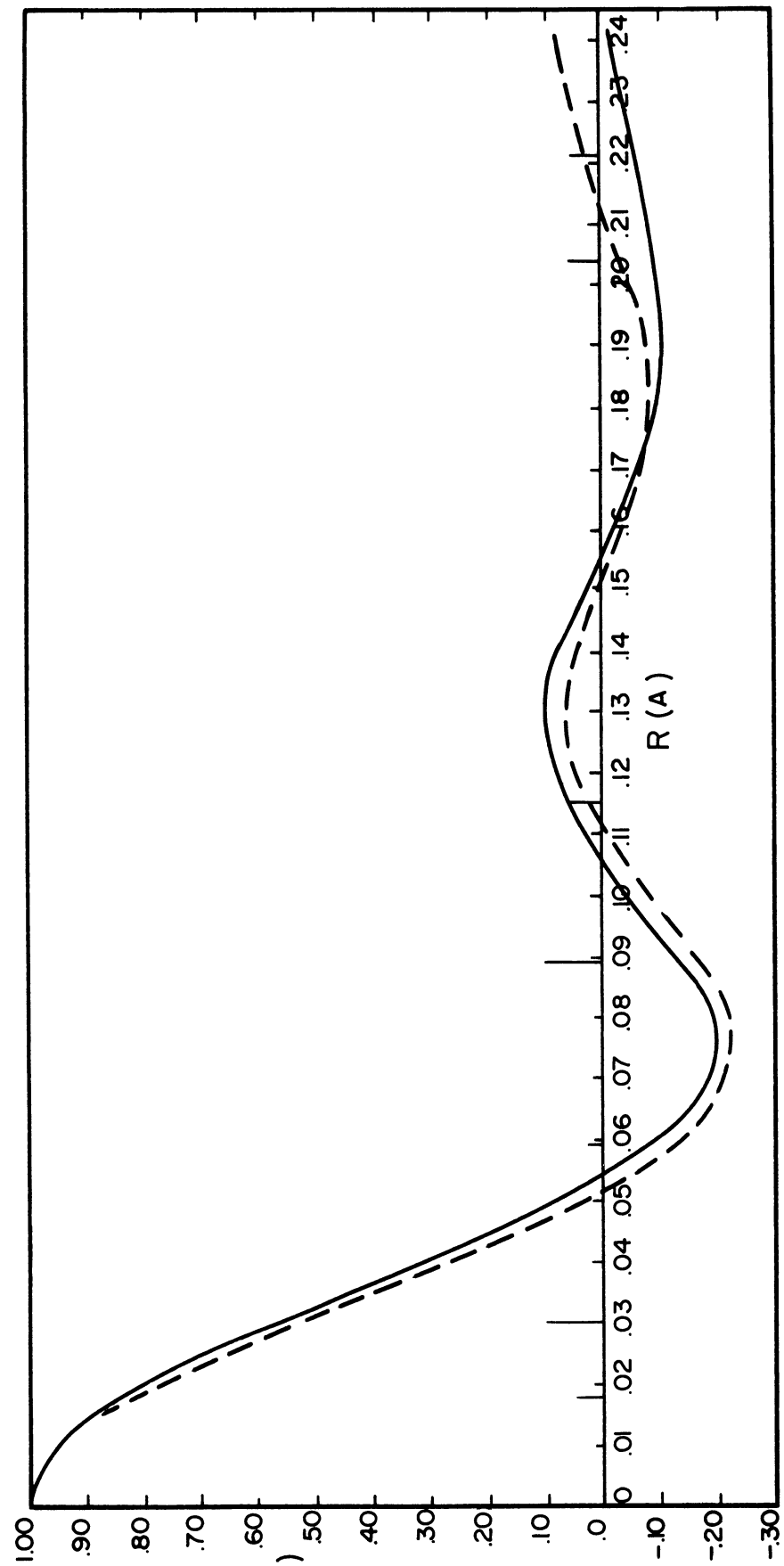

Figure 5-6 Equatorial transforms of the cylindrical units. The solid curve represents the equatorial transform of hollow cylinders located at r=7.8A, r=10A, r=3A and r=5A weighted 1/2, 1/4, 1/8, and 1/8 respectively. The dotted curve represents the equatorial transform of hollow cylinders at r=8A, r=5A, and r=10A weighted 1/2, 1/4, and 1/4 respectively plus 5% water at r=3A. Vertical lines indicate estimated intensities for equatorial reflections of feather keratin.

lattice is the product of the structure factor of the set of unit scatterers described above and the structure factor for an individual cylindrical unit:

$$F_T(h\,k\,o) = F_c(R_{hko})\,G_{hko} \qquad (5\text{-}7)$$

where $F_{T(hk0)}$ represents the transform of the 7-cylinder unit evaluated at the reciprocal lattice points for the hexagonal lattice, $d_{hk0} = \frac{67.2A}{\sqrt{4/3(h^2 + hk + k^2)}}$ and $R_{hk0} = 1/d_{hk0}$. The resulting intensities are as usual proportional to $(F_T)^2$. The Lorentz and polarization factors were computed as small and were omitted. To obtain the final intensities, the values of $F_T^2(hk0)$ were multiplied by the multiplicity factor which gives the number of reflecting Bragg planes for a given spacing. The results of the calculation are shown in Table V-I.

Certain of the important features of the equatorial diffraction pattern are well explained by this model. The very strong "33.5A" equatorial reflection, is predicted to have the highest intensity for any of the equatorial spots for structure 1 and is predicted to be only slightly weaker than the intense 11.2A reflection for structure 2. Thus, the very strong 33.5A and 11.2A spots are well explained. In addition, the "55A" equatorial reflection is predicted to be a strong reflection as observed.

The agreement with the data is less satisfactory for the 8.85A equatorial reflection. This reflection, which is weak in the diffraction pattern of turkey, is predicted to have zero intensity. (The 8.85A equatorial reflection is a medium intensity reflection in sea gull quill.) The reason for the discrepancy is not clear as the transform of the cylindrical unit of structure is small at $R = 1/8.85A^{-1}$. The model also predicts a strong or medium intensity reflection at 7.30A which is not ob-

TABLE V-I

Equatorial Reflections of the Proposed Feather Structure (1)*

Calculated			Observed	
Reflection	Spacing (A)	Intensity	Spacing (A)	Intensity
100	58.0	4152	~55	s
110	33.5	7380	33.5	vs
200	29.0	1134	~26(?)	w
300	19.4	264		
220	16.8	216	17.1	mw
410	12.7	1740		
330	11.2	5370	11.2	vs
600	9.65	66		
610	8.85	—	8.84	w(?)
630	7.30	4764		
900	6.43	—		
660	5.58	2640	~ 5.8	w
930	5.36	6240		
1200	4.84	244		
1120	4.80	374		
770	4.80	198		
860	4.80	94		
950	4.74	83		
1040	4.67	284	~ 4.66	m(diffuse)
1210	4.63	63		
1130	4.57	54		
1300	4.48	19		
870	4.48	37		
960	4.45	94		

* The experimental equatorial spacings and intensities used were based on the data obtained from an earlier diffraction photograph than that employed in compiling Table II-I.

TABLE V-I (Continued)

Equatorial Reflections of the Proposed Feather Structure (2)

Calculated			Observed	
Reflection	Spacing (A)	Intensity	Spacing (A)	Intensity
100	58.0	4020	~55	s
110	33.5	6840	33.5	vs
200	29.0	1056	~26(?)	w
300	19.4	264		
220	16.8	288	17.1	mw
410	12.7	2328		
330	11.2	8520	11.2	vs
600	9.65	594		
610	8.85	—	8.84	w(?)
630	7.30	1776		
900	6.43	120		
660	5.58	1980	~ 5.8	w
930	5.36	3300		
1200	4.84	235		
1120	4.80	241		
770	4.80	12		
860	4.80	6		
950	4.74	—		
1040	4.67	—	~ 4.66	m(diffuse)
1210	4.63	—		
1130	4.57	4		
1300	4.48	8		
870	4.48	16		
960	4.45	117		

served and a strong or medium reflection at about 5.8A which is observed weak. Examination of Table V-I indicates that the predicted intensity for these reflections is sensitive to the approximation used. In addition, the relative intensity of these reflections with respect to the reflections at smaller R values would be lowered if the atomic scattering factors and the temperature factor were taken into account. It is therefore likely that these difficulties will be at least partially overcome by knowledge of the exact structure of the cylindrical unit.

A very broad reflection around 4.66A is expected as there are many Bragg planes which have spacings in this region. A very diffuse strong reflection with a peak at 4.66A is observed.

The contribution of the side chains and of amorphous material to the scattering is a serious problem in fibrous structures. In addition, the exact form of the packing is not known with certainty. For example, if the results of a wide-angle scattering experiment prove the reality of the 81.8A and 115A equatorial reflections, the unit cell would have to be modified. The agreement, in the present case, is comparable to that which has been obtained for the more well known structures of silk fibroin[17] and poly-L-alanine.[30] It is concluded that the present cylindrical model is basically capable of explaining the equatorial diffraction pattern, but some of the details are not yet well-defined.

Ramachandran[51] has suggested another possibility for the packing of cylindrical units which he believes may apply to feather keratin as well as to collagen. Figure 5-7 shows a cylindrical lattice of three sheets of the type Ramachandran has proposed. The packing arrangement for a cylindrical lattice is pseudo-hexagonal. The three lattice points on the first sheet form an equilateral triangle of side a_o.

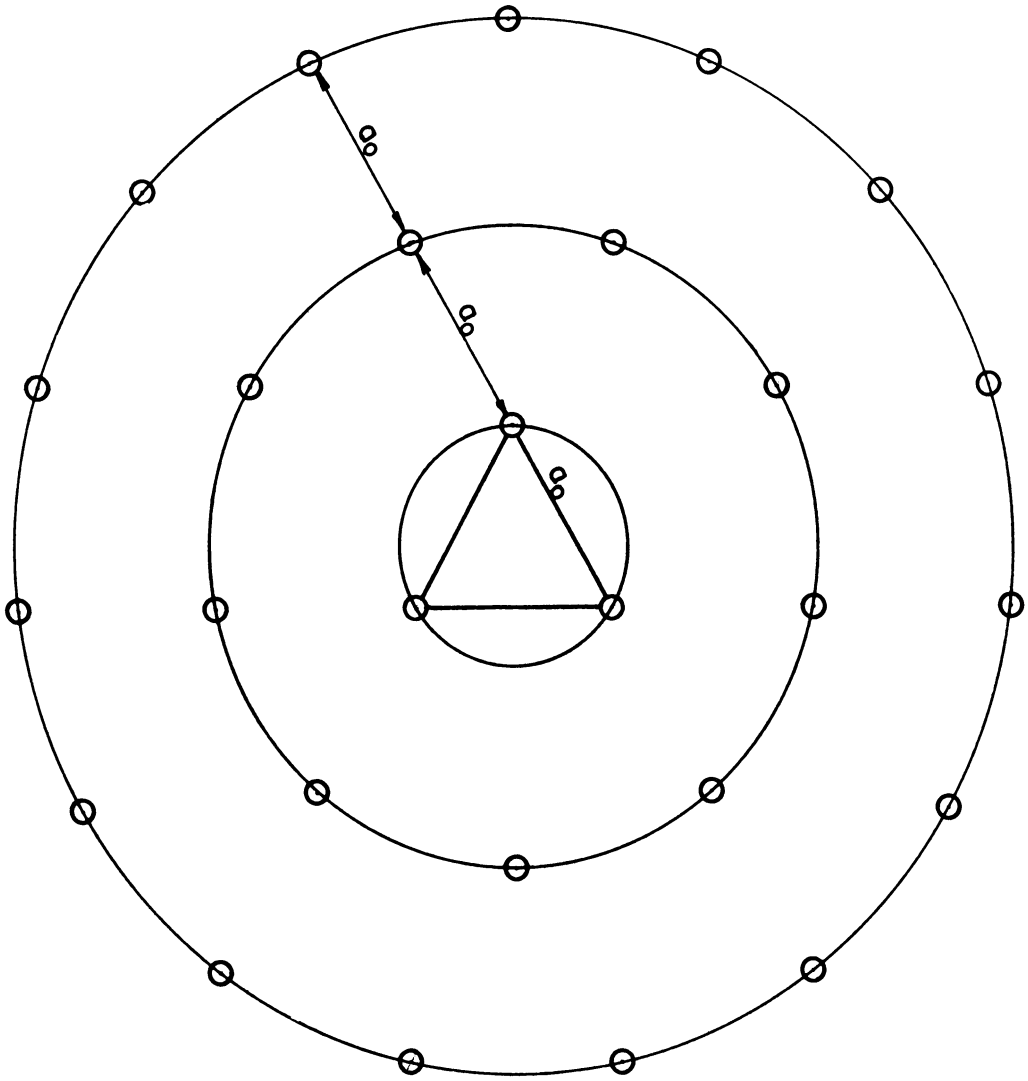

Figure 5-7 Cylindrical lattice of three sheets. Circles indicate lattice points.

It can be shown that the radius of the nth sheet of a cylindrical lattice is given by: $r_n = \frac{a_o \sqrt{3}}{3} \sqrt{3n^2 + 3n + 1}$. The arc distance between adjacent lattice points on any sheet is b_o and the number of lattice points on successive sheets increases by 6 (3,9,15,21,...). It follows that $6\, b_o \cong 2\pi a_o$ or $b_o \cong a_o$. An interesting consequence of the near-equality of b_o and a_o appears to be that although the lattice is two-dimensional the reflections from the lattice can be indexed on the basis of only one parameter. Thus, the lattice predicts equatorial reflections at $d \cong \frac{a_o}{n}$. It is natural to suppose that this type of lattice could explain the formation of row lines which are a prominent feature of the x-ray diffraction pattern of sea gull quill and to a lesser extent in turkey quill. The other interesting feature of a cylindrical lattice is that it has the potentialities of explaining the existence of the long equatorial spacings as due to the contributions of cylinders placed at large radii.

For feather keratin, Ramachandran has proposed a value for a_o of 34A. The scattering from a cylindrical lattice of three-sheets has therefore been calculated for the case of a_o = 34A. The results are shown in Figure 5-8. Only the cylindrically symmetric part of the scattering is indicated. This part of the scattering was calculated from the superposition of hollow cylinders placed at radii r_1, r_2, r_3 and weighted by the factors 1, 3, and 5 respectively (the ratio of the number of cylinders on each sheet). Calculations including Bessel functions of higher order, for example $J_3(2\pi r_1 R)$, $J_6(2\pi r_1 R)$, and $J_9(2\pi r_1 R)$ for the first sheet and $J_9(2\pi r_2 R)$, $J_{18}(2\pi r_2 R)$, and $J_{27}(2\pi r_2 R)$ for the second sheet show that the scattering does not differ significantly from the cylindrically symmetric

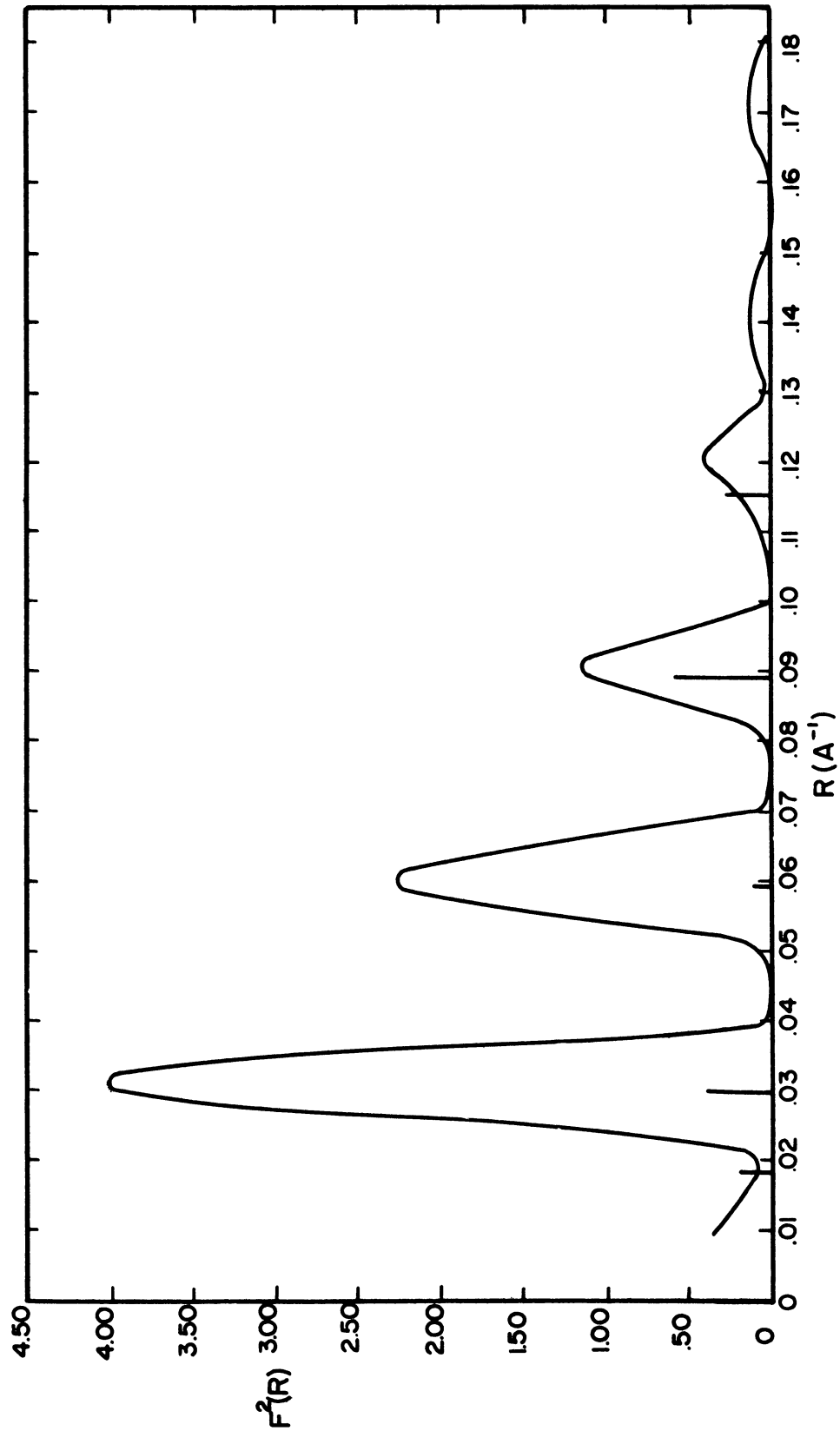

Figure 5-8 Equatorial scattering from a cylindrical lattice of three sheets for a =34A. The vertical lines indicate the estimated relative intensities of the ^{o}re-flections in the feather keratin diffraction pattern.

part alone. The calculations, which actually went up to six sheets, indicated a certain amount of stability in the region $R \geq 0.03A^{-1}$ as the number of sheets increased. It was also noted that the intensity showed a tendency to drop more rapidly near the origin of reciprocal space as the lattice became more complete.

More recently, Ramachandran[87] has suggested that the structures of feather keratin and collagen are similar on a molecular level. It is therefore of interest to determine how a collagen-like structure would fit into a cylindrical lattice of a_o = 34A and satisfy reasonable density requirements. The average residue weight for collagen is about 93, and there are three residues per cylindrical unit of structure in an axial projection of 2.86A.[8] From these facts, it can be shown that the only way in which the triple-stranded collagen units can pack into a cylinder of diameter 34A and give an adequate density is for the cylinder to contain seven such units. For this packing arrangement, the calculated density for the cylinder of diameter 34A is about 1.25. Five or six cylindrical units would not be likely to fill up a cylinder of diameter 34A, but on the contrary would leave holes in the 34A diameter cylinder. The density on the basis of four cylindrical units would be about 0.7, which is entirely too low. If seven cylindrical units fill up the 34A diameter cylinder, the diameter of the individual cylindrical unit is about 11.3A. The centers of the six cylinders which surround the central cylinder lie on a circle which is concentric with the central cylinder and whose radius is 11.3A. The inter-particle separation for collagen is sensitive to the moisture content of the sample. The minimum separation

occurs for a dry sample and is about 12A[8]. The diameter of 11.3A determined above is thus less than the minimum separation of the cylindrical units indicated by the x-ray data. This criticism is not a very strong one, as it is possible that a collagen-like molecule could have a diameter of 11.3A. The hypothesis that collagen-like molecules fill up the 34A diameter cylinders may be criticized more strongly on other grounds. The very intense 33.5A and 11.2A equatorial reflections in feather keratin are of comparable intensity. The equatorial transform of the model described above is given approximately by the product of three factors: 1) the transform of the lattice, 2) the transform of the seven points in central hexagonal arrangement, and 3) the transform of the cylindrical unit of structure. We shall now evaluate the ratio of the transform at 34A to that at 11.2A. For a cylindrical lattice of three-sheets (a_o = 34A) the ratio of the transform of the lattice evaluated at 34A to that evaluated at 11.2A is about 2/1 (Figure 5-8).* The transform of six equally spaced unit scatterers located on a circle of radius r_o is approximately $6\ J_o(2\pi r_o R)$[88]. The transform of seven unit scatterers in central hexagonal arrangement is approximately $\{1 + 6\ J_o(2\pi r_o R)\}$, where r_o is the radius of the circle surrounding the central point. For r_o = 11.3A, the ratio of the transform of the seven points evaluated at 34A to that evaluated at 11.2A is approximately 0.8. Three concentric cylinders located at radii of 1A, 3A, and 5A and, weighted 1/4, 1/2, and 1/4 respectively represents a reasonable approximation to a collagen-like unit of structure[35]. For this simplified model, the value of the transform at 34A is approximately 0.91 while the value at 11.2A is

* The intensity transform is shown in Figure 5-8. The intensity transform is proportional to the square of the Fourier transform discussed above.

approximately 0.39. The ratio of the predicted intensity at 34A to that at 11.2A is:

$$\frac{I(34A)}{I(11.2A)} \approx \left(\frac{2 \times 0.8 \times 0.9}{0.4}\right)^2 \approx \frac{14}{1}$$

which is in gross contradition to the experimental facts.

The possibility of packing the cylindrical units postulated in the present work into a Ramachandran lattice with a_o = 22A was also considered. As the calculated scattering does not exhibit a maximum near 34A, this type of packing is also unacceptable. The final possibility considered was the packing of the postulated 7-cylinder units into a Ramachandran lattice with a_o = 67A. Such a packing arrangement, which would be locally the same as the one presented in the present work, would predict a strong 67A reflection which is not found and would not predict the strong 55A reflection which is observed. This packing arrangement would be likely to enhance the intensity of the 8.7A equatorial reflection relative to that obtained for the packing arrangement that has been proposed in this work. The difficulties indicated above, however, are probably sufficient to rule out this possibility.

It is concluded that the hypothesis that collagen-like molecules fill up the 34A diameter cylinders in the manner described is not valid. The type of lattice Ramachandran has proposed for feather keratin remains to be proven correct. Until a definite unit of structure is given and its equatorial transform calculated, final judgment should be reserved.

5.3 Meridional Diffraction Pattern

The meridional diffraction pattern of feather keratin is exceedingly complex. It will ultimately be necessary to make a detailed structure factor calculation in order to compare the observed and predicted intensities. There are however several difficulties connected with this direct approach: 1) the coordinates given for the atoms in the main chains may differ somewhat from the "theoretical" coordinates which correspond to the configuration of minimum potential energy, 2) the detailed positions for the atoms in the side chains which contain practically half the scattering power in the structure are unknown, and 3) the scattering from many cylindrical units will have to be taken into account. It is therefore of value to make a preliminary semi-quantitative calculation in order to determine some of the major features of the predicted diffraction pattern.

We will first consider the scattering from the main chains of one cylindrical unit of the idealized model. For a given β-helix, there are eight amino acid residues in the assymetric unit of structure. Transform theory[29] shows that the helix imposes a selection rule on the orders of the Bessel functions comprising the scattering on the layer lines:

$$n + 8m = \ell \quad (m = 0, \pm 1, \pm 2, \ldots) \qquad (5\text{-}8)$$

where n represents the order of the Bessel function and ℓ represents the layer-line index. Corresponding atoms on adjacent helices are related by a 10-fold rotation axis. The existence of the 10-fold rotation axis restricts the orders of the Bessel functions comprising the transform of the 10-chain unit to values:[29]

$$n = 10k \quad (k = 0, \pm 1, \pm 2, \ldots.) \qquad (5\text{-}9)$$

These are the only general restrictions on the scattering which can be deduced from the symmetry of the proposed structure. It should be realized that deviations from this simplified model may result due to the influence of the side chains and/or adjacent cylindrical units on the main chain configuration. Nevertheless, the scattering from the atoms in the main chains of the idealized model for one cylindrical unit (see Figure 5-9) can account for certain of the important features of the diffraction pattern.

Before considering the predictions based on the model, a mathematical point must be introduced. Consider the meridian of reciprocal space, i.e., the line R = 0. Since $J_0(0) = 1$ and $J_n(0) = 0$ for $n \neq 0$, only zero order Bessel functions contribute to the intensity of the meridional reflections.[29] It follows from equation (5-8) that meridional reflections would be predicted to occur only on layer lines whose orders are multiples of eight. Since n = 0 is a solution of equation (5-9) for any l, the existence of a 10-fold rotation axis does not impose any additional selection rule on the layer lines for which meridional reflections can occur.

The most striking feature of the diffraction pattern of feather keratin is the intense and persistent, 8th order, 23.6_4A meridian reflection. This reflection is accounted for by the regular sequence of proline residues, which are located 23.6_4A apart in the z direction. Water molecules are probably hydrogen-bonded to the free CO groups on the proline residues, thus adding another 10 electrons per proline in

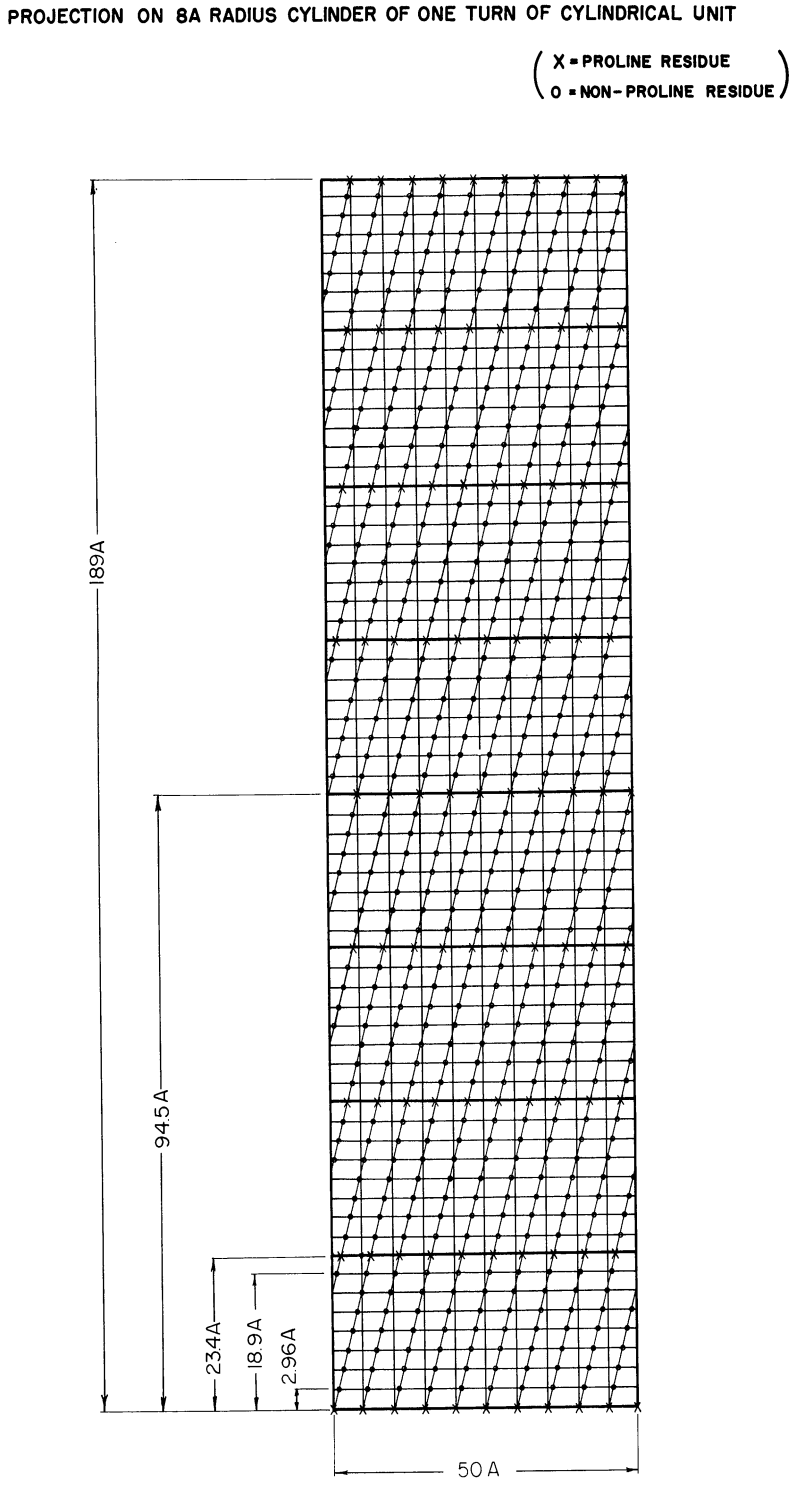

Figure 5-9 - Diagrammatic representation of idealized model of the proposed cylindrical unit of structure.

a relatively fixed spatial configuration. Rougvie[48] has proposed that the 23.6_4A meridian reflection would be explained by the scattering of regularly placed sulfur atoms. We believe this is not the case. The atomic scattering factor for sulfur does not fall off sufficiently rapidly to explain the large decrease in the intensity of the higher orders of the 23.6_4A which is observed. On the other hand, the discrete atoms of the proline residues are spread out over a region of several angstroms and a more rapid fall-off of the scattering factor with increasing Bragg angle is possible.

On the basis of the proposed model, the medium-weak meridional reflection at 2.96A represents the <u>average</u> axial projection of an amino acid residue. An examination of the expression of the structure factor for a meridional reflection shows that if all the residues in a structure are equally spaced in the z direction the meridional reflection corresponding to the rise per residue would be predicted to be very intense. In the present case, the proline residues introduce discontinuities into the chain configuration which results in some amino acid residues having an axial projection greater than 2.96A and other residues, particularly the prolines having an axial projection less than 2.96A. Thus, the model predicts the weakening of the 2.96A meridian reflection which is observed. The 2.96A meridian reflection is considerably weaker than the neighboring 3.15A layer-line spacing. In order to determine whether the predicted intensity of the 3.15A layer-line spacing is stronger than the 2.96A meridian reflection, a detailed structure factor calculation is required. The fact that the 3.15A layer-line spacing is stronger than the 2.96A meridian spacing implies the existence of discontinuities, such

as prolines, in the feather structure.

A strong reflection in the 1A meridian region is usually observed in the β-keratins. This reflection is interpreted as arising from the increase of approximately 1A in the vertical projection of successive atoms in a straight extended polypeptide chain. The residues in the proposed model are tipped with respect to the fiber axis and the CONH atoms for a given residue fall more closely on a horizontal plane. A reflection in the 1A meridian region would therefore not be expected to be strong, and none is observed.

An inspection of equations (5-8) and (5-9) shows that the idealized model for the atoms in the main chains of the cylindrical unit of structure permits reflections only on even layer lines of the 189A fiber axis repeat. Thus, a pseudo-repeat at 94.5A is predicted. Physically, a pseudo-repeat at about 94.5A is expected, as 94.5A is the least common multiple of the distance between successive prolines (23.64A) and the average vertical distance between adjacent chains (18.9A). The fact that the proposed structure possesses a pseudo-repeat at 94.5A is in agreement with the observation that only a few medium-weak reflections are observed which are odd orders of the 189A identity period.

In addition to the reflections at 23.64A and 2.96A, other meridional reflections in the diffraction pattern have indices which are multiples of 8. The weak reflection at about 11.8A in the diffraction pattern of turkey calamus is possibly meridional. (A medium intensity meridional reflection is observed at 11.8A in the diffraction pattern of sea gull quill.) Meridional reflections are also observed at 3.94A

(weak 48th order) and 3.37A (very very weak 56th order). It will be necessary to make detailed structure factor calculations in order to predict the intensities of these reflections. The higher orders of the 23.6_4A meridian reflection which are not present in the diffraction pattern may be explained by the fact that their structure factors vanish.

The near-meridional reflections (small R values) cannot be accounted for by the scattering from the atoms in the main chains of one cylindrical unit of structure. For the atoms in the main chains, the mean radius is about 8A. The contribution of $J_{10}(2\pi 8R)$ to the scattering is negligible at small R values. The contribution of Bessel functions whose order is higher than 10 is, of course, even smaller.

The contribution to the scattering of the "non-ideal" components of the structure will now be considered. The main effects are due to the atoms in the side chains which contain approximately half the scattering power of the structure. For the atoms in the side chains, there is no longer a ten-fold rotation axis relating corresponding atoms on adjacent chains. Thus, equation (5-9) no longer holds. In addition, the side chains are not expected to form perfect helices. The number of electrons in the side chains varies significantly from residue to residue and the axial projection from the center of charge of one side chain to another also varies. Hence, equation (5-8) no longer holds and there are, in general, no restrictions on the orders of the Bessel functions which can occur on any layer line. Because of limited knowledge of the positions of the atoms in the side chains, a detailed quantitative estimate of the scattering cannot be made and only the

qualitative features of the scattering will be discussed.

Since adjacent side chains are related by an average translation of $\frac{189}{10}$A in the z direction, an enhancement of the intensity on layer lines whose orders are multiples of 10 might be expected in the diffraction pattern. An inspection of Table II-I shows that this is the case. A medium-weak layer line reflection is observed at 18.6A (10th order), a strong layer-line reflection is observed at 9.38A (20th order), and a strong layer-line reflection is observed at 3.15A (60th order). The 3.15A layer-line reflection is close to the amino acid repeat of 2.96A and might be expected to be strong.

The 6.30A (30th order) and 4.96A (38th order) meridional reflections are intense. As has been noted, the side chains can contribute meridional reflections on any layer line. A mechanism is therefore possible to explain the existence of these reflections but the details are not clear. In particular, the 4.96A meridional reflection does not appear to be related to any obvious periodicity in the proposed structure. It is of interest to note that similar difficulties arise even in the discussion of the diffraction patterns of the synthetic polypeptides where the possibilities for variations in the side chains are considerably less than in the proteins. For example, there is a meridional reflection at 4.4A in the x-ray diffraction pattern of α poly-L-alanine.[89] The structure of this polymer is based on the α-helix. An undistorted α-helix, however, cannot account for a meridional reflection at 4.4A as the only meridional spacings which should occur correspond to spacings smaller than 1.5A. It has been suggested that slight distortions

of the methyl groups might suffice to give the observed reflection.

It is concluded: 1) the present cylindrical model is capable of explaining many of the salient features of the meridional and near-meridional diffraction pattern of feather keratin, and 2) a detailed quantitative study of the effects of taking various approximations for the distribution of the atoms of the side chains, of permitting deviations from the idealized model for the atoms in the main chains, and of considering the scattering from many cylindrical units is required before a final judgment relative to the difficulties discussed above can be made.

5.4 Radial Fourier Synthesis

For a cylindrically symmetric system the signs of the equatorial reflections are either plus or minus. If the signs could be determined unambiguously, it would be possible to construct the function $\rho(r)$, which represents the projected electron density in a plane perpendicular to the fiber axis as a function of the radial distance r from the axis. A knowledge of $\rho(r)$ would indicate the mean radius of the atoms in the main chains as well as the more variable radii of the atoms in the side chains. If a centro-symmetric system approximates to cylindrical symmetry, it is still possible to calculate the cylindrically symmetric part of the structure from the equatorial reflections, provided the signs of these reflections are known.

We shall first consider the case when the projected electron density is cylindrically symmetric. Then: $\rho(\vec{r}) = \rho(\underline{r},\underline{z})$ (5-10)
where $\vec{r}$ is the usual three-dimensional radius vector and $\underline{r},\underline{z}$ are cylindrical polar coordinates. The projected electron density is given by:

$$\rho(r)=\int_{-\infty}^{+\infty}\left[\int_0^{\infty}\int_0^{2\pi}\int_{-\infty}^{+\infty} F(\underline{R},\zeta)\, e^{i2\pi(\vec{\underline{R}}\cdot\vec{\underline{r}}+z\zeta)}\, \underline{R}\,d\underline{R}\,d\psi\,d\zeta\right] dz \qquad (5\text{-}11)$$

where the reciprocal vector has been broken up into a component (ζ) along the axial direction and a component ($\underline{R}$) in a plane perpendicular to ζ. The integral over z is the delta function $\delta(\zeta)$. Hence:

$$\rho(r)=2\pi\int_0^{\infty}\int_0^{2\pi} F(\underline{R},0)\, e^{i2\pi \underline{R}\,\underline{r}\cos\phi}\, \underline{R}\,d\underline{R}\,d\phi \qquad (5\text{-}12)$$

where φ is the angle between $\underline{R}$ and $\underline{r}$. Performing the integral over φ we obtain:

$$\rho(r)=2\pi\int_0^{\infty} F(R,0)\, J_0(2\pi r R)\, R\,dR \qquad (5\text{-}13)$$

For the usual case, when the reflections are discrete the integration may be replaced by a summation. Dropping the unessential factor of 2π, we have:

$$\rho(r)=\sum_R R\,F(R,0)\, J_0(2\pi r R) \qquad (5\text{-}14)$$

The main difficulty in solving equation (5-14) for $\rho(r)$ is the lack of knowledge of the signs of the equatorial reflections. One approach to this problem is to assume the approximate size and density distribution for the scattering unit. A set of signs may then be calculated and these may be used to determine a $\rho(r)$ which may be tested for consistency with the assumed model.

Next, we consider the case when the structure (and therefore the transform) is not cylindrically symmetric, but is oriented at random about its axial direction. The result for the projected electron density is:

$$\rho(r,\alpha)=\int_{-\infty}^{+\infty}\rho(r,\alpha,z)\,dz=\int_0^{\infty}\int_0^{2\pi}F(R,\psi,0)\,e^{i2\pi rR\cos(\alpha-\psi)}\,R\,dR\,d\psi \quad (5\text{-}15)$$

where r,α, and z are cylindrical polar coordinates. Averaging $\rho(r,\alpha)$ over α, we obtain an average radial electron distribution function:

$$\overline{\rho(r)}=\frac{1}{2\pi}\int_0^{2\pi}\rho(r,\alpha)\,d\alpha=2\pi\int_0^{\infty}R\,\overline{F(R,0)}\,J_0(2\pi rR)\,dR \quad (5\text{-}16)$$

where:

$$\overline{F(R,0)}=\frac{1}{2\pi}\int_0^{2\pi}F(R,\psi,0)\,d\psi \quad (5\text{-}17)$$

For the usual case, when the reflections are discrete, we may write, apart from unessential factors of proportionality:

$$\overline{\rho(r)}=\sum_R R\,\overline{F(R,0)}\,J_0(2\pi rR) \quad (5\text{-}18)$$

where $\overline{F(R,0)}$ is defined by equation (5-17). The only difference between equation (5-14) and equation (5-18) is the replacement of $F(R,\phi)$ by $\overline{F(R,0)}$ and $\rho(r)$ by $\overline{\rho(r)}$. In order to employ equation (5-18), it is necessary to know the relationship of $\overline{F(R,0)}$ to the experimentally determined intensities I(R,0). I(R,0) is proportional to the average of the square of the structure factor over the angle ψ:

$$I(R,0)=\frac{1}{2\pi}\int_0^{2\pi}F^2(R,\psi,0)\,d\psi \quad (5\text{-}19)$$

For a centrosymmetric structure, $F(R,\psi,0)=\overset{*}{F}(R,\psi,0)$. We employ Schwartz's inequality:

$$\left|\int fg\,d\tau\right|^2\leq\int|f|^2\,d\tau\int|g|^2\,d\tau \quad (5\text{-}20)$$

Let $f = F(R,\psi,0)$, $g = 1$ then:

$$\left|\int F(R,\psi,0)\,d\psi\right|^2 \leq 2\pi\int_0^{2\pi} F^2(R,\psi,0)\,d\psi \qquad (5\text{-}21)$$

from which we obtain:

$$\left|\overline{F(R,0)}\right|^2 \leq I(R,0) = \frac{1}{2\pi}\int_0^{2\pi} F^2(R,\psi,0)\,d\psi \qquad (5\text{-}22)$$

The equality sign in Schwartz's inequality holds if, and only if, f and g are directly proportional, which would be true if, and only if, $F(R,\psi,0)$ is independent of ψ. Since $F(R,\psi,0)$ is not independent of ψ, the magnitude of $F(R,0)$ for the non-cylindrically symmetric case is determined from the observed intensities only within the limits established by equation (5-22), i.e., F is never greater than $\sqrt{I}$. As the main features of $\rho(r)$ are much more sensitive to the assumed choice of the signs of the reflections than they are to small errors in the choice of the amplitudes, it is expected that the limitations discussed above would not be serious for structures approximating cylindrical symmetry.

We will now assume that equation (5-18) is applicable to the case of feather keratin and investigate the consequences of this assumption. The intensities and positions of the "strong" equatorial reflections of feather keratin are listed below:

TABLE V-II

Intensities and Positions of the Equatorial Reflections of Feather Keratin

d(A)	$R(A^{-1})$	I_{peak}	$F = \sqrt{I_{peak}}$	RF
33.5	0.030	1.25	1.12	0.034
17.1	0.059	0.07	0.26	0.016
11.2	0.089	0.38	0.62	0.055
8.7	0.115	0.08(?)	0.28	0.032
4.66	0.215	0.41(?)	0.64	0.138

As has been mentioned, the main difficulty in solving equation (5-18) is lack of knowledge of the signs of the equatorial reflections. We do not have an unambiguous estimate of the approximate size and density distribution for the scattering unit which is independent of the structural hypotheses and model which have previously been discussed. Hence, the powerful arguments based on the finite size of the scattering unit impressing a minimum wave-length on the resulting transform [90,91] cannot be used to limit the possibilities of choosing different sign combinations. We will therefore use other approaches: 1) the signs determined from a single cylindrical unit of structure of the proposed model will be used to calculate a $\rho(r)$ which can be tested for consistency with the model, 2) the consequences of choosing different sign combinations independent of any structural assumptions will be investigated.

The first choice of the signs for the equatorial reflections is based on the transform of structure 1, i.e., the transform of a hollow cylinder of radius 7.8A weighted 1/2, a hollow cylinder of radius 10A weighted 1/4 and hollow cylinders at 3 and 5A each weighted 1/8 (Figure 5-6). The signs are: 33.5A(+), 17.1A(-), 11.2A(-), 8.7A(+), 4.66A(-). The scattering of both crystalline and amorphous regions of structure contribute to the intensity of the 4.66A equatorial reflection. Consequently, $\rho(r)$ has been calculated on the assumption that the amorphous contribution to the intensity of this reflection is 0,1/2, and 2/3. The results are shown in Figure 5-10.

The main features of $\rho_1(r)$ are maxima at about 3A, 8A, and 12A. The curves for $\rho_2(r)$ and $\rho_3(r)$ are qualitatively similar to that for $\rho_1(r)$.

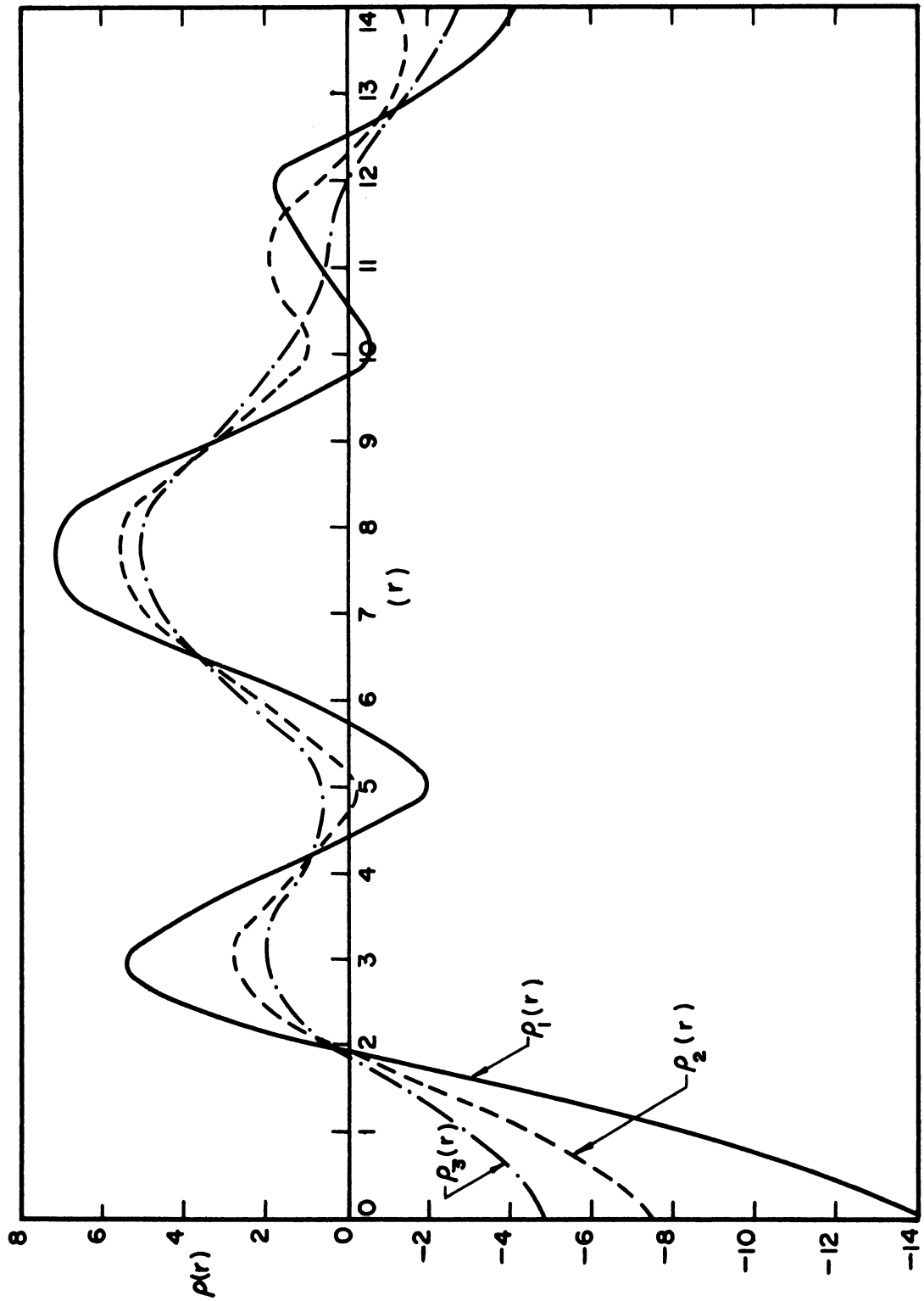

Figure 5-10 Radial fourier[1] turkey calamus based on the following signs for the equatorial reflections: 33.5A(+), 17.1A(-), 8.7A(+), and 4.66A(-). The subscripts 1,2,3 represent the cases for which the contribution of the amorphous scattering to the 4.66A reflection is assumed to be 0,1/2, and 2/3 respectively.

The model is self consistent in the sense that no electron density was assumed at the origin and the computed electron density at r = 0 is low. The large peak at about 8A is in agreement with the model, but this cannot be considered as a strong check on the assumed unit of structure because the signs used in the calculations are consistent with 1/2 the charge being located at 7.8A and one would naturally expect a peak in the calculated $\rho(r)$ at about 7.8A. This point can be understood most easily by considering a highly idealized model whose unit of structure is a single uniform hollow cylinder of radius r_o. The transform of such a cylinder is $F(R,0) = J_o(2\pi r_o R)$. Examination of equation (5-14) shows that $\rho(r_o) = \sum_R R|F(R,0)\ J_o(2\pi r_o R)|$, i.e., all the terms in the summation are positive. We would therefore expect the computed value of $\rho(r_o)$ to be "near" a maximum. The fact that a "peak" is automatically expected near r_o for arbitrary r_o constitutes one of the chief drawbacks in this use of the radial Fourier method of verifying an assumed unit of structure.

Considering the other approach, there are thirty two possible sign combinations of the five reflections listed in Table V-II. Many of these combinations have been considered in detail and the resulting functions for $\rho(r)$ fall into two distinct classes depending upon whether the sign of the 4.66A reflection is chosen as positive or negative. If the sign of this reflection is chosen as negative, functions similar to $\rho_1(r)$ are obtained. If the sign of the 4.66A reflection is chosen as positive, functions are obtained which are similar to $\rho_4(r)$ (Figure 5-11). This function peaks at r = 0, has a minimum at r = 3A and maxima at about

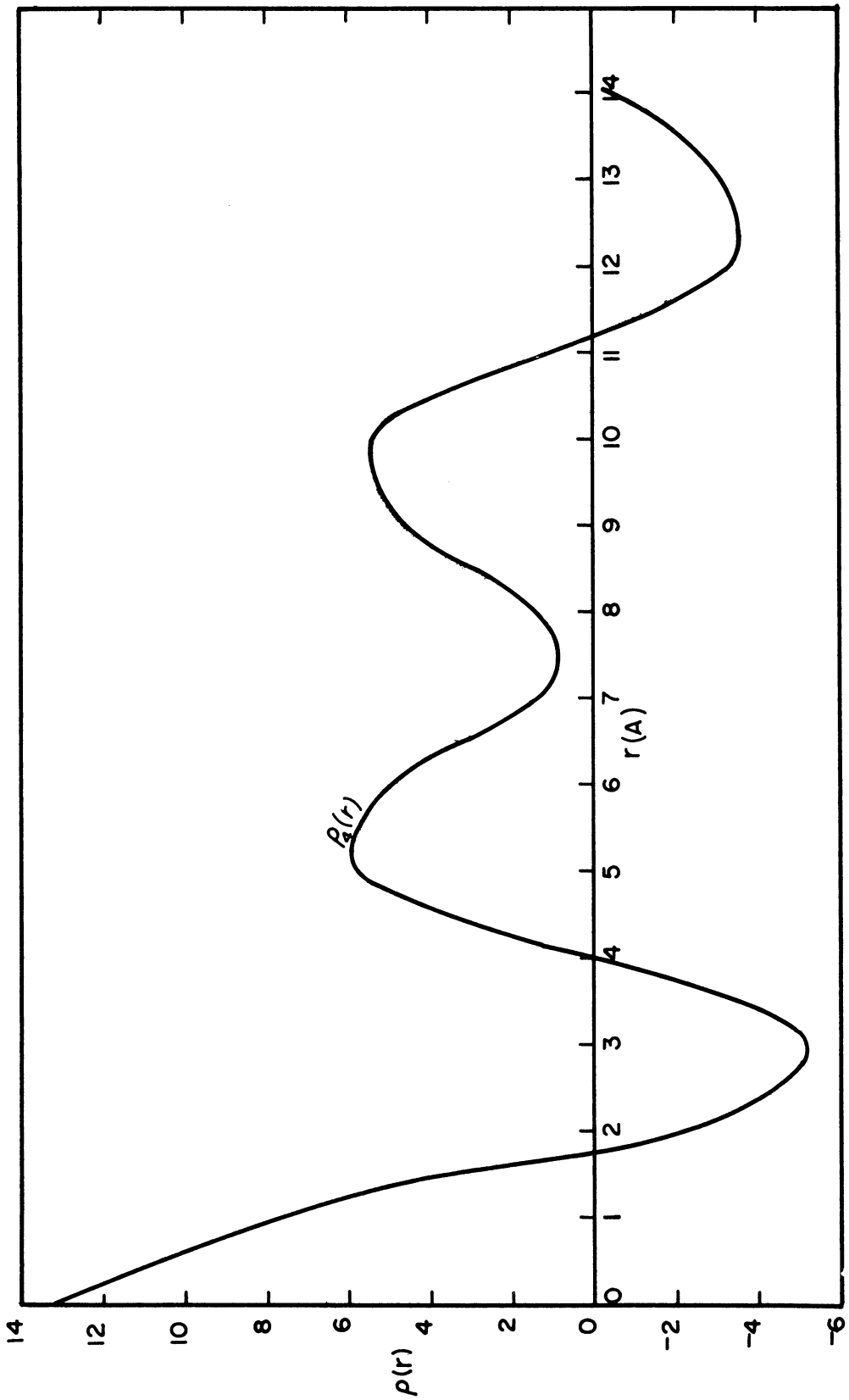

Figure 5-11 Radial fourier synthesis of turkey calamus based on the following signs for the equatorial reflections: 33.5A(+), 17.1A(-), 11.2A(-), 8.7A(+), and 4.66A(+). No amorphous scattering was assumed.

r = 5 and 10A. No physically realizable model with such characteristics has been suggested by the data.

There is in fact a method by which it is possible to obtain some indication of a reasonable choice of signs for the equatorial reflections. We will assume that the structure is composed of essentially similar cylindrical units. The transform of such a unit can be approximated by $J_o(2\pi\bar{r}R)$ where $\bar{r}$ represents the mean radius of the atoms in the unit. The sign of the 33.5A equatorial reflection for such a unit is almost certainly positive. The first node of $J_o(x)$ occurs for x = 2.40. Hence, if the 33.5A ($R = 0.03A^{-1}$) reflection were negative (on the basis of a single cylindrical unit of structure), the smallest value for the radius of the unit would be: $\bar{r} = \frac{2.40}{(2\pi)(.03)} = 12.7A$. The radius would actually be considerably larger than this value since the 33.5A equatorial reflection is very intense, implying in this case that the first node of $J_o(2\pi\bar{r}R)$ occurs for an R value considerably less than $0.03A^{-1}$. It is difficult to understand how a stereochemically satisfactory structure could be built with such a high value for the radius of the unit. We will therefore assume that the sign of the 33.5A equatorial reflection is positive. Since no intense reflections occur between $R = 0.03A^{-1}$ and $R = 0.09A^{-1}$, it is probable that a node in the transform of the cylindrical unit occurs between these two R values and that the sign of the 11.2A equatorial reflection is negative. The important question of whether the 4.66A equatorial reflection is positive or negative still cannot be decided without recourse to further argumentation. An examination of the equatorial diffraction pattern shows that there is a relatively

large region extending from about R = $0.13A^{-1}$ to R = $0.20A^{-1}$ in which the intensity of the scattering is very low. This observation implies that the value of the transform of the hypothesized cylindrical unit of structure is very small in this region. If we demand that the transform of the cylindrical unit be approximately represented by $J_0(2\pi\bar{r}R)$, be positive at R = $0.03A^{-1}$, negative at R = $0.09A^{-1}$, and low in the region from about R = $0.13A^{-1}$ to R = $0.20A^{-1}$, the sign of the transform evaluated at R = $\frac{1}{4.66}$ A^{-1} is negative. As has been discussed, this choice of sign for the 4.66A equatorial reflection yields a $\rho(r)$ which is low at the origin and has a large peak at about r = 8A in agreement with the $\rho(r)$ expected for the ten-chain model. Although the assumptions which have been introduced above are not compelling, they are the most reasonable ones suggested by the data. Thus, the radial Fourier analysis lends support to a model of the type proposed. If it should prove experimentally possible either to establish the signs of the equatorial reflections with greater certainty, or to obtain an independent estimate of the size of the scattering unit, the function $\rho(r)$ will serve as a more stringent test of the model.

5.5 Cylindrical Patterson Function

An attempt will be made to evaluate the extent of agreement of the ten-chain model with the cylindrical Patterson function. For purposes of comparison, the peaks in the "cylindrical Patterson function" for the highly idealized model shown in Figure 5-9 have been calculated. The model consists of one cylindrical unit of structure. Each of the ten polypeptide chains is represented by a helix of radius 8A and pitch

189A. The amino acid residues, with the exception of the prolines, are indicated by dots and the prolines by crosses. Every eighth residue on a given chain is a proline. Successive residues are assumed to have the same vertical spacing of 2.96A. Corresponding residues on adjacent chains are at the same vertical level and are related by a rotation of 36° around the helix axis. Because of lack of detailed knowledge, the effect of the side chains, additional cylindrical units of structure, and the details of the structure of the main chain atoms have been omitted from the calculation. Thus, the resolution of the "calculated Patterson function" is very low and only very rough conclusions can be drawn about the positions of the resulting peaks. The "interatomic" vectors in the range z = 0 to z = 28A and r = 0 to r = 12A have been determined for the model described above, and the resulting positions are designated by crosses in Figure 5-12. A P next to a cross designates a proline-proline vector in addition to vectors between non-proline residues.

The method of calculation will now be described. The (r,z) coordinates of the "interatomic vectors" from a helical wire of diameter d and pitch P are determined by writing the equation for r as a function of z:

$$r = d \sin\left(\frac{\pi z}{P}\right) \qquad (5\text{-}23)$$

The continuous line marked A in Figure 5-12 shows these intrahelical vectors for the case d = 16A and P = 189A. If a number of equally spaced atoms ($z = mz_o$, m integral) lie on the locus of a helix, the interatomic vectors consist of the set of points:

$$r_m = d \sin\left(\frac{\pi m z_o}{P}\right) \qquad m = 0, \pm 1, \pm 2, \cdots \qquad (5\text{-}24)$$

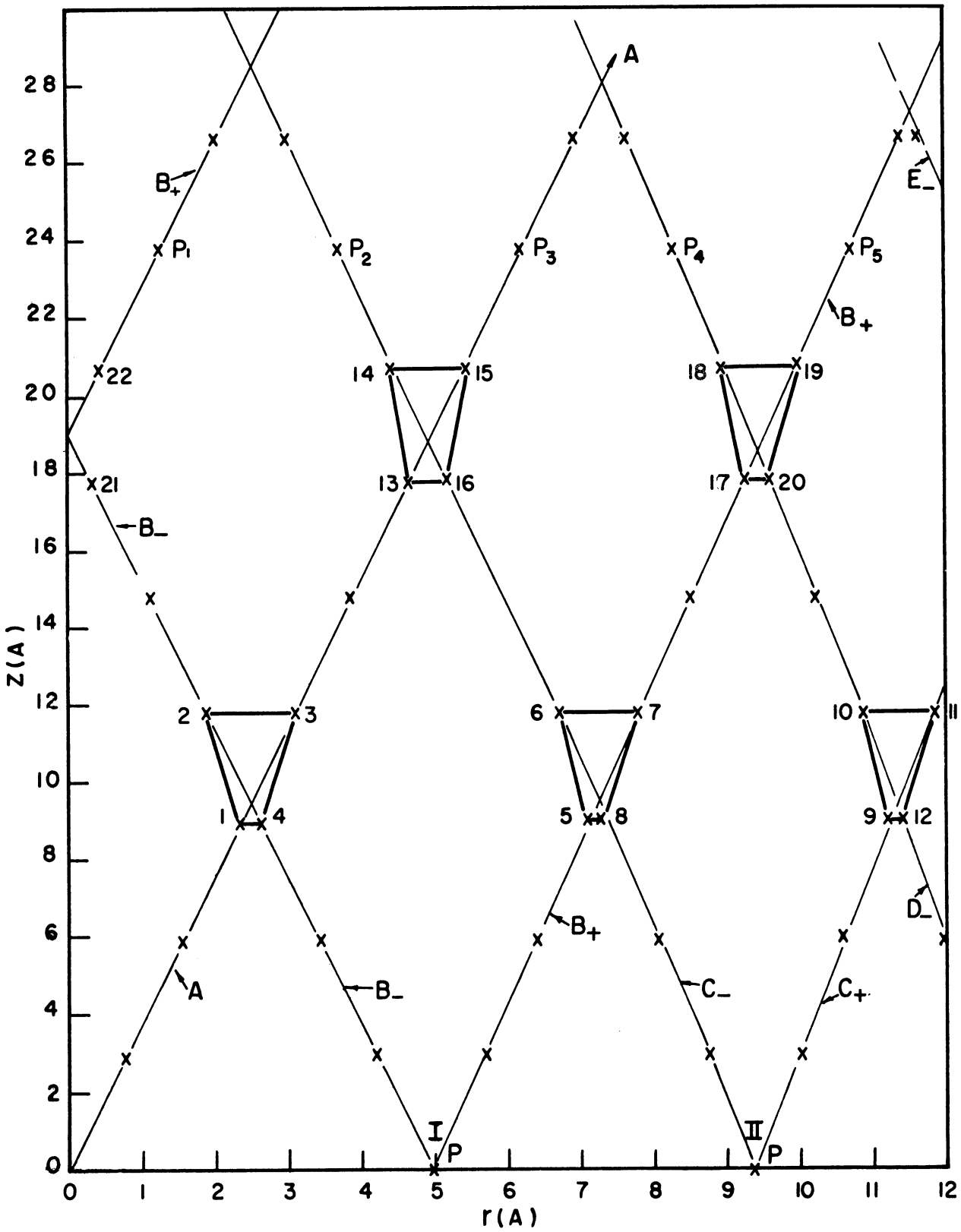

Figure 5-12 Calculated "Patterson function" for idealized model of a cylindrical unitof structure.

Thus, the crosses on line A, which are spaced 2.96A apart in the vertical direction, represent the intrahelical vectors for the model described above. We next consider the interatomic vectors from a given atom a located on helix A to the atoms on the neighboring helices B_- and B_+, where B_- is determined from A by a rotation of -36° and B_+ is determined from A by a rotation of +36°. The (r,z) coordinates of the interatomic vectors from a to the set of atoms on B are given by the equation:

$$r_m = d \sin \pi \left(\frac{m z_o}{P} - \frac{1}{10} \right) \qquad m = 0, \pm 1, \pm 2, \cdots \quad (5\text{-}25)$$

Similarly, the (r,z) coordinates of the interatomic vectors from a to the set of atoms on B_+ are given by:

$$r_m = d \sin \pi \left(\frac{m z_o}{P} + \frac{1}{10} \right) \qquad m = 0, \pm 1, \pm 2, \cdots \quad (5\text{-}26)$$

In an analogous manner, the crosses on lines C_- and C_+ represent the vectors from a to the atoms on the helices which are next nearest neighbors to A etc.

The peaks marked I and II on the line z = 0 (Figure 5-12) would be expected to be very strong as they represent the lateral distance between adjacent polypeptide chains and next nearest neighbors respectively. These peaks would be expected to be enhanced by any partially oriented amorphous β chains which are present in the feather keratin structure. In addition, it should be noted that for z = 0, $P(0,r) = \sum_{\ell} A_\ell(r) \cos \left(\frac{2\pi \ell z}{P}\right) = \sum A_\ell(r)$, and any error due to the use of incorrect intensities or to an incorrect assignment of a layer-line index will not contribute significantly to a diminution of the intensity of the expected peaks. Consequently, we would expect an enhancement of the peaks on the

line z = 0 relative to the other peaks in the pattern. The resulting set of interatomic vectors shown in Figure 5-12 exhibits five areas where the interatomic vector density is high. These are designated by the quadrilaterals (1,2,3,4), (5,6,7,8), (9,10,11,12), (13,14,15,16) and (17,18,19,20) respectively. Peaks might therefore be expected to be found in the Patterson function calculated from the experimentally determined intensities at or near these regions. Peaks are in fact observed in the cylindrical Patterson function (Section 2.6) at P(2,9) (near quadrilateral 1,2,3,4), at P(5, 19-20)(in quadrilateral 13,14,15,16) and at P(9,20)(near quadrilateral 17,18,19,20) in agreement with the predictions based on the idealized model. No peaks in the cylindrical Patterson function are observed, however, near quadrilaterals (5,6,7,8) and (9,10,11,12). Pattersons 2 through 5 exhibit peaks at about P(4-25) while Patterson_1 has a peak at about P(5-25). The peak in this region is close to the peak marked P_2 in Figure 5-12. Patterson 1 shows peaks at about P(10,25) while Pattersons 2 through 5 exhibit peaks at about P(9,26). The peak in this region is close to the peak marked P_4. The large peaks on the line P(0,z) at P(0,6-7), P(0,13-15), P(0,19) and P(0,24) require special attention. In a general way, the peak at P(0,19) is expected, since adjacent chains are related by an average translation of $\frac{189}{10}$ A $\simeq$ 19A in the z direction. Many interactions between side chain and main chain atoms as well as interactions between the atoms of the side chains only would be expected in this region, in addition to the main chain-main chain vectors marked 21 and 22 in Figure 5-12. The peak at P(0,24) is interpreted as arising from proline-proline interactions marked P_1.

Although P_1 has an r coordinate of 1.2A, a peak at P(0,24) would still be expected to occur, as a result of overlap of electron density, poor resolution, and "computational enhancement" of the function P(0,z).

It is difficult to evaluate the correctness of a fiber structure from a consideration of the cylindrical Patterson function alone. The only guide is the extent of the agreement between the observed and the calculated maps. The agreement obtained here is better than that obtained with other fibrous structures.[56] In the present case, the most serious difficulties are that some of the peaks predicted on the basis of the idealized model are not found in the cylindrical Patterson function that has been calculated from the experimentally determined intensities. On the other hand, many of the prominent peaks in the cylindrical Patterson function are readily interpretable on the basis of the ten-chain model, and none of the remaining peaks are inconsistent with the type of model that has been proposed. In addition, some false detail due to lack of knowledge of the correct intensities tends to shift and/or alter peak values. It is therefore concluded that the ten-chain model is consistent with the observed cylindrical Patterson function.

5.6 Alterations in the Diffraction Pattern

Effects of Stretching

It has been shown that samples of turkey calamus can be stretched approximately 5% before rupturing. Both the wide-angle and the low-angle meridian and layer-line spacings increase by the same amount, i.e., about 5%. No significant changes in the relative intensities of the reflections

were observed. The positions and intensities of the equatorial reflections remained unchanged.

The previously existing proposals for the configuration of the polypeptide chains in feather keratin cannot easily account for the stretching data. The elastic properties of feather keratin are markedly different from the elastic properties of α-keratin. The α-keratin configuration can be converted into the β configuration by stretching. The resulting x-ray diffraction pattern is essentially different from the α-pattern, showing a strong meridional arc at 3.33A. In the case of feather keratin, we have noted that no significantly new pattern is obtained by stretching the specimen. It is therefore probable that the essential molecular configuration of feather keratin is unaltered during the stretching process. In addition, there is no reason to believe that an α-helix would remain stable if it were extended 5% by increasing the length of the hydrogen bonds. (An approximately 2% increase in the 5.15A and the 1.5A meridian spacings of α-keratin has been reported during the early stages of the stretching to the β form.[92] These considerations would tend to serve as objections to an all-α model as proposed by Pauling[1].

The elastic properties of collagen and feather keratin also differ significantly. Whereas, in the case of feather keratin the long and short spacings change by the same percentage upon stretching the sample, the diffraction pattern of stretched collagen shows that the long and short spacings change by different percentages[74]. For example, for a 5% increase in the fiber length, the 640A macroperiod of

collagen increases by approximately 4% while the 2.86A meridian spacing only increases by about 1%. It is noteworthy that collagen is more easily extensible than feather keratin, in the sense that the wide-angle meridian spacings of collagen can increase by as much as 15% upon stretching. It is therefore probable that there are significant structural differences between feather keratin and collagen.

It is also not easy to account for the elastic properties of feather keratin on the basis of a structure which contains two basic types of polypeptide chain configurations or in terms of a micelle structure.

On the other hand, the ten-chain model appears to give good agreement with the stretching data. In the unstretched case, the parameters of the helix are: P = 189A, θ = 14.5°, l = 3.06A, r = 7.83A. The 5% increase in the meridian and layer-line spacings upon stretching would be accounted for by a 5% increase in the pitch of the helix. The fact that the equatorial spacings remain unchanged suggests that the radius of the cylindrical unit of structure remains constant during the stretching process. A value θ stretched = 13.8° is obtained from equation (4-1) for P = 198.5A (1.05 x 189A) and r = 7.83A. Thus, only a very small decrease in the pitch angle of about 0.7° will account for the data. Since the pitch angles for the two cases are approximately equal and the radii are equal, the hydrogen bonding distance between adjacent polypeptide chains, as determined from equation (4-3), would not change significantly. From equation (4-2), the residue length is 3.06A for the unstretched case and 3.19A for the stretched case. An

increase in the residue length of 0.13A might be expected to introduce a significant amount of strain into the polar pleated-sheet configuration. The $C_{\alpha 1}$-$C_{\alpha 2}$-$C_{\alpha 3}$ angle for the unstretched case is approximately $107^{\circ}30'$ while the corresponding angle for the stretched case is approximately $114^{\circ}30'$. A 7° increase in this angle (which is close to the corresponding change in the tetrahedral angle) is "large" and it is likely that the polar structure would rupture before increasing the $C_{\alpha 1}$-$C_{\alpha 2}$-$C_{\alpha 3}$ angle still further. Another possibility is that by increasing the length of the residues beyond 3.19A, the residues would adopt an anti-polar configuration. An examination of the proposed model (Section 4.6), however, shows that this is not possible without first breaking the hydrogen bonds and completely disrupting the structure. It is therefore concluded that the proposed model provides a reasonable mechanism to account for the elastic properties of feather keratin: 1) up to extensions of about 5% the basic molecular configuration of feather keratin remain unchanged and only a change in scale occurs, 2) for extensions greater than 5% the strain on the polar sheet configuration becomes too large and the specimen ruptures.

Effects of Water on the Equatorial Diffraction Pattern

It has been noted that the intensity of the "33.5A" equatorial reflection is extremely sensitive to the water content of the sample. As the humidity varies from complete dryness to saturation, the intensity of this spot diminishes from a value comparable to the very intense 23.6A meridian spacing to essentially zero.

On the basis of the proposed model, it would be expected that the water molecules would tend primarily to fill up the "holes" in the lattice shown in Figure 5-5. A semi-quantiative estimate of the effect on the intensity of the "33.5A" equatorial reflection of water in these "holes" will be made. As computed from the amino acid composition (Section 3.2), the average number of electrons per residue of feather keratin is close to 52. Hence, one turn of the cylindrical unit of structure contains 64 x 10 x 52 $\cong$ 33,000 electrons. If each "hole" in the lattice were completely filled with water, it would contain an estimated $\pi(11.2)^2(189)(10^{-24}) \times \frac{10}{18} \times 6.02 \times 10^{23} \cong$ 25,000 electrons. For purposes of making an order of magnitude calculation, it is assumed that the scattering from the "holes" in the lattice can be approximated by solid cylinders of radii 11.2A and that each "hole" is completely filled with water, i.e., contains approximately 25,000 electrons. Taking into account the positions of the centers of the holes [(1/3, 2/3);(2/3,1/3)] , and employing the formula for the scattering from a solid cylinder of radius 11.2A ($F(R) = \frac{2J_1[(2\pi)(11.2)R]}{(2\pi)(11.2)\,R}$), the equatorial scattering from structure 1 (Section 5-2) has been recalculated for the "33.5A" equatorial reflection ($R = \frac{1}{33.5} A^{-1}$). The resulting value for F^2 is 23, in good agreement with the observation that the intensity of this reflection in the diffraction pattern obtained from a water-soaked sample is essentially zero. If the "holes" in the lattice were partially filled with amorphous β-chains in addition to water, the result for the decrease in the intensity of the strong "33.5A" equatorial reflection upon water-soaking would be very similar to the result determined above.

The spacing of the "33.5A" equatorial reflection is also a function of the water content of the sample. The spacing obtained in the present work is 31.2A for an air-dried sample and 32.6A for a water-soaked sample (Table II-II). Other workers have obtained somewhat higher values for this spacing, e.g., Kraut obtained a value of 33.5A. An examination of the photographs of sea gull quill taken by Bear and Rugo indicates that upon soaking in water there is an approximately 5% increase in this spacing. On the basis of the proposed model, the increase of the spacing of the "33.5A" equatorial reflection which is observed as the humidity of the sample is raised is interpreted as a swelling effect: 1) the 7-cylinder unit may separate slightly as a result of water entering between the cylindrical units, 2) the 7-cylinder units may expand slightly as a result of water entering between the cylinders comprising the units, 3) the diameters of the individual cylinders may increase slightly as a result of water entering the empty space near their axes. We would expect the first effect to predominate.

It is concluded that the proposed model readily explains the fact that the intensity of the "33.5A" equatorial reflection diminishes from a value comparable to the very intense 23.6_4A meridian reflection for a sample at room humidity to essentially zero for a water-soaked sample. The change in the spacing of this reflection is interpreted as a swelling effect. In fact, these effects would be very difficult to understand on the basis of the more conventional close-packed β structures or on the basis of a collagen-like structure.

5.7 Agreement with the Infrared Data

Parker[58] has shown that a perpendicular dichroic ratio of 4.8/1 for the residual NH stretching band of feather keratin is obtained after non-oriented OH and NH groups are removed by exchanging with D_2O. This result requires that any proposed structure for feather keratin must yield a dichroic ratio of at least 4.8/1. The dichroism of the ten-chain model can be estimated if we assume that there is a distribution of NH dipoles, each making an angle θ with the fiber axis and having random orientation about the axis. In this case, the perpendicular dichroism is $1/2 \tan^2 \theta$ [93,94]. To a good approximation, for the NH dipoles in the present model, θ is equal to the complement of the angle which the chains make with respect to the fiber axis. For the ten-chain model, $\theta = 75.5°$, yielding a dichroism of about 7.5/1. The observed infrared dichroism is thus adequately accounted for by the proposed structure.*

The infrared data are supposedly capable of yielding further information relative to the configuration of the polypeptide chains other than that given by the dichroism. Ambrose and Elliott[68,69] have proposed, as a result of a study of the infrared spectra of polypeptides and proteins, that the value of the CO stretching frequency is characteristic of the state of folding of the polypeptide chains. This frequency is near 1660 cm^{-1} in the α or folded form while in the β or extended form it is close to 1630 cm^{-1}. On the bais of the observed doubling of the CO stretching frequency in the infrared spectra of feather keratin, they have concluded that there is a proportion of α protein in the structure.[95] As the

* If we set $1/2 \tan^2 \theta = 4.8$, $\theta \cong 72°$. Hence, the pitch angle of the chains with respect to the fiber axis should not exceed 18°.

intensities of the two components are about equal, the acceptance of the frequency criterion would imply that feather keratin contains comparable amounts of folded and extended chains. From the x-ray point of view, it is difficult to accept this conclusion as there is no firm evidence for the existence in the diffraction pattern of either the 5.1A or the 1.5A meridional reflections which are characteristic of the α-fold. It does not seem possible to explain the absence of these spacings in a natural way if we assume that the α-helix is a major component of the structure.

Until a more fundamental explanation of the frequency criterion is presented, it is not obligatory to accept it. For example, Sutherland and Wood[96] have listed the frequencies found in various synthetic polypeptides and fibrous proteins which were judged by x-ray diffraction or infrared dichroism criteria to be either in the α or the β forms. The absorption peak varies in position a great deal and is often found in positions intermediate between those suggested by Ambrose and Elliott. The average position of this band for the 8 α proteins which were considered is 1649 ± 4 cm^{-1}. The β proteins show similar variations. Sutherland and Wood observed that whereas the α proteins all have only one band in this region all of the β proteins have at least two. They suggested that a better criterion for distinguishing between α and β proteins might be the number of bands in the region between 1600 and 1660 cm^{-1}. No reason for such a criterion was suggested.

In summary, if judgment on the validity of the Ambrose-Elliott frequency criterion is reserved, the ten-chain model is in

good agreement with the infrared data.*

5.8 Agreement with the Chemical Data

The main features of the chemical data are: 1) the observed proline content of feather keratin, 2) upon solubilization homogeneous units are obtained of approximately 10,000 molecular weight, 3) the axial ratio of these units, on the basis of the assumption of their shape being a prolate ellipsoid of revolution, is greater than 5/1, 4) there are almost no detectable end-groups, and 5) reconstitution of the solubilized material gives a substance whose diffraction pattern exhibits some of the characteristics of that of the native feather.

In the light of the chemical data, three hypotheses relative to the structure of feather keratin will be considered: 1) the hypothesis of Bear-Rugo-Rougvie, 2) the hypothesis of Woodin, 3) the present hypothesis of the ten-chain cylindrical unit of structure.

---

* A recent paper by Elliott, Hanby, and Malcomb[97] strongly suggests that the frequency criterion proposed by Ambrose and Elliott is not valid. For an α-helix, a value for the C = O stretching frequency is expected in the neighborhood of 1652-1655 cm^{-1}. These authors have found, however, that for water soluble films of Bombyx-mori silk fibroin (which gives an x-ray diffraction pattern characteristic of amorphous material) the value of the C = O stretching frequency is 1660 cm^{-1}. On the basis of the Ambrose-Elliott frequency criterion, a value for the C = O stretching frequency of 1660 cm^{-1} would indicate the presence of the α-helix in the structure of silk fibroin. The authors remarked that it is difficult to understand why the x-ray diffraction pattern did not show any of the characteristics of the α-helix. Further studies on the dispersion of optical rotation for water-soluble films of Bombyx-mori gave a low value for b_o in Moffit's equation which indicates a low value for the helical content of the sample. The absence of the carbonyl stretching band at 1630 cm^{-1} shows that these films are also not in the extended or β-configuration. On the basis of these and other observations, the authors have been led to the conclusion that the presence of a carbonyl band at about 1660 cm^{-1} is observed in polypeptide spectra not only with the α-helix and collagen folds but also in what, in the absence of further evidence, seems to be a disordered state. Since the x-ray and infrared evidence indicates the existence of a large component of amorphous material in the feather keratin structure, the intense band at 1650 cm^{-1} which is observed

As has been previously discussed, Bear and Rugo have proposed a micelle type structure for feather keratin, with globular particles arranged around "equivalent nodal points" of a net. Rougive obtained a monomer and dimer of cysteic acid-keratin. The monomer could be described as a prolate ellipsoid of revolution with a major axis equal to 100A and a minor axis equal to 14.7A, while the dimer had the dimensions of 220A and 14.2A respectively. Reconstitution of this material gave a substance whose diffraction pattern exhibited some of the characteristics of the diffraction pattern of the original feather. Rougvie interpreted these observations as implying that the native feather keratin consists of monomeric units of extended polypeptide chains held together by -S-S- and hydrogen bonds. The fact that the dimer had the same width and approximately twice the length of the monomer was taken as evidence of the end-to-end aggregation of particulate units. The work of Rougvie was thus thought to substantiate the hypothesis of Bear and Rugo that the structure of feather keratin was based on the aggregation of globular units. In particular, the length of the monomer (100A) is fairly close to the fiber axis identity period of 95.4A.** It will now be shown that this interpretation of the data encounters many difficulties. The hypothesis of Bear is open to criticism on purely x-ray grounds. As has been mentioned, the centers of the particles in

---

* in the infrared spectrum of feather may be attributable to amorphous material. The ten-chain model is therefore in good agreement with the infrared data.

** This spacing is considered a pseudo-identity period in the present work.

the "unit cell" with respect to the x,z coordinate axes are located at: (0,0), (0,1/2), (1/2,1/4), and (1/2,3/4), In a general way, a pseudo-halving of the unit cell in the lateral direction would be expected to arise from such a distribution of scattering centers. Thus, a strong equatorial reflection would be predicted at 17A and a weak equatorial reflection would be predicted at 34A. The diffraction pattern of feather keratin exhibits a very strong equatorial reflection at about 34A and a weak equatorial reflection at about 17A, which is inconsistent with Bear's model. The Bear-Rougvie model is not sufficiently well-defined at the present time to make more detailed x-ray criticisms. From the chemical point of view, the assumption that the shape of the monomer of feather keratin in solution can be approximated by a prolate ellipsoid of revolution is of doubtful validity. The axial ratio of 6.83/1 (prolate ellipsoid assumption, 30% hydration), which was determined from the sedimentation - diffusion data, is not in good agreement with the axial ratio as determined from the viscosity data, viz. 9.77/1. On the other hand, there is much better agreement with the dimensions calculated on the basis of a random coil model from the viscosity data and from the sedimentation-diffusion data. For a random coil, Rougvie obtained a value of 85A for the root-mean-square end-to-end length of the particle $(\bar{r}^{\,2})^{1/2}$ from the Flory-Fox equation:

$$M[\eta] = 2.1 \times 10^{21} [\overline{r^2}]^{3/2} \qquad (5\text{-}27)$$

For a random coil, the root mean square end-to-end length of the particle may also be calculated from the sedimentation data according to the equation: (98)

$$s_o[\eta]^{1/3}[M^{-2/3}] = \frac{[2.1\times10^{21}]^{1/3}[1-\bar{v}\rho]}{\eta_o N\ [5.11]} \qquad (5\text{-}28)$$

where ρ is the density of the solution, η_o is the viscosity of the solution at 20°C, s_o is the sedimentation constant, and N is Avogadro's number, Substituting the expression for $[\eta]^{1/3}$ from the Flory-Fox equation, and using quoted values for ρ and η_o of 1.00 and 10^{-2} respectively we obtain a value for $[\bar{r}^2]^{1/2}$ of 78A. (The other quantities necessary to solve these equations have been give in Table III-II). The value of 78A determined from equation (5-28) is sufficiently close to the value of 85A determined from equation (5-27) to warrant the conclusion that the shape of the particle in solution can more accurately be approximated by a random coil than by a rigid rod. Thus, the assumption that the shape of the monomeric unit can be approximated by a prolate ellipsoid of revolution whose axial ratio is 6.83/1 remains to be proven correct. As no viscosity measurements were reported for the dimer, its shape is even more questionable. The hypothesis of Bear-Rugo-Rougvie encounters another difficulty. When the -SH groups of solubilized preparations of feather keratin are oxidized to $-SO_3H$ groups, the 33.5A equatorial reflection disappears but the meridian reflection at 23.6A (observed at approximately 22A) remains. It is not easy to understand, on the basis of a model which assumed that -S-S- linkages bind the monomer together in both the lateral and the longitudinal directions, why one reflection should disappear and not the other. In order to explain this result, it would be necessary to postulate that the longitudinal -S-S- linkages are more resistant to oxidation than the lateral -S-S- linkages.

Woodin concluded on the basis of the absence of end-groups that the feather keratin monomer is an unbranched cyclic peptide. He remarked[66] that a cyclic polypeptide chain of 90 residues would have a maximum length of about 140A for a rise per residue of 3.1A. If the diameter of the double chain was assumed to be from 14A-20A, the axial ratio for a hydration of 0-30% would be in the range 10 to 7, in agreement with Woodin's viscosity data. The suggestion of Woodin is unsatisfactory, however, in several respects: 1) the fact that the feather keratin monomer may be cyclic in solution does not imply that the structure of the native feather is based on cyclic polypeptide chains; 2) it is difficult to understand how a double-chain β structure could form a stereochemically satisfactory hydrogen-bonded system; 3) the length of 140A (or sub-multiples of 140A) bears no relation to the identity period of feather keratin.

On the basis of certain reasonable assumptions, the ten-chain model can be shown to be in agreement with the chemical data.

The proline content of the ten-chain model is in good agreement with the observed proline content of feather keratin. Since the structure of the protein is essentially similar in different species, the observed constancy of the proline content[60] between different species is well explained by the model.

The model can account for the existence of approximately 10,000 molecular weight units in solution if it is assumed that upon solubilization the polypeptide chains are ruptured at regular intervals along the chain. One of the most probable sites for such a break is at the proline residues.[99] A unit of molecular weight

9,700 would result if every 12th proline peptide bond were particularly labile. It is not known whether the solubilization treatment (10M urea, 0.1M $NaHSO_3$, extracted for 24 hours at 40°C at pH6 or alternatively reaction with thioglycol) can result in the hydrolysis of peptide bonds. Although it would be unusual for hydrolysis to occur under such mild conditions, it may not be impossible. Cystine residues tend to occur close to proline residues[62] and if, for example, certain neighboring peptide bonds were thereby subject to strain they could be more susceptible to hydrolysis. Definitive data on the conditions of the partial hydrolysis of proteins which would exclude the possibility of the hypothesized hydrolysis is not yet available. Since there would probably be no large constraining forces which would tend to keep the particle in a fixed spatial configuration, it is likely that such a segment of a polypeptide chain would assume a configuration similar to a random coil in solution. As has been discussed, the solution data indicates that this is probably the case for the feather keratin monomer.

The absence of end-groups is more difficult to explain. The tentative hypothesis may be advanced that the free chain tends to cyclize in solution. On the basis of this hypothesis, the reconsitution process would involve opening the cycles under the influence of mechanical stress. It should also be noted that in certain cases the determination of end-groups in not an unambiguous procedure. For example, a masking effect can occur with N-terminal proline and serine[100]. In addition, unusual effects also occur with the carboxypeptidase method[101], for example, proline is not attacked. Thus, it may be wise to reserve final judgement on the interpretation of the end-group studies.

On the basis of the proposed model, it is possible to conceive the outlines of a mechanism for the reconstitution of the dissovled keratin. The chain fragments would re-group into units similar to the ten-chain cylindrical structures, the proline residues reaggregating at the same vertical level. The presence of the 189A fiber axis identity period and the 95A pseudo-period would not be expected since the chains are not long enough, but the sequence of proline residues still gives rise to a strong $\sim$ 23.6A meridian reflection. The fiber diagram of the reconstituted material is not sufficiently detailed to conclude that the 189A fiber axis identity period is reproduced. The packing of the cylinders will yield the strong 33.5A equatorial spacing. When the -SH groups are oxidized to $-SO_3H$ groups, the regular sequence of the cylinders is disrupted and this side-to-side spacing does not appear.

It is concluded that although the explanation of the chemical data is not yet sufficiently certain, the experimental facts do not preclude the existence of a continuous chain structure of the type proposed.

5.9 Agreement with the Density

Kraut[50] has obtained a value of 1.28 gm/cc for the density of feather keratin. (The density of most fibrous proteins is about 1.3 gm/cc.) From the amino acid compositon of feather keratin as determined by Schroeder and co-workers[60], the value for the average residue weight is 101. If the form of the packing is that proposed in the present work, the density of the structure can be determined. The calculated value for the density will be subject to uncertainties involving the amounts and distribution of disordered material and water.

The density of a single cylindrical unit of ten polypeptide chains of diameter 22.4A is: $d = \frac{10 \times 64 \times 101 \times 1.66 \times 10^{-24}}{3.14(11.2 \times 10^{-8})^2 \times 189 \times 10^{-8}} =$ 1.44 gm/cc. The effect of moisture on the equatorial spacings shows that the water content of feather keratin is variable but a figure of 5% seems reasonable (102). The addition of 5% water would raise the density of the cylindrical unit to 1.51 gm/cc. The density of a 7-unit group based on the envelope of the aggregate (the dotted line in Figure 5-5), is 1.13 without water and 1.19 with 5% water. If 7-unit groups are packed into the hexagonal lattice of Figure 5-5, the density is 1.02 without water and 1.07 with 5% water. The calculated density is too low to be in agreement with the measured density of 1.28 gm/cc.

The density discrepancy could possibly be explained by a consideration of the following three factors: 1) the large component of amorphous material in the structure has not been taken into account in calculating the density of the model; 2) the units may pack more closely than indicated in Figure 5-5, 3) the percentage of water may be somewhat higher than 5%. As has been previously discussed, the x-ray and infrared data indicate that feather keratin has a considerable component of amorphous material. If sufficient amorphous material is present in the holes in the structure, the density for the model may be satisfactory. Complete hexagonal packing of the units yields a density of 1.31 gm/cc without water and 1.37 gm/cc with 5% water. Thus, if the 7-unit groups packed space in a pseudo-hexagonal manner, a satisfactory density could be obtained. (If this were the case, the question of the agreement of the model with the equatorial diffraction pattern would have to be re-examined.)

It is interesting to note that there are density anomalies (not as great as in the present case) with structures based on the α-helix. The

calculated density of poly-γ-methyl-L-glutamate based on an α-helix model was 1.28 gm/cc while the measured density was 1.31 gm/cc [89]. A revision of the unit cell brought the calculated density up to 1.304 gm/cc. The calculated density of 1.304 gm/cc is extremely close to the measured density of 1.31 gm/cc. The significant point, however, is that the calculated density is less than the measured density, which is contrary to what is expected. When the α proteins are considered, the discrepancies are much greater. Measurements on a "highly crystalline" sample of porcupine quill indicate that the average volume of a residue is $140A^3$ while the value calculated on the basis of the Pauling-Corey model and the Huggins model for α-keratin are $150A^3$ and $143A^3$ respectively [103]. Thus, neither model would appear to be sufficiently compact to account for the data. This result is particularly surprising in view of the fact that the α-helix is a very tightly wound spiral whose structure is known.

In the present case, it is concluded that the proposed model is capable of satisfying the density requirements. Whether it does so in a "natural" manner cannot be determined until a more certain knowledge of the amounts and distribution of disordered material, the three-dimensional lattice, and the percentage of water in the structure is available.

CHAPTER VI

CONCLUSIONS

6.1 Experimental Results

One of the most significant experimental results of this work is the fact that the "3.07A spacing", which had been previously thought to be a meridional reflection, is actually a 3.15A layer-line spacing. The interpretation of the 3.07A spacing, as the axial projection of a single amino acid residue along a β-polypeptide chain is therefore no longer tenable. In fact, a meridional reflection is found at 2.96A which has been interpreted as the amino acid repeat. The fiber axis identity period for feather keratin had previously been considered to be 94.5A. The 7.60A, 7.09A, 3.57A, and 2.39A layer-line spacings would have close to half-integral indices on the basis of a 94.5A fiber axis identity period which indicates that 94.5A is probably not the true repeat. The average c_o obtained in the present studies is 189A, in agreement with the value obtained from the most accurately measurable meridian spots, those at 23.6_4, 6.30, and 4.97A. Only a few reflections (medium-weak) are odd orders of the new identity period. Therefore, 94.5A remains a pseudo-identity period. The equatorial spacing at approximately 50A, which Bear had attributed to radiation artifacts, has been clearly observed on photographs taken in the present work. We therefore conclude that the existence of this reflection must be accounted for by any model proposed for feather keratin.

The cylindrical Patterson function for feather keratin has been obtained. The Patterson function shows no similarity to that expected for an α-helix. The peaks in the 4-5A and the 9-10A regions are, however, indicative of the presence of β chains. Thus, the cylindrical Patterson

function helps establish the fact that feather keratin is a β protein and not an α protein, as had been suggested prior to this work.

Two types of alterations in the x-ray diffraction pattern were investigated: 1) the effects on the diffraction pattern of stretching the sample, 2) the effects on the diffraction pattern of water-soaking and treatment with chemical reagents. The sample ruptures at elongations much greater than 5%. The meridian and layer-line spacings change by the same percentage upon stretching, i.e., approximately 5% for a 5.5% elongation of the sample, but the equatorial spacings remain unchanged. The relative intensities of the reflections (judged visually) for both the stretched and the unstretched cases are the same. These results are interpreted as implying that both the long and the short spacings in the feather keratin diffraction pattern are intimately connected and that only one type of polypeptide chain predominates in the structure. We have confirmed Bear's result that the intensity of the "32.6A" equatorial reflection is very weak in the diffraction pattern obtained from a water-soaked sample. (This reflection is very intense in the diffraction pattern of a sample at room humidity.) It is believed that the great diminution of the intensity of the 32.6A equatorial reflection which is observed upon water-soaking represents a significant aspect of the feather keratin structure.

6.2 Structural Conclusions

An analysis of the available x-ray, chemical and infrared data strongly suggests that the α-helix, the usual forms of extended chains, and the three-stranded collagen configuration are not major components of the feather keratin structure. In order to account for the unique features of the x-ray and chemical data, we have introduced the following structural

hypotheses: 1) there is a regular sequence of proline residues along the β-polypeptide chain, 2) the chain assumes a helical configuration of pitch 189A, i.e., fiber axis identity period. We have designated such a configuration of the polypeptide chain as a β-helix.* An analysis of the implications of these assumptions has led to a unique cylindrical unit of structure for feather keratin. The unit consists of ten coaxial β-helices which are hydrogen-bonded to each other. In any given chain, there are 64 amino acid residues in one turn of the helix (189A), every eighth residue being a proline. The proline residues on adjacent chains pack together at the same vertical level in order to form a maximum number of hydrogen bonds. The remaining residues are in a modified polar pleated-sheet configuration. The helix is right-handed and, viewed from the outside of the cylindrical surface, the CO bonds on the non-proline residues point to the left. Corresponding atoms in the main chains of adjacent helices are related to each other by a rotation of $\frac{2\pi}{10}$ around the helix axis. The atoms in the side chains, however, are not necessarily related by a 10-fold rotation axis. Since 94.5A is the least common multiple of the vertical distance between successive prolines ($23.6\frac{1}{4}$A) and the average vertical distance between adjacent chains (18.9A), the structure possesses a pseudo-repeat of 94.5A. Using scale models of the polypeptide chain, we have constructed a stereochemically satisfactory structure whose hydrogen bond lengths and angles are within the acceptable range and whose van der Waals contacts are satisfactory. The coordinates as determined from model building have been "refined" by mathematical calculation and a preliminary set of coordinates for the atoms in the main chains have been presented.

---

* When the proline residues in a β-helix are replaced by ordinary residues, the resulting configuration is designated as a pure β-helix.

A detailed evaluation of the extent of agreement of the predictions based on the proposed model with the data has been made. The following questions have been considered: 1) the agreement of the model with the equatorial diffraction pattern, 2) the agreement of the model with the meridional and near-meridional diffraction pattern, 3) the consistency of the model with a radial Fourier synthesis, 4) the consistency of the model with the cylindrical Patterson function, 5) the ability of the model to explain the alterations in the diffraction pattern produced by chemical and physical treatment of the sample, and 6) the agreement of the model with the infrared, chemical, and density data.

One of the most satisfactory aspects of the proposed structure is that it predicts the presence of the intense equatorial reflections, which are observed at about 55A, 33.5A, and 11.2A. There are two points where agreement with the data is less satisfactory. The intensity of the 8.85A equatorial reflection, which is a weak reflection in the turkey pattern,* is predicted to be practically zero. In addition, a medium to strong intensity reflection is predicted at 7.30A which is not observed and a medium to strong reflection at about 5.8A is predicted. As the intensity in this region is sensitive to the exact approximation to the structure which is employed, it is probable that this difficulty will be overcome by a more detailed knowledge of the structure of the cylindrical units. It is concluded that the present cylindrical model is basically capable of explaining the equatorial diffraction pattern, but some of the details are not yet well-defined.

Certain of the important features of the meridional and near-meridional diffraction pattern of feather keratin are predicted on the

*The 8.85A equatorial reflection is a medium intensity reflection in the pattern of sea gull quill.

basis of the scattering of the main chains of the cylindrical unit of structure: 1) the very intense and characteristic 23.6$_4$A meridional reflection which is the most striking feature of the low-angle diffraction pattern, 2) the medium-weak 2.96A meridional reflection, 3) the absence of a reflection in the 1A meridian region which is characteristic of the β-keratins, 4) the fact that most of the reflections are even orders of the 189A identity period, 5) the presence of many meridional reflections in the diffraction pattern whose orders are multiples of 8, e.g., 8(vs), 48(w), 56(vvw), 64(mw), 6. the presence of many reflections on layer-lines whose orders are multiples of 10, e.g., 10(mw), 20(s), 50(vw), and 60(s). There are, however, some aspects of the diffraction pattern which are not fully understood at the present time: 1) the strong meridional reflections at 6.30A and 4.97A, 2) the medium-weak 10.4A meridional reflection, and 3) the strength of the 3.15A layer-line reflection. It is thought that side chain effects could account for most of these points. It is therefore concluded: 1) the present cylindrical model is capable of explaining many of the salient features of the meridional and near-meridional diffraction pattern, and 2) a detailed quantitative study of the effects of taking various approximations for the distribution of the atoms of the side chains, of permitting deviations from the idealized model for the atoms in the main chains, and of considering the scattering from many cylindrical units is required before final judgment relative to the difficulties discussed above can be made.

The results of the radial Fourier analysis based on the equatorial diffractions (Section 5.4) lend support tc the proposed model. In particular, a cylindrical structure with a mean radius for the atoms in the main chains of about 8A is indicated.

Many of the peaks in the cylindrical Patterson function, such as the peaks at P(4-5, 0), P(9-10, 0), P(5, 19-20), and P(9-20), are in agreement with those expected on the basis of the ten-chain model. The model also offers a reasonable explanation of the large peaks found at P(0, 19) and P(0, 24). A detailed explanation for the existence of the large peaks at P(0, 6-7) and P(0, 13-15) is not known at the present time. The existence of these peaks, however, is not inconsistent with the type of model proposed and is thought to arise from interactions involving side chains and/or disordered material. Some of the peaks which would be predicted on the basis of the model, e.g., those at about P(7-8, 9-12), P(11-12, 9-12), P(6,24), P(8,24) are not found in the cylindrical Patterson function. It is concluded that the cylindrical Patterson function is consistent with the ten-chain model even though some of the details are not yet clear.

The model is capable of explaining the changes in the diffraction pattern which are produced by stretching the sample. The following deductions concerning the elastic properties of feather keratin are shown to be reasonable: 1) up to extensions of about 5% the basic molecular configuration of feather keratin remains unaltered, and 2) for extensions greater than 5% the strain on the "polar sheet configuration" becomes too large and the specimen ruptures. It is also shown that the model readily explains the observed fact that, upon water-soaking, the intensity of the "33.5A" equatorial reflection diminishes from a value comparable to the very intense 23.6_4A meridian reflection to essentially zero.

Since the Ambrose-Elliott frequency criterion is probably not valid for proteins like feather keratin which have a large percentage of amorphous material in their structure, the model is in good agreement

with the infrared data.

The explanation of the chemical data is not yet sufficiently clear. The experimental facts, however, do not preclude the existence of a continuous chain structure of the type proposed.

The model proposed is capable of satisfying the density requirements. Whether it does so, cannot be determined until a more certain knowledge of the amounts and distribution of disordered material, the three-dimensional lattice, and the percentage of water in the structure is available.

6.3 Perspectives

The model for feather keratin proposed in the present work appears to be in agreement with a considerable proportion of the presently available data. If it is tentatively assumed that the proposed model is on the right general lines, the importance of proline residues in influencing the spatial configuration of a polypeptide chain will have been demonstrated. As the scattering from the idealized model for the main chains of the proposed cylindrical unit of structure cannot account for some of the significant features of the meridional and near-meridional diffraction pattern, these reflections must arise from the scattering of the atoms in the side chains, and/or from deviations in the main chain configuration due to the influence of the side chains. The signifcance of the side chains in determining some of the important features of the diffraction pattern of a fibrous protein has not always been fully appreciated. Since the side chains contain approximately half the scattering power in a fibrous protein and are not subject to the "rigid symmetry conditions" which are satisfied by the atoms in the main chains, it is

probable that they make a significant contribution to the diffraction pattern. It is therefore suggested that a detailed quantitative study of the effects of taking various reasonable approximations to the coordinates of the atoms in the main chains and in the side chains of the proposed model be made. In addition, it will be necessary to consider the scattering from many cylindrical units of structure. If the results of these studies are positive, the importance of the side chains in determining (either directly or indirectly) some significant features of the diffraction pattern of feather keratin will have been demonstrated.

APPENDIX A

THE APPLICATION OF THE THEORY OF FOURIER TRANSFORMS TO THE DIFFRACTION OF A SIMPLE HELIX

The theory of the diffraction of a simple helix has played an important role in the study of the fibrous proteins. It is therefore of interest to determine the diffraction pattern of a helix as derived from the basic relations of Fourier transform theory. The relevant ideas and examples have been taken from James[104], Cochran, Crick, and Vand[29], and Stokes[105].

The fundamental relations of Fourier transform theory determine the magnitudes and phases of the scattered waves as a function of the electron charge distribution and vice versa. The equations are:

$$T(\vec{R}) = \int \rho(\vec{r})\, e^{i2\pi(\vec{r}\cdot\vec{R})}\, d\vec{r} \qquad \text{(A-1)}$$

$$\rho(\vec{r}) = \int T(\vec{R})\, e^{-i2\pi(\vec{r}\cdot\vec{R})}\, d\vec{R} \qquad \text{(A-2)}$$

where $\rho(\vec{r})$ is the density of scattering matter expressed in electrons per unit volume, $\vec{r}$ is the radius vector in real space from the origin of the cooridnate system, $\vec{R} = \frac{\vec{s}-\vec{s}_o}{\lambda}$, where $\vec{s}_o$ and $\vec{s}$ are unit vectors in the direction of incidence and the direction of scattering respectively, and λ is the wave-length of both the incident and scattered radiation. The integration is to be taken throughout all real and reciprocal space in equations (A-1) and (A-2) respectively. Absorption of radiation and rescattering are neglected.

$T(\vec{R})$, which represents the amplitude and phase of the scattered waves, can be represented geometrically as a distribution in the space defined by a vector having the direction and magnitude of $\vec{R}$. This space is

known as reciprocal space. The distribution $T(\vec{R})$ completely characterizes the Fraunhofer diffraction pattern that can be produced by $\rho(\vec{r})$ for any wave-length and under any conditions of incidence and scattering. If, in the distribution $T(\vec{R})$, we draw the "sphere of reflection" whose radius is $\frac{1}{\lambda}$ and whose center P is located at $\frac{-\vec{s}_o}{\lambda}$, the value of $T(\vec{R})$ at any point Q on the sphere gives the amplitude scattered in the direction $\overrightarrow{PQ}$. The most frequent application of the theory is to the case of three-

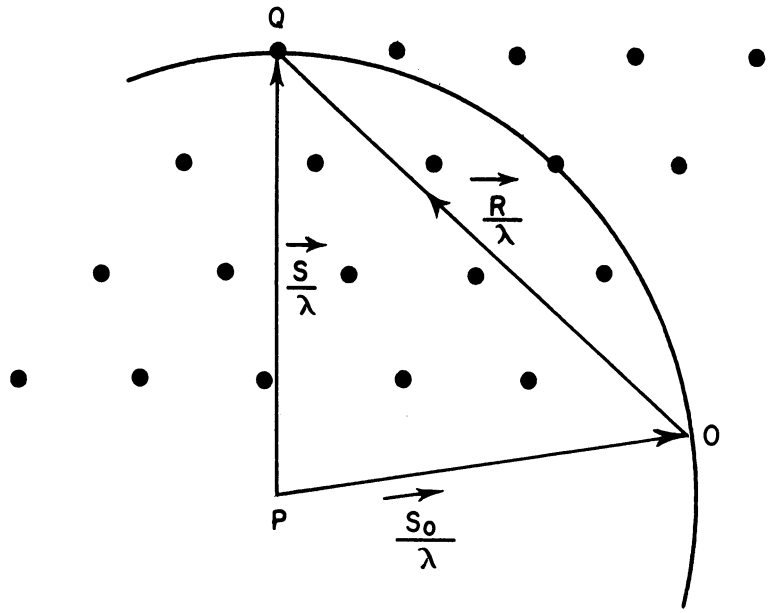

Figure A-1. Ewald's construction for the diffraction maxima using the reciprocal lattice and the sphere of reflection.

dimensionally periodic single crystals where it can be shown that $T(\vec{R})$ vanishes except at the points of a lattice reciprocal to the space-lattice of the crystal. The method of constructing this reciprocal lattice from the crystallographic lattice is well known. An x-ray reflection from a single crystal is observed when a point of the reciprocal lattice intersects

the sphere of reflection. For a non-periodic distribution of scattering matter, the distribution of scattering amplitude in reciprocal space is in general continuous and the "reflections" are determined by the intersection of the sphere of reflection with the distribution $T(\vec{R})$.

In order to derive the scattering from a helix, it is convenient to prove the convolution theorem which gives the transform of the product of two functions $f(x)$ and $s(x)$. Let $F(\xi)$ and $S(\xi)$* be the transforms of $f(x)$ and $s(x)$. Then:

$$F(\xi) = \int f(x)\, e^{i2\pi\xi x}\, dx \qquad S(\xi) = \int s(x)\, e^{i2\pi\xi x}\, dx$$

$$f(x) = \int F(\xi)\, e^{-i2\pi\xi x}\, d\xi \qquad s(x) = \int S(x)\, e^{-i2\pi\xi x}\, d\xi \tag{A-3}$$

The transform of the product is given by:

$$\int f(x)\, s(x)\, e^{i2\pi xX}\, dx = \iint F(\xi)\, s(x)\, e^{i2\pi x(X-\xi)} dx d\xi = \int F(\xi)\, S(X-\xi)\, d\xi \tag{A-4}$$

The integral on the right hand side of equation (A-4) is known as the convolution or folding of the functions $F(\xi)$ and $S(\xi)$. The theorem states that the transform of the product of two functions is the convolution of their transforms. The generalization to three dimensions is:

$$\int f(\vec{u}) s(\vec{u}) e^{i2\pi(\vec{R}\cdot\vec{u})}\, d\vec{u} = \int F(\vec{t})\, S(\vec{R}-\vec{t})\, d\vec{t} \tag{A-5}$$

$$\int F(\vec{R}) S(\vec{R}) e^{-i2\pi(\vec{R}\cdot\vec{u})}\, d\vec{R} = \int f(\vec{r})\, s(\vec{u}-\vec{r})\, d\vec{r} \tag{A-6}$$

Let the coordinates of $\vec{R}$ be (ξ,η,ζ) (see Figure A-2). For any distribution of scattering matter periodic with period P along the z axis, it can be shown that the transform $T(\xi,\eta,\zeta)$ of the distribution in reciprocal

* Here, ξ is used as a cartesian coordinate.

space effectively vanishes unless $\zeta = \frac{n}{P}$ n = 0, $\pm$ 1, $\pm$ 2,..... Let the transform of 1 period be denoted by $T(\xi,\eta,\zeta)$. Then by equation (A-1) the transform for N periods of the resulting distribution is:

$$T'(\xi,\eta,\zeta) = T(\xi,\eta,\zeta)\left[1 + e^{i2\pi P\zeta} + e^{i2\pi 2P\zeta} + \ldots\ldots\ldots e^{i2\pi(N-1)P\zeta}\right]$$

The intensity distribution is given by:

$$T'\overset{*}{T}' = T\overset{*}{T}\frac{\sin^2(N\pi P\zeta)}{\sin^2(\pi P\zeta)}$$

where the * represents the complex conjugate. For large N,

$$\frac{\sin^2(N\pi P\zeta)}{\sin^2(\pi P\zeta)} = N^2 \text{ for } \zeta = \frac{n}{P} \text{ and } 0 \text{ for } \zeta \neq \frac{n}{P}.$$

We now derive the scattering from a helix. First, the case of a wire of uniform electron density, radius r, pitch P, and infinite length will be considered. The helix may be defined by the equations:

$$\begin{aligned} x &= r\cos\left(\frac{2\pi z}{P}\right) \\ y &= r\sin\left(\frac{2\pi z}{P}\right) \\ z &= z \end{aligned} \qquad \text{(A-7)}$$

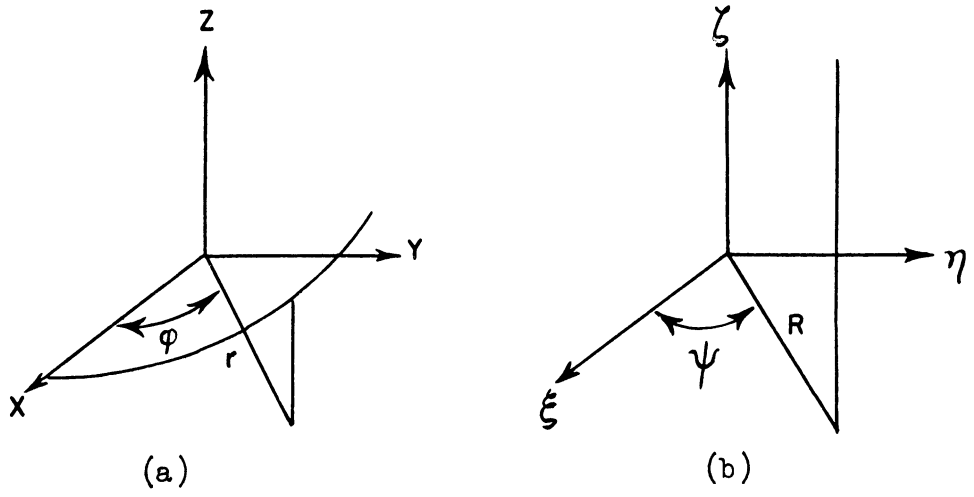

Figure A-2. Coordinates of a point on a helix.

(a) Cartesian (x,y,z) and cylindrical polar (r,φ,z)

(b) Corresponding coordinates of a point in reciprocal space.

The value of the Fourier transform at a point (ξ,η,ζ) in reciprocal space is given by:

$$T(\xi,\eta,\zeta) = \int le^{i2\pi(x\xi + y\eta + z\zeta)}\, dV$$

where dV may be taken proportional to dz. Substituting the values of the coordinates from equation (A-7) we obtain apart from unessential constants of proportionality:

$$T(R,\psi,\zeta) = \int_0^P e^{i2\pi(Rr\cos\{\frac{2\pi z}{P} - \psi\} + z\zeta)}\, dz \qquad \text{(A-8)}$$

From the previous considerations, we need only consider the transform at values $\zeta = \frac{n}{P}$:

$$T(R,\psi,\tfrac{n}{P}) = \int_0^P e^{i2\pi[Rr\cos(\frac{2\pi Z}{P} - \psi) + \frac{nz}{P}]}\, dz \qquad \text{(A-9)}$$

The integral in equation (A-9) may be evaluated by using the identity $\int_0^{2\pi} e^{iX\cos\varphi} e^{in\varphi} d\varphi = 2\pi i^n J_n(X)$. Taking $X = 2\pi rR$ and $\varphi = \frac{2\pi Z}{P}$ the result is:

$$T(R,\psi,\tfrac{n}{P}) = J_n(2\pi rR)\, e^{in(\psi + \frac{\pi}{2})} \qquad \text{(A-10)}$$

The main features of the intensity distribution expected from a continuous helix are shown below. The distribution is characterized by an X shaped array of spots centered at the origin of reciprocal space and an empty region near the meridian of reciprocal space. From the properties of Bessel functions it can be shown that the angle α is approximately equal to the pitch angle of the helix, i.e., the angle between the tangent vector to the helix and the helix axis. The pitch P can be determined from the layer-line spacing.

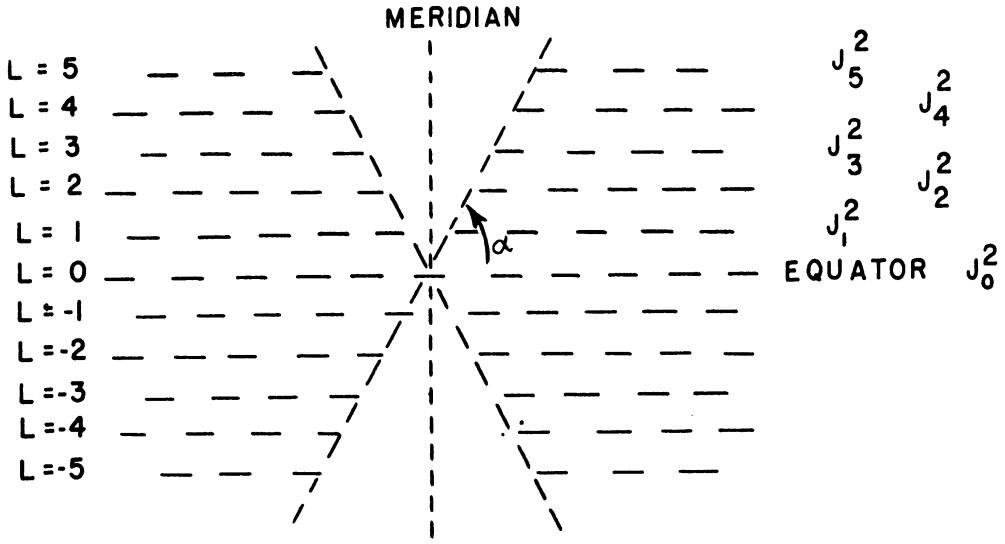

Figure A-3. The maxima of the squares of bessel functions.

We now consider the case of a discontinuous helix. A discontinuous helix may be defined as a set of points of vertical spacing p on the locus of a continuous helix of pitch P. The discontinuous helix may be considered as the product of two functions H and G such that H = 1 on the helix and 0 everywhere else and G = 1 on a set of horizontal planes of spacing p and 0 everywhere else. The transform of H is given by equation (A-10) and has values different from 0 only on the planes $\zeta = \frac{n}{P}$. The transform of G, g, can be shown to be equal to 1 for $\xi = \eta = 0$, $\zeta = \frac{m}{p}$ (m integral), and 0 elsewhere. Substituting in equation (A-5) the convolution of the transforms of H and G, which is the transform of HG, is:

$$C(X,Y,Z) = \int T(X-\xi,\ Y-\eta,\ Z-\zeta)\ g(\xi,\eta,\zeta)\ d\xi d\eta d\zeta \qquad \text{(A-11)}$$

$T(X-\xi,Y-\eta,Z-\zeta)$ vanishes unless $Z-\zeta = \frac{n}{P}$, with no restrictions on ξ and η. The function $g(\xi,\eta,\zeta)$ vanishes unless $\xi = \eta = 0$ and $\zeta = \frac{m}{p}$. Thus $C(X,Y,Z)$ will be different from 0 only when:

$$Z = \frac{n}{P} + \frac{m}{p} \qquad \text{(A-12)}$$

The transform of a discontinuous helix is therefore zero except over the set of planes given by equation (A-12). In general, P and p will not be commensurable and the identity period c will be some multiple of P. We may write:

$$Z = \frac{n}{P} + \frac{m}{p} = \frac{\ell}{c} \qquad \text{(A-13)}$$

where ℓ is an integer designating the layer-line index. For a given layer line ℓ, all pairs of integers (n,m) which satisfy equation (A-13) may be determined. The transform of the discontinuous helix evaluated on the ℓth layer line is given by:

$$T(R,\psi,\ell/c) = \left[J_{n_1}(2\pi rR)e^{in_1(\psi + \frac{\pi}{2})} + J_{n_2}(2\pi rR)e^{in_2(\psi + \frac{\pi}{2})} + \ldots \right] \qquad \text{(A-14)}$$

where $(n_1, n_2, \ldots)$ are solutions of equation (A-13). Thus, the transform of the discontinuous helix is the sum of terms of the form given by equation (A-10) for the continuous case.

To bring out the nature of the solution for a simple case, let us consider an example in which P and p are commensurable. Suppose $P/p = 4$. Solving equation (A-13) for the lowest order Bessel functions J_n as a function of ℓ we obtain: $(\ell,n) = (0,0),(1,1),(2,2),(3,-1),(4,0)$. The intensity transform* for a given ℓ is obtained by substituting the value of n into equation (A-14) and squaring. Figure A-4 shows a schematic diagram of the array of spots expected from this discontinuous helix.

* The contribution to the transform of the higher order Bessel functions has been neglected.

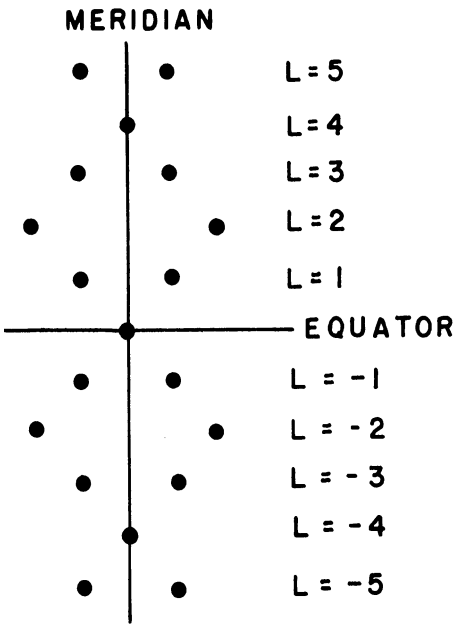

Figure A-4. Schematic representation of the diamond shaped array of spots expected from a discontinuous helix (P = 4p).

The resultant pattern has empty diamond shaped regions above and below the center. The first meridional reflection occurs on the 4th layer line, i.e., the order of the layer line on which the first meridional reflection occurs is equal to the number of points in the identity period. The diffraction pattern in reciprocal space is periodic, with period $\frac{1}{P} = \frac{1}{4p}$.

In the more general case, P and p are not commensurable. The diffraction pattern is more complicated but its essential features can be determined from equations (A-13) and (A-14). It is true in general that the first meridional reflection occurs on the layer line whose index is equal to the number of points (residues) in the identity period.

In many of the cases which have been studied, the diffraction patterns of the materials under consideration have been similar or identical

to that expected on the basis of the theory of the diffraction of a simple helix. In these simple cases, it has been possible to determine the pitch of the helix, the number of units per turn of the helix, and the number of turns of the helix in the identity period with relatively little ambiguity.

APPENDIX B

CONSTRUCTION OF PURE β-HELICES

By a pure β-helix is meant a configuration of the polypeptide chain which is locally β and which follows a helical path of large pitch. The configuration of a pure β-helix is determined by the coordinates of the first two residues and by the helical operation. The problem will be considered in two stages: 1) the determination of the coordinates of the α-carbon atoms. 2) the determination of the other coordinates in the amide group.

It is desired to twist a planar zig-zag chain of α-carbon atoms in such a way that the even and odd numbered α-carbon atoms shown in Figure B-1 form two coaxial helices.

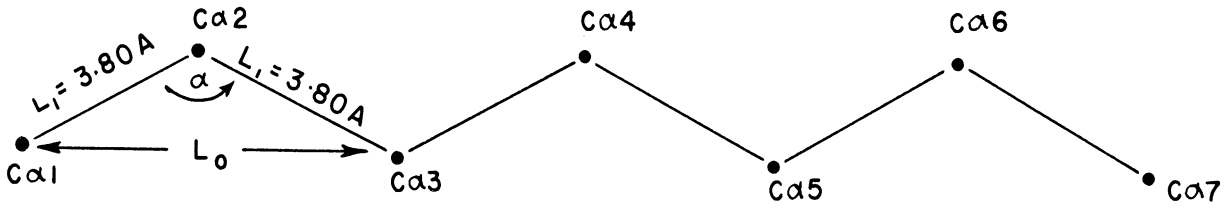

Figure B-1. Skeleton of α-carbon atoms.

Consider a left-handed set of coaxial helices whose pitch is P with N atoms per pitch of each helix.* The helix operation H which maps α-carbon$_1$

* The original formulation of the problem was in terms of left-handed helices. In order for the results to be comparable to those of the right-handed helix discussed in the text, the necessary changes will be made at the end of the discussion.

into α-carbon$_3$ and α-carbon$_2$ into α-carbon$_4$ is: $\varphi_H = \frac{-2\pi}{N}$ and $\Delta Z_H = \frac{P}{N}$ where φ is the rotation angle around the helix axis and z is the coordinate measured along the helix axis. Starting with the 1st α-carbon atom, the radius of the odd numbered atoms is determined by the relation:

$$(r\varphi_H)^2 + (\Delta Z_H)^2 = L_o^2 \qquad \text{(B-1)}$$

Substituting the values for φ_H and ΔZ_H we obtain:

$$r = \frac{1}{2\pi}\left[N^2L_o^2 - P^2\right]^{1/2} \qquad \text{(B-2)}$$

Two right-handed rectangular coordinate systems $x_oy_oz_o$ and $x_1y_1z_1$ are introduced below. The z axes are perpendicular to the plane of the paper. The unit vector along y_1 is tangent to the circle of radius r at the point O_1. Point O designates the "center" of the helix. The transformation connecting the two systems is:

$$\begin{aligned} x_o &= x_1 + r \\ y_o &= y_1 \\ z_o &= z_1 \end{aligned} \qquad \text{(B-3)}$$

Let the first α-carbon atom be located at the point O_1. By applying the helix operation, we obtain the coordinates of the third α-carbon atom:

$$\begin{aligned} x_{1C_{\alpha 3}} &= r[\cos(\tfrac{2\pi}{N})-1] \\ y_{1C_{\alpha 3}} &= -r[\sin(\tfrac{2\pi}{N})\ ] \\ z_{1C_{\alpha 3}} &= P/N \end{aligned} \qquad \text{(B-4)}$$

We now require that the configuration of the β-helix should be locally similar to the polar pleated-sheet configuration. On the basis of an

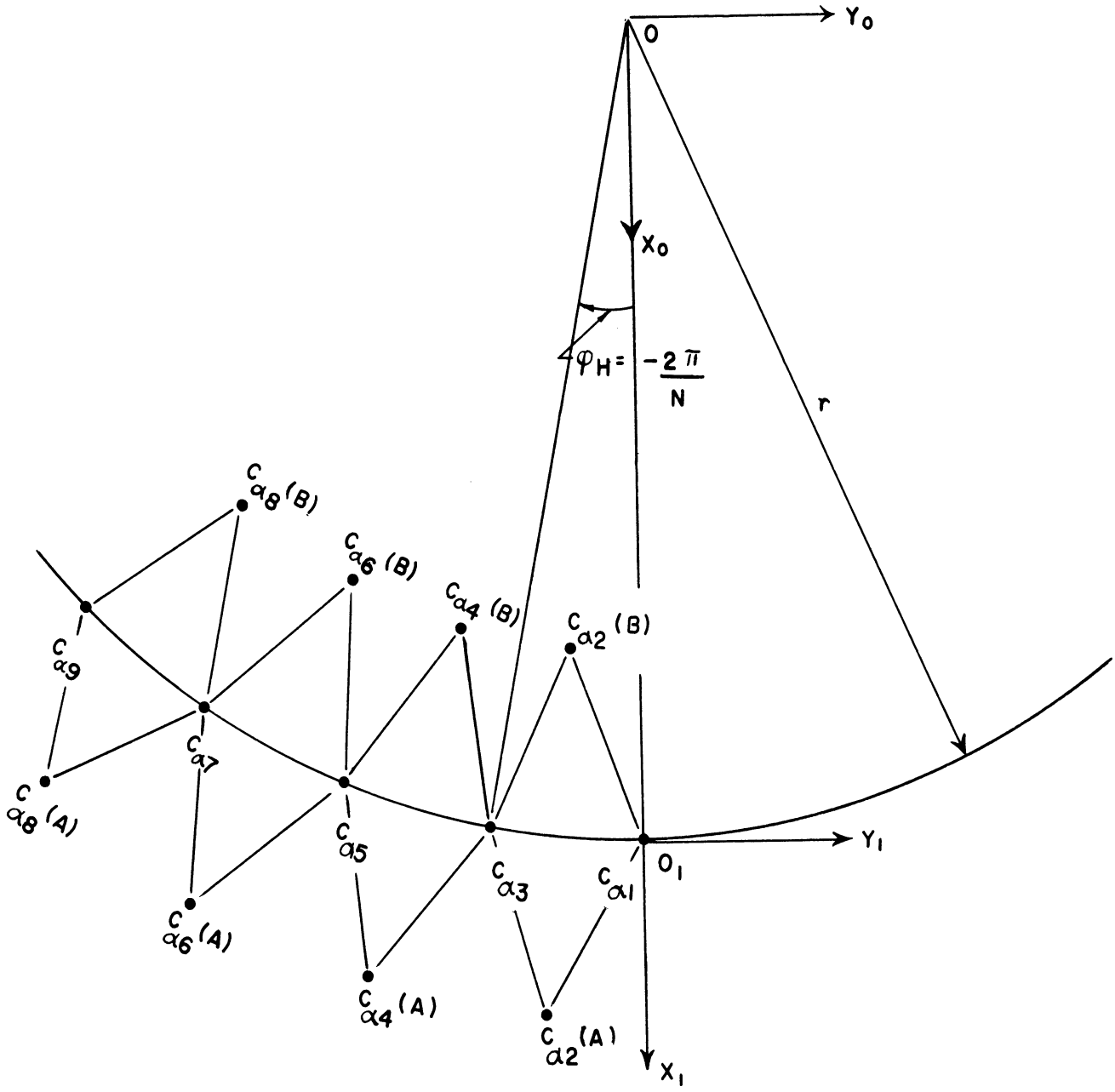

Figure B-2. Coordinate systems.

examination of a model of the polar pleated-sheet, it is reasonable to expect that the (φ,z) coordinates of the second α-carbon atom will be approximately 1/2 the corresponding coordinates for the third α-carbon atom. The two positions for the second α-carbon atom for which the (φ,z) coordinates are 1/2 the corresponding coordinates for the third α-carbon

atom are marked by A and B in Figure B-2. Using the fact that the distance between successive α-carbon atoms is a constant (approximately 3.80A for any configuration), the coordinates of the second α-carbon atom can easily be calculated by elementary geometrical methods for any particular case.

The second part of the problem involves the positioning of the other atoms in the planar amide groups. The parameters in Figure B-3 are based on the latest values for the distances and bond angles in the polypeptide chain.[77]

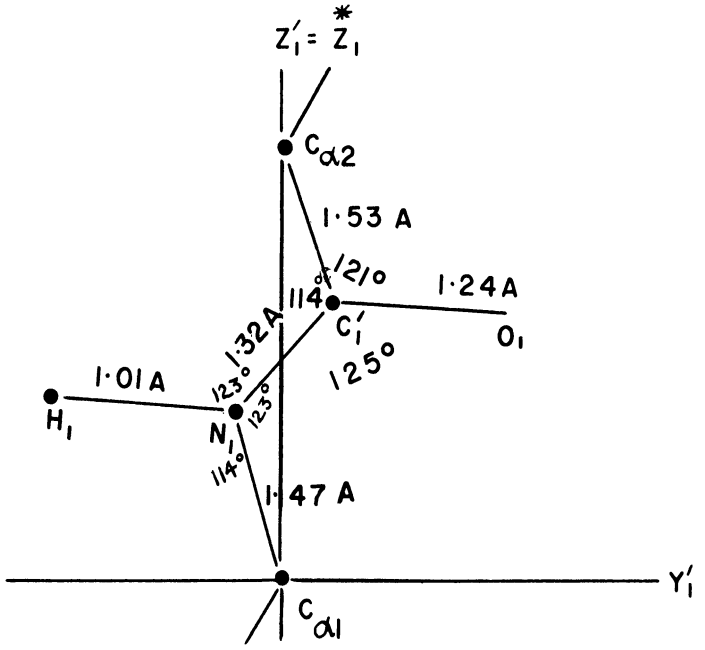

Figure B-3. Parameters in the amide group.

Table B-I lists the coordinates of the atoms in the amide group for the orientation shown in Figure B-3.

TABLE B-I

Coordinates of the Atoms in the Amide Group (in A)

	x_1'	y_1'	z_1'
$C_{\alpha 1}$	0.00	0.00	0.00
N_1	0.00	-0.34	1.43
H_1	0.00	-1.33	1.62
C_1'	0.00	0.58	2.38
O_1	0.00	1.80	2.19
$C_{\alpha 2}$	0.00	0.00	3.80

It is now convenient to introduce the Euler angles which relate the $(x_1 y_1 z_1)$ system to a rotated $(X_1 Y_1 Z_1)$ system, both coordinate frames having the same origin at O_1. The line of nodes is defined as the intersection of the plane through O_1 perpendicular to the Z_1 axis and the $(x_1 y_1)$ plane. Following the conventions of Goldstein,(106) the Euler angles relating the $(x_1 y_1 z_1)$ system and the $(X_1 Y_1 Z_1)$ system are: $(\theta,\psi,\varphi) = (\theta,0,\varphi)$ for X_1 along the line of nodes. The transformation between the two coordinate systems is given by:

$$\begin{pmatrix} x_1 \\ y_1 \\ z_1 \end{pmatrix} = \begin{pmatrix} \cos\varphi & -\cos\theta\sin\theta & \sin\theta\sin\varphi \\ \sin\varphi & \cos\theta\cos\varphi & -\sin\theta\cos\varphi \\ 0 & \sin\theta & \cos\theta \end{pmatrix} \begin{pmatrix} X_1 \\ Y_1 \\ Z_1 \end{pmatrix} \quad \text{(B-5)}$$

We now introduce a coordinate system $(\overset{*}{x}_1 \overset{*}{y}_1 \overset{*}{z}_1)$ with the vector from $C_{\alpha 1}$ to $C_{\alpha 2}$ as the $\overset{*}{z}_1$ axis. The Euler angles connecting this system to the $(x_1 y_1 z_1)$ system are taken as: $(\theta_1,\psi_1,\varphi_1) = (\theta_1,0,\varphi_1)$. The angle γ_1 measures the rotation of the amide group aronnd the $\overrightarrow{C_{\alpha 1} - C_{\alpha 2}}$ axis;

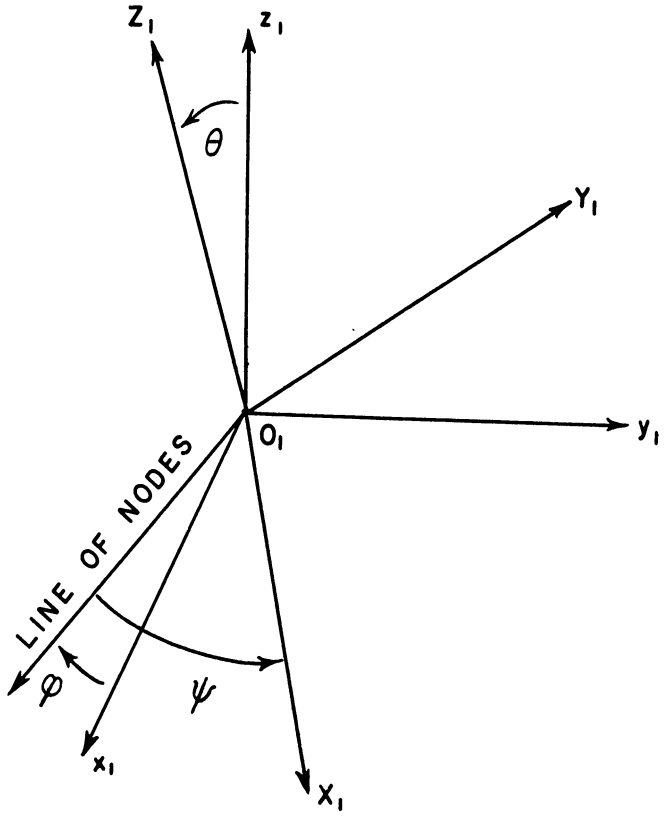

Figure B-4. The Euler angles.

$\gamma_1 = 0$ when the plane of the amide group coincides with the $\overset{*}{z}_1\overset{*}{y}_1$ plane.

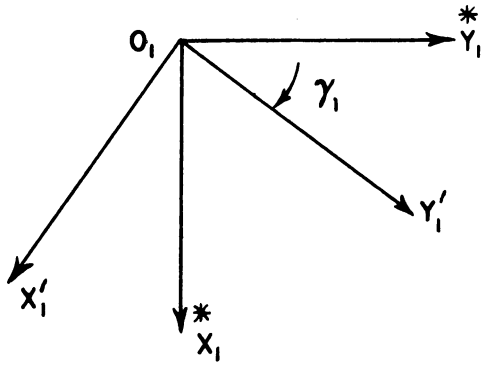

Figure B-5. Orientation of the amide group.

The relationship between the $(x_1'y_1'z_1')$ system and the $(\overset{*}{x}_1\overset{*}{y}_1\overset{*}{z}_1)$ system is:

$$\begin{aligned}\overset{*}{x}_1 &= x_1' \cos\gamma_1 - y_1' \sin\gamma_1 \\ \overset{*}{y}_1 &= y_1' \cos\gamma_1 + x_1' \sin\gamma_1 \\ \overset{*}{z}_1 &= z_1'\end{aligned} \qquad \text{(B-6)}$$

For the plane of the amide group, we may take $x_1' = 0$ (Table B-I).

Equation B-6 simplifies to :

$$\begin{aligned}\overset{*}{x}_1 &= -y_1' \sin\gamma_1 \\ \overset{*}{y}_1 &= +y_1' \cos\gamma_1 \\ \overset{*}{z}_1 &= z_1'\end{aligned} \qquad \text{(B-7)}$$

For a given γ_1, the $(x_1y_1z_1)$ coordinates for the ith atom of the amide group of the first residue is given by the equation:

$$\begin{pmatrix} x_{1i}^{(1)} \\ y_{1i}^{(1)} \\ z_{1i}^{(1)} \end{pmatrix} = \begin{pmatrix} \cos\varphi_1 & -\cos\theta_1 \sin\varphi_1 & \sin\varphi_1 \\ \sin\varphi_1 & \cos\theta_1 \cos\varphi_1 & -\sin\theta_1 \cos\varphi_1 \\ 0 & \sin\theta_1 & \cos\theta_1 \end{pmatrix} \begin{pmatrix} \overset{*}{x}_{1i} \\ \overset{*}{y}_{1i} \\ \overset{*}{z}_{1i} \end{pmatrix} \qquad \text{(B-8)}$$

where $(\overset{*}{x}_{1i}, \overset{*}{y}_{1i}, \overset{*}{z}_{1i})$ are determined from equation (B-7) and $(y_{1i}' \; z_{1i}')$ are given in Table B-I. The values of θ_1 and φ_1 can be obtained easily from the coordinates of the $C_{\alpha 2}$ atom.

In order to determine the coordinates of the atoms of the amide group of residue 2, a coordinate system $(\underline{x}_1\underline{y}_1\underline{z}_1)$ is introduced which is related to the $(x_1y_1z_1)$ system by the equations:

$$\begin{aligned}\underline{x}_1 &= x_1 - x_{1C_{\alpha 2}} \\ \underline{y}_1 &= y_1 - y_{1C_{\alpha 2}} \\ \underline{z}_1 &= z_1 - z_{1C_{\alpha 2}}\end{aligned} \qquad \text{(B-9)}$$

,i.e., a translation of the origin of the $(x_1y_1z_1)$ system by the vector $\overrightarrow{C_{\alpha 1}\text{-}C_{\alpha 2}}$. The system $(\overset{*}{x}_2\overset{*}{y}_2\overset{*}{z}_2)$ is introduced with $\overset{*}{z}_2$ lying along the $\overrightarrow{C_{\alpha 2}\text{-}C_{\alpha 3}}$ vector. The Euler angles which connect the $(\overset{*}{x}_2\overset{*}{y}_2\overset{*}{z}_2)$ system to the $(x_1y_1z_1)$ system are taken as: $(\theta_2,\psi_2,\varphi_2) = (\theta_1,0,\varphi_2)$. The angle γ_2 measures the rotation of the amide group around the $\overrightarrow{C_{\alpha 2}\text{-}C_{\alpha 3}}$ axis; $\gamma_2 = 0$ when the plane of the amide group coincides with the $(\overset{*}{z}_2\overset{*}{y}_2)$ plane. For the atoms of the planar amide group, x_1' may be equated to zero and we obtain for z_1' lying along the $\overrightarrow{C_{\alpha 2}\text{-}C_{\alpha 3}}$ axis:

$$\begin{aligned} \overset{*}{x}_2 &= -y_1' \sin\gamma_2 \\ \overset{*}{y}_2 &= +y_2' \cos\gamma_2 \\ \overset{*}{z}_2 &= z_1 \end{aligned} \qquad \text{(B-10)}$$

The coordinates of the ith atom of residue 2 are given by:

$$\begin{pmatrix} x_{1i}^{(2)} \\ y_{1i}^{(2)} \\ z_{1i}^{(2)} \end{pmatrix} = \begin{pmatrix} \cos\varphi_2 & -\cos\theta_2\sin\varphi_2 & \sin\theta_2\sin\varphi_2 \\ \sin\varphi_2 & \cos\theta_2\cos\varphi_2 & -\sin\theta_2\cos\varphi_2 \\ 0 & \sin\theta_2 & \cos\theta_2 \end{pmatrix} \begin{pmatrix} \overset{*}{x}_{2i} \\ \overset{*}{y}_{2i} \\ \overset{*}{z}_{2i} \end{pmatrix} + \begin{pmatrix} x_{1C_{\alpha 2}} \\ y_{1C_{\alpha 2}} \\ z_{1C_{\alpha 2}} \end{pmatrix} \qquad \text{(B-11)}$$

The values of φ_2 and $\theta_2 = \theta_1$ can easily be obtained from the coordinates of $C_{\alpha 2}$ and $C_{\alpha 3}$. Examination of equations B-8; B-11; B-7 and B-10 shows that the z difference between corresponding atoms of residues 1 and 2 will be equal if and only if: $\cos\gamma_1 = \cos\gamma_2$ or $\gamma_2 = \pm\gamma_1$ (B-12)

To summarize: a general method has been presented whereby, given the pitch, the number of residues per turn, and the distance between every other α-carbon atom, a system of coaxial helices may be constructed which has maximum symmetry. The 2nd α-carbon atom may be put in either of two positions marked A and B in Figure B-2. As a consequence of equation B-12

the coordinates of the atoms of the amide group are determined essentially by one additional parameter the angle γ_1, which must be chosen with the following criteria in mind: 1) the distortions at the tetrahedral carbon atom must not be "too large" 2) the structure must be in agreement with the infrared dichroism 3) the helix generated by γ_1 must be able to hydrogen-bond satisfactorily to the adjacent polypeptide chains with acceptable van der Waals contacts.

We have "constructed" a left-handed β-helix for which $L_o \cong 6.14A$ (Pauling's polar pleated-sheet) $\alpha = 107° 30'$, N = 32 and P = 190A. For this choice of parameters, the $(x_1 y_1 z_1)$ coordinates for the α-carbon atoms in position B are: $C_{\alpha 1}(0.00,0.00,0.00)$, $C_{\alpha 2}(-2.31A,-0.55A,2.97A)$, $C_{\alpha 3}(-0.15A, -1.55A,5.94A)$. We considered the case $\gamma_1 = +68°$ and $\gamma_2 = -68°$. The coordinates for two adjacent chains related by a rotation of 36° around the z_0 axis are given in Table B-II. The coordinates for the right-handed helix can be obtained from the coordinates of the left-handed helix by the transformation: $x_{RHH} = x_{LHH}$; $y_{RHH} = -y_{LHH}$ and $z_{RHH} = z_{LHH}$.* The basal projection for the right-handed helix is shown in Figure B-6. The distance from O_1 on chain 2 to N_1 on chain 1 = 2.65A, while the distance from O_2 on chain 2 to N_2 on chain 1 = 2.70A. For most substances with NH....O bonds, the distance from the nitrogen atom to the hydrogen-bonded oxygen atom varies from about 2.7A to 2.9A.[81] The hydrogen bond lengths quoted above are therefore slightly short. These lengths would almost certainly be brought into the correct range if the 1st α-carbon atom had been located at a

* RHH = right-handed helix and LHH = left handed helix

TABLE B-II*

Coordinates (in A) for the Atoms of a Possible Pure β-Helix

Chain 1	x_1	y_1(LHH)	y_1(RHH)	z_1	x_o	r	φ(LHH)	φ(RHH)
$C_{\alpha 1}$	0.00	0.00	0.00	0.00	7.97	7.97	0	0
N_1	-0.89	-0.53	0.53	1.04	7.07	7.07	--4°30'	4°30'
H_1	-1.08	-1.52	1.52	0.95	6.89	7.06	-12°30'	12°30'
C_1'	-1.41	0.22	-0.22	2.00	6.56	6.56	2°	- 2°
O_1	-1.21	1.43	-1.43	2.13	6.76	6.91	12°	-12°
$C_{\alpha 2}$	-2.31	-0.55	0.55	2.97	5.66	5.68	- 5°30'	+ 5°30'
N_2	-1.54	-1.25	1.25	4.01	6.43	6.55	-11°	-11°
H_2	-1.56	-2.26	2.26	3.92	6.41	6.79	-19°30'	19°30'
C_2'	-0.89	-0.62	0.62	4.97	7.08	7.11	- 5°	5°
O_2	-0.84	0.61	-0.61	5.10	7.12	7.15	5°	- 5°
$C_{\alpha 3}$	-0.15	-1.55	1.55	5.94	7.81	7.97	-11°30'	+11°30'
N_3	-1.13	-1.90	1.90	6.98	6.83	7.09	-15°30'	+15°30'
Chain 2								
$C_{\alpha 1}$	-1.52	-4.68	4.68	0.00	6.44	7.97	-36°	+36°
N_1	-2.56	-4.59	4.59	1.04	5.41	7.09	-40°30'	+40°30'
H_1	-3.29	-5.29	5.29	0.95	4.68	7.06	-48°30'	+48°30'
C_1'	-2.53	-3.68	3.68	2.00	5.43	6.56	-34°	+34°
O_1	-1.66	-2.82	2.82	2.13	6.31	6.91	-24°	+24°
$C_{\alpha 2}$	-3.72	-3.77	3.77	2.97	4.25	5.68	-41°30'	+41°30'
N_2	-3.50	-4.78	4.78	4.01	4.46	6.55	-47°	+47°
H_2	-4.11	-5.59	5.59	3.92	3.86	6.79	-55°30'	+55°30'
C_2'	-2.60	-4.66	4.66	4.97	5.37	7.11	-41°	+41°
O_2	-1.85	-3.70	3.70	5.10	6.12	7.15	-31°	+31°
$C_{\alpha 3}$	-2.56	-5.85	5.85	5.94	5.41	7.97	-47°30'	+47°30'
N_3	-3.56	-5.56	5.56	6.98	4.41	7.09	-51°30'	+51°30'

* LHH = left-handed helix and RHH = right-handed helix. The coordinates of right-handed helix are determined from those of the left-handed helix by a reflection in the $(x_1 z_1)$ plane.

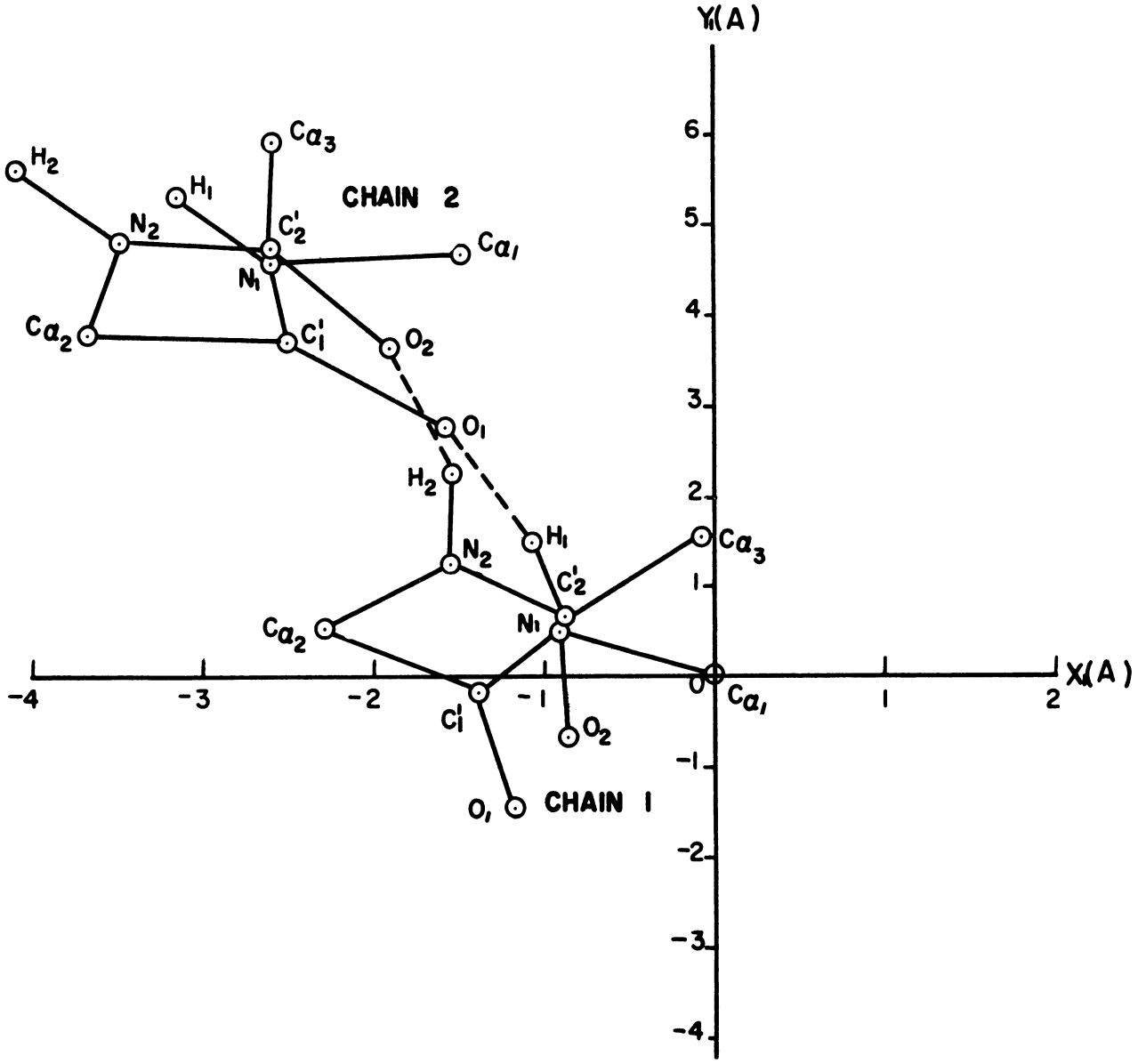

Figure B-6 Basal projection of the atoms in the main chains of a possible pure β-helix.

greater radius, i.e.,about 8.7A. The angles, for the NH....O bonds, between the NO vectors and the NH vectors are less than 30°, which agrees well with the criterion used by Pauling and Corey.[25] The C_2' -$C_{\alpha 3}$ -N_3 angle = 106° and the angle C_1' -$C_{\alpha 2}$-N_2 = 112°. Variations in the "tetrahedral" carbon angle of larger than 3° are known to occur in organic crystals related to proteins. For example, a "tetrahedral" carbon angle of 113.7° is found in N, N' hexamethylenebisproprionamide[107]; a "tetrahedral" carbon angle of 113° is quoted for the N, N' diacetylhexamethylenediamine molecule[108]. In addition, Donohue[28] has estimated, on the basis of semi-quantitative considerations, that the value of the instability due to a "tetrahedral" angle of 100° would only be about 0.3 kcal per mole per residue.*

The coordinates for the β-carbon atom attached to $C_{\alpha 2}$, i.e., $C_{\beta 2}$ and the H atom attached to $C_{\alpha 2}$, i.e., H_2' were determined by a subsidiary calculation. The resulting $(x_1 y_1 z_1)$ coordinates for the H_2' atom and the C_β^2 atom on chain 1 are (-2.92, -0.22A, 3.44A) and (-3.27A, 1.45A, 2.19A) respectively. The angle between $\overrightarrow{C_{\alpha 2}C_{\beta 2}}$ and $\overrightarrow{C_{\alpha 2}H_2'}$ is 106.5°. The largest deviation from a tetrahedral angle occurs for the H_2'-C_α-C_1' angle which is 104.5°. The contact between the $C_{\beta 2}$ atom on chain 1 and the H_2' atom on chain 2 is approximately 1.90A This contact could very likely be made equal to or greater than 2A by increasing the radius of the 1st α-carbon atom from 8.1A to about 8.7A The $C_{\alpha 2}$ atom on chain 1 has a short van der Waals contact of about 2.5A with O_1 on chain 2. Briegleb quotes a value of 1.3A for the van der Waals

* The C'-C_α-N angle equals 100° for the 4.3_{14} helix.

radius of an aliphatic carbon atom (σ-electons, Section 4.5), while the value of the van der Waals radius for oxygen is 1.4A according to Pauling (Section 4.6). Hence, a carbon oxygen contact should be 2.7A or greater. In order to determine whether the short contacts and the hydrogen-bonding distances could simultaneously be brought into the appropriate range, we have as a first approximation increased the radii of all of the atoms in the structure by 0.7A. The contact between $C_{\alpha 2}$ on chain 1 and O_1 on chain 2 becomes 2.72A, while the contact between $C_{\beta 2}$ on chain 1 and H_2' on chain 2 becomes 2A. The distance between O_1 on chain 2 to N_1 on chain 1 is 2.82A and the distance from O_2 on chain 2 to N_2 on chain 1 is 2.90A. The contacts and the hydrogen bond lengths are in the acceptable range and it is very probable that a more exact solution could be found. The CO and NH bonds are tipped with respect to the fiber axis by an angle of about 5°. The helix is therefore in agreement with the observed infrared dichroism.

It is therefore concluded that it is possible to "construct" a pure β-helix of the type discussed with satisfactory hydrogen bonds and satisfactory van der Waals contacts. To construct such a helix which would better satisfy the required criteria, it would be necessary to make additional calculations of the type that have been indicated in this discussion.

APPENDIX C

ROUGH CALCULATIONS OF THE COORDINATES OF A β - Helix

An attempt has been made to determine the coordinates of the ten-chain model by mathematical calculations employing the measured coordinates of the α-carbon atoms determined from model building. The analytical geometry employed involved a generalization of the techniques used in Appendix B. As the details of the calculation are tedious and do not involve any essential new principles, they will not be discussed. It should be emphasized that as a result of the fact that many parameters in the system had to be estimated the cumulative error was large and the coordinates given are very rough. The coordinates for the atoms in the main chain for eight residues of chain 1 are given in Table C-1. The φ coordinates for the atoms in chain 2 are 36° greater than the corresponding coordinates for the atoms in chain 1 while the r and z coordinates are the same.

TABLE C-1

Rough Coordinates (in A) for the Atoms of a Possible β-Helix

Chain 1	x_0	y_0	z_0	r	φ
C_{α_1}	3.93	5.28	3.14	6.57	53°30'
C'_1	4.62	6.11	4.23	7.66	53°
O_1	5.74	5.82	4.64	8.17	45°30'
N_1	3.89	7.13	4.66	8.12	61°30'

TABLE C-I (Cont.)

Chain 1	x_0	y_0	z_0	r	φ
H_1	2.97	7.34	4.31	7.92	68°
$C_{\alpha 2}$	4.36	8.05	5.70	9.15	61°30'
C_2'	3.67	7.83	7.05	8.65	65°
O_2	3.54	8.75	7.86	9.44	68°
$N_{2(proline)}$	3.27	6.59	7.24	7.36	64°
$C_{\alpha 3(proline)}$	2.57	6.14	8.47	6.65	67°30'
C_3'	3.14	7.01	9.60	7.68	66°
O_3	4.33	6.94	9.92	8.18	58°
N_3	2.25	7.82	10.15	8.14	74°
H_3	1.28	7.85	9.86	7.95	81°
$C_{\alpha 4}$	2.58	8.74	11.24	9.07	73°30'
C_4'	2.89	7.80	12.42	8.32	70°
O_4	4.04	7.46	12.68	8.48	61°30'
N_4	1.81	7.42	13.08	7.64	76°30'
H_4	0.88	7.72	12.84	7.77	83°30'
$C_{\alpha 5}$	1.88	6.53	14.25	6.80	74°

TABLE C-I (Cont.)

Chain 1	x_0	y_0	z_0	r	φ
C'_5	2.19	7.41	15.47	7.73	73°30'
O_5	3.36	7.65	15.80	8.36	66°30'
N_5	1.11	7.85	16.10	7.93	82°
H_5	0.17	7.63	15.80	7.63	89°
$C_{\alpha 6}$	1.19	8.69	17.29	8.80	82°30'
C'_6	1.55	1.90	18.55	8.05	79°
O_6	2.73	7.76	18.90	8.23	70°30'
N_6	0.50	7.43	19.21	7.45	86°
H_6	-0.45	7.57	18.90	7.58	93°30'
$C_{\alpha 7}$	0.62	6.67	20.46	6.68	84°30'
C'_7	0.71	7.55	21.71	7.58	84°30'
O_7	1.80	7.97	22.12	8.17	77°30'
N_7	-0 46	7.80	22.27	7.81	93°30'
H_7	-1.33	7.45	21.91	7.57	100°
$C_{\alpha 8}$	-0.62	8.66	23.49	8.68	93°

TABLE C-I (Cont.)

Chain 1	x_0	y_0	z_0	r	φ
C'_8	-0.21	7.97	24.80	7.98	91°30'
O_8	0.93	8.13	25.27	8.18	83°30'
N_8	-1.16	7.23	25.33	7.32	99°
H_8	-2.08	7.12	24.92	7.42	106°30'

Although the coordinates given in Table C-I are only approximate, they can be used to determine a zeroth order approximation to the transform of the atoms in the main chain. By taking reasonable variations of these coordinates the changes in the transform which result can be determined and a better estimate of the scattering can be obtained.

BIBLIOGRAPHY

1. L. Pauling, "The Configuration of Polypeptide Chains in Proteins," Les Proteines: Rapports et Discussions, ed. R. Stoops (Bruxelles: Institut International de Chimie Solvay, 1953), 63.

2. B. W. Low and J. T. Edsall, "Aspects of Protein Structure," Currents in Biochemical Research, ed. David E. Green (London: Interscience Publishers, Ltd., 1956), 378.

3. S. Mizushima, Structure of Molecules and Internal Rotation, Academic Press Inc., New York, 1954), Chapter VI.

4. F. H. C. Crick and A. Rich, Nature 176, 915 (1955).

5. F. Sanger and H. Tuppy, Biochemical J. 49, 481 (1951).

6. F. Sanger and E. O. P. Thompson, Biochemical J. 53, 353, 366 (1953).

7. M. L. Anson, "The Denaturation of Proteins," Les Proteines: Rapports et Discussions, ed. R. Stoops (Bruxelles: Institut International de Chimie Solvay, 1953), 201.

8. R. S. Bear, "The Structure of Collagen Fibrils," Advances in Protein Chemistry, eds. M. L. Anson, K. Bailey, and J. T. Edsall (New York: Academic Press Inc., 1952), VII, 69.

9. W. T. Astbury, Textile Fibers Under the X-Rays (Kynoch Press, Birmingham).

10. W. T. Astbury, Trans. Far. Soc. 34, 378 (1938).

11. W. T. Astbury and H. J. Woods, Nature 126, 913 (1930).

12. M. F. Perutz, Nature 167, 1053 (1951).

13. J. C. Kendrew, "Structure Proteins I," The Proteins, eds. H. Neurath and K. Bailey (New York: Academic Press Inc., 1954), II, B Chapter XXIII.

14. R. S. Bear and H. J. Rugo, Ann. New York Acad. Sci. 53, 627 (1951).

15. R. Brill, Ann., 434, 204 (1923).

16. K. H. Meyer and H. Mark, Ber. 61, 1932 (1928).

17. R. E. Marsh, R. B. Corey, and L. Pauling, Biochem. et Biophys. Acta 16, 1 (1955).

18. L. Pauling and R. B. Corey, Proc. Nat. Acad. Sci. (U.S.) 37, 729 (1951).

19. B. W. Low, "The Structure and Configuration of Amino Acids, Peptides and Proteins," The Proteins, eds. H. Neurath and K. Bailey (New York: Academic Press Inc., 1954), I, A, Chapter IV.

20. R. B. Corey and J. Donohue, J. Amer. Chem. Soc. 72, 2899 (1950).

21. W. T. Astbury and F. O. Bell, Nature 147, 696 (1941).

22. M. L. Huggins, Chem. Rev. 32, 195 (1943).

23. E. J. Ambrose and W. E. Hanby, Nature 163. 483 (1949).

24. E. J. Ambrose, A. Elliott, and R. B. Temple, Nature 163, 859 (1949).

25. L. Pauling, R. B. Corey, and H. R. Branson, Proc. Nat. Acad. Sci. (U.S.) 37, 205 (1951).

26. L. Pauling and R. B. Corey, Proc. Nat. Acad. Sci. (U.S.) 37, 235 (1951).

27. C. Robinson and E. J. Ambrose, Trans. Far. Soc. 48, 854 (1952).

28. J. Donohue, Proc. Nat. Acad. Sci. (U.S.) 39, 470 (1953).

29. W. Cochran, F. H. C. Crick, and V. Vand, Acta Cryst. 5, 581 (1952).

30. L. Brown and I. F. Trotter, Trans, Far. Soc. 52, 537 (1956).

31. F. H. C. Crick, Acta Cryst. 6, 685 (1953).

32. D. P. Riley and U. W. Arndt, Phil. Trans. Roy. Soc., A247, 409 (1955).

33. P.M.Cowan, A.C.T.North, and J.T.Randall, "High-Angle X-Ray Diffraction of Collagen Fibres, "Nature and Structure of Collagen, Ed. J.T.Randall, F.R.S. (London: Butterworths Scientific Publications, 1953), 241.

34. G. N. Ramachandran and G. K. Ambady, Current Sci. 23, 349 (1954).

35. G. N. Ramachandran and G. Kartha, Proc. Indian Acad. Sci. A42, 215 (1955).

36. P. M. Cowan and S. McGavin, Nature 176, 501 (1955).

37. F. H. C. Crick and A. Rich, Nature 176, 780 (1955).

38. M. L. Huggins, Proc, Nat. Acad. Sci. (U.S.) 43, 209 (1957).

39. K. M. Rudall, Riochem. et Biophys. Acta 1, 549 (1947).

40. W. T. Astbury and T. C. Marwick, Nature 130, 309 (1932).

41. W. T. Astbury and R. Lomax, Nature 133, 794 (1934).

42. R. B. Corey and R. W. G. Wycoff, J. Biol. Chem. 114, 407 (1936).

43. W. T. Astbury and F. O. Bell, Tabulae Biologicae 17, 90 (1939).

44. R. S. Bear, J. Amer. Chem. Soc. 66, 2043 (1944).

45. W. T. Astbury, S. V. Perry, R. Reed, and L. C. Spark, Biochem. et Biophys. Acta 1, 379 (1947).

46. C. Cohen and J. Hanson, Biochem. et Biophys. Acta 21, 177 (1956).

47. R. S. Bear and C. C. Selby, J. Biophys. and Biochem. Cytology 2, 55 (1956).

48. M. A. Rougvie, PhD. Thesis, M.I.T., (1954).

49. L. Pauling and R. B. Corey, Proc. Nat. Acad. Sci. (U.S.), 37, 256 (1951).

50. J. Kraut, PhD. Thesis, California Institute of Technology, (1954).

51. G. N. Ramachandran and V. Sasisekharan, Arch. Biochem. and Biophys. 63, 255 (1956).

52. C. H. MacGillavry and E. M. Bruins, Acta Cryst. 1, 156 (1948).

53. G. H. Vineyard, Acta Cryst. 4, 281 (1951).

54. Radiography in Modern Industry, (Eastman Kodak Company, X-Ray Div., Rochester New York, 1947), 37.

55. C. W. Bunn, Chemical Crystallography, (Oxford University Press, Great Britain, 1946), 149.

56. H. L. Yakel and P. N. Schatz, Acta Cryst. 8, 22 (1955).

57. C. W. Bunn and E. V. Garner, Proc. Roy. Soc. A189, 39 (1947).

58. K. D. Parker, Biochem. et Biophys. Acta 17, 148 (1955).

59. H. Lipson and W. Cochran, The Crystalline State Vol. III, The Determination of Crystal Structures, (G. Bell and Sons Ltd., London, 1953), 215.

60. W. A. Schroeder, L. M. Kay, B. Lewis, and N. Munger, J. Amer. Chem. Soc. 77, 3901 (1955).

61. W. H. Ward, C. H. Binkley, and N. S. Snell, Textile Res. J. 25, 314 (1955).

62. W. A. Schroeder, L. M. Kay, N. Munger, N. Martin, et al, J. Amer. Chem. Soc. 79, 2769 (1957).

63. W. H. Ward, L. M. High, and H. P. Lundgren, J. Polymer Res. 1, 22 (1946).

64. A. M. Woodin, Biochem. J. 57, 99 (1954).

65. A. M. Woodin, Nature 176, 1117 (1955); 173, 823 (1954).

66. A. M. Woodin, Biochem. J. 63, 576 (1956).

67. G. Ehrlich and G. B. B. M. Sutherland, First Interim Report, DA-44-109-qm-1037, March 1953.

68. E. J. Ambrose and A. Elliott, Proc. Roy. Soc. A205, 47 (1951).

69. E. J. Ambrose and A. Elliott, Proc. Roy. Soc. A208, 75 (1951).

70. S. Krimm, J. of Chem. Phys. 23, 1371 (1955).

71. C. L. Angell, Unpublished.

72. L. Pauling and R. B. Corey, Proc. Nat. Acad. Sci. (U.S.), 37, 251 (1951).

73. L. Pauling and R. B. Corey, Proc. Nat. Acad. Sci. (U.S.) 39, 253 (1951).

74. P. M. Cowan, A. P. T. North, and J. T. Randall, "X-Ray Diffraction Studies of Collagen Fibres," Symposia of the Society for Experimental Biology: Fibrous Proteins and Their Biological Significance, eds. R. Brown and J. F. Danielli (New York, Academic Press Inc., 1955), No. IX, 115.

75. H. R. Crane, Scientific Monthly 70, June (1950).

76. S. Krimm and R. Schor, J. Chem. Phys. 24, 922 (1956).

77. R. B. Corey and L. Pauling, Proc. Roy. Soc. B141, 10 (1953).

78. J. M. Bijvoet, A. F. Peerdeman, and A. J. van Bommel, Nature 168, 271, (1950).

79. R. E. Marsh, Abstracts of the Communications, The International Union of Crystallography, (Fourth International Conference, Montreal, July 10-19, 1957), 86.

80. H. A. Stuart, Die Physik Der Hochpolymeren, Die Struktur Des Frien Molekuls, (Springer-Verlag, Berlin, 1952), Band I, 99.

81. J. Donohue, J. Phys. Chem. 56, 502 (1952).

82. L. Pauling, Nature of the Chemical Bond, (Cornell University Press, New York, 1940), 189.

83. H. A. Stuart, Die Physik Der Hochpolymeren, Die Struktur Des Frien Molekuls, (Springer-Verlag, Berlin, 1952), Band I, 56.

84. M. el Nadi, Journal of Chemical Physics 19, 503 (1951).

85. L. Pauling, Nature 171, 59 (1953).

86. G. Oster and D. P. Riley, Acta Cryst. 5, 272 (1952).

87. G. N. Ramachandran, Abstracts of the Communications, The International Union of Crystallography, (Fourth International Conference, Montreal, July 10-19, 1957), 87.

88. J. Waser, Acta Cryst. 8, 142 (1955).

89. C. H. Bamford, A. Elliott, and W. E. Hanby, Synthetic Polypeptides (Academic Press Inc., New York, 1956), Chapter VII.

90. W. L. Bragg and M. F. Perutz, Proc. Roy. Soc. A213, 425 (1952).

91. W. L. Bragg, Proc. Phys. Soc. B65, 833 (1952).

92. W. T. Astbury and J. W. Haggith, Biochem. et Biophys. Acta 10, 483 (1953).

93. R. D. B. Fraser, J. Chem. Phys. 21, 1511 (1953).

94. P. W. Higgs, Proc. Roy. Soc. A220, 472 (1953).

95. E. J. Ambrose and A. Elliott, Proc. Roy. Soc. A206, 206 (1951).

96. G. B. B. M. Sutherland and D. L. Wood, Progress Report No. 2, DA-44-109-qm-1037, April 1953 - December 1953.

97. A. Elliott, W. E. Hanby, and B. R. Malcom, Nature 180, 1340 (1957).

98. P. J. Flory, Principles of Polymer Chemistry, (Cornell University Press, Ithaca, New York, 1953), 627.

99. W. A. Schroeder et al., J. Amer. Chem. Soc. 76, 3556 (1954)

100. C. B. Anfinsen and R. R. Redfield, "Protein Structure in Relation to Function and Biosynthesis," Advances in Protein Chemistry, eds. M. L. Anson, K. Bailey, and J. T. Edsall (New York: Academic Press Inc., 1956), XI,2.

101. F. Sanger, "The Chemistry of Simple Proteins," Symposia of the Society for Experimental Biology: Fibrous Proteins and Their Biological Significance, eds. R. Brown and J. F. Danielli (New York, Academic Press Inc., 1955), No. IX, 10.

102. D. L. Wood, private communication.

103. R. D. B. Fraser, T. P. MacRae, and D. H. Simmonds, Biochem. et Biophys. Acta 25, 654 (1957).

104. R. W. James, The Crystalline State Vol. II, The Optical Principles of the Diffraction of X-Rays, (G. Bell and Sons Ltd., London, 1954), Appendix V.

105. A. R. Stokes, "The Theory of X-Ray Fiber Diagrams," Progress in Biophysics, eds. J. A. V. Butler and J. T. Randall F. R. S. (New York and London: Pergamon Press, 1955), V, Chapter V.

106. H. Goldstein, Classical Mechanics (Addison-Wesley Press Inc., Cambridge Mass., 1951) Chapter IV.

107. L. H. Jensen, S. Krimm, R. G. Parrish, and D. L. Wood, Acta Cryst. 10, 528 (1957).

108. M. Bailey, Acta Cryst. 8, 575 (1955).

UNIVERSITY OF MICHIGAN
3 9015 03525 1837